Co-culturing sensory neurons and glial cells on microelectrode arrays platforms for functional studies on pain

Dissertation

zur Erlangung des Grades eines
Doktors der Naturwissenschaften

der Mathematisch-Naturwissenschaftlichen Fakultät
und
der Medizinischen Fakultät
der Eberhard-Karls-Universität Tübingen

vorgelegt von

Francesca Izzi
aus Valdagno, Italien

2021

Tag der mündlichen Prüfung:	20.09.2021
Dekan der Math.-Nat. Fakultät:	Prof. Dr. Thilo Stehle
Dekan der Medizinischen Fakultät:	Prof. Dr. Bernd Pichler
1. Berichterstatter:	Dr. Paolo Cesare
2. Berichterstatter:	Prof. Dr. Philipp Kahle
Prüfungskommission:	Dr. Paolo Cesare
	Prof. Dr. Philipp Kahle
	Prof. Dr. Ulrich Rothbauer
	Dr. Franziska Denk

Erklärung/Declaration

Ich erkläre, dass ich die zur Promotion eingereichte Arbeit mit dem Titel "Co-culturing sensory neurons and glial cells on microelectrode arrays platforms for functional studies on pain" selbstständig verfasst, nur die angegebenen Quellen und Hilfsmittel benutzt und wörtlich oder inhaltlich übernommene Stellen als solche gekennzeichnet habe. Ich versichere an Eides statt, dass diese Angaben wahr sind und dass ich nichts verschwiegen habe. Mir ist bekannt, dass die falsche Abgabe einer Versicherung an Eides statt mit Freiheitsstrafe bis zu drei Jahren oder einer Geldstrafe bestraft wird.

I hereby declare, that I have authored the work filed for the doctorate with the title "Co-culturing sensory neurons and glial cells on microelectrode arrays platforms for functional studies on pain" myself, only used the sources and auxiliary materials cited and have labeled as such places adopted literally or with regards to content. I affirm under penalty of perjury that these statements are true and that I have concealed nothing. I am aware that the submission of a false affirmation under penalty of perjury is punishable by imprisonment of up to three years or a fine.

Tübingen, den: ....

Datum/Date Unterschrift/Signature

Statement of Contributions

All the experiments involving cell cultures, and recording with MEA, ICC, were performed by me. Dr. Paolo Cesare helped me in dissecting the mice for single-cell sequencing and part of microfluidics experiments, due to the large quantities of cells required for such experiments. Dr. Patrizia Rizzu (Deutsches Zentrum für Neurodegenerative Erkrankungen e.V. in Tübingen) helped in designing the single-cell sequencing experiment. Noémia-Rita Alves Fernandes (Deutsches Zentrum für Neurodegenerative Erkrankungen e.V.in Tübingen) generated the libraries and performed single-cell sequencing. Dr. Sara Villa Hernandez and Dr. Franziska Denk (Wolfson Centre for age-related diseases at King's College London) analysed the libraries produced with single-cell sequencing, provided the results displayed in Figure 3.55 and suggested the possible targets reported in Table 3.11.

"*If we fail, we hope that someone, somewhere, finds these notes to know that we may not have succeeded but that we tried.*"

Pandemic Legacy: Season 2

Summary

One in five adults suffers from chronic pain, which frequently aggravates into neuropathic pain. This constitutes a significant cause of long-term sick leave and forced early retirement, placing a financial burden on both individuals and healthcare systems. Many analgesic compounds are already available, which, although they do have therapeutic utility in some acute pain states, are ineffective in between one and two-thirds of patients suffering from chronic pain conditions. These drugs also suffer from drawbacks in clinical use, with common side-effects, especially in long-term applications. Therefore, despite extensive research programs by biopharmaceutical companies and academia, there is a significant and unmet need for improved analgesic compounds, either based on novel or existing mechanisms.

Furthermore, several cases of chronic pain eventually aggravate into neuropathic pain.

Because of the large number of cases and the lack of targeted therapies, there has been considerable interest in the mechanisms that underpin neuropathic pain. One of the major surprises to have emerged over the last decades is that in experimental models of neuropathic pain, non-neuronal cells play a very active role in developing sensory abnormalities. In particular, multiple studies have demonstrated a critical role for Schwann cells and satellite glial cells (SGCs) in the PNS. However, to move these advancements towards their translational application, sufficient basic knowledge on neuropathic pain neuron-glia pathways, and tools for target and compounds discovery and validation, is still needed. In particular, it is not clear how exactly glial cells induce the hyper-excitable state in pain-signaling neurons. Moreover, pain mechanisms are not always controlled in the same way in preclinical species and humans.

This work illustrates how the excitability of sensory neurons is strongly affected by the presence of glial cells. The absence of glial cells leads to an almost complete silencing of sensory neurons without affecting their survival. It has been proved that sensory neurons deprived of their glial cells can still generate action potentials. However, there is a delay in the onset of an action potential, as they require a higher stimulation to generate such action potential.

It also shows that most glial cells in ganglia are represented by Schwann cells, leading to the hypothesis that these cells are essential for neuronal excitability in the PNS. It also demonstrates that these glial cells are not required to be in strict contact with DRG neurons to affect neuronal excitability but is sufficient for them to be in the same culture media. Furthermore, this work assesses a downregulation of specific genes in sensory neurons grown without glial cells, which correlates with the same genes being upregulated in established in vivo pain models.

These findings support the hypothesis that glial cells play a crucial role in the excitability of sen-

sory neurons. Therefore, they may be deeply involved in the generation of painful states, including those typical of neuropathic pain.

Zusammenfassung

Einer von fünf Erwachsenen leidet unter chronischen Schmerzen, die sich häufig zu neuropathischen Schmerzen entwickeln. Dies ist eine wesentliche Ursache für Langzeitkrankenstände und erzwungene Frühverrentungen und stellt sowohl für den Einzelnen als auch für die Gesundheitssysteme eine enorme Belastung dar. Zwar sind bereits viele verschiedene Analgetika verfügbar, die bei einigen akuten Schmerzen eine gute Wirksamkeit zeigen, aber bei einem bis zwei Dritteln der Patienten mit chronischen Schmerzzuständen unwirksam sind. Insbesondere bei langfristiger Anwendung dieser Medikamente treten häufig Nebenwirkungen auf. Daher besteht auch heute noch trotz intensiver Forschung von biopharmazeutischen Unternehmen und Hochschulen ein massiver Bedarf an der Entwicklung von verbesserten analgetischen Wirkstoffen, die entweder auf bekannten oder neuen Mechanismen basieren.

Eine der größten überraschenden Entdeckungen der letzten Jahrzehnte ist, dass in experimentellen Modellen gezeigt wurde, dass für neuropathischen Schmerz nicht-neuronale Zellen eine sehr aktive Rolle bei der Entwicklung sensorischer Anomalien spielen. Insbesondere haben mehrere Studien eine zentrale Rolle für Schwann-Zellen und Satelliten-Gliazellen (SGCs) im PNS gezeigt. Wie genau Gliazellen den hypererregbaren Zustand in schmerzsignalisierenden Neuronen induzieren ist aktuell noch unklar. Für die Anwendung dieser Erkenntnisse im klinischen Alltag, fehlt es jedoch noch an ausreichendem Grundlagenwissen über die Neuronen-Glia-Signalwege im PNS sowie an Tools für die Entdeckung und Validierung von Targets und Wirkstoffen.

Außerdem werden Schmerzmechanismen in präklinischen Studien an Tieren und beim Menschen nicht immer auf die gleiche Weise gesteuert.

Diese Arbeit veranschaulicht, dass die Erregbarkeit von sensorischen Neuronen durch die Anwesenheit von Gliazellen stark beeinflusst wird. Die Abwesenheit von Gliazellen führt zu einer fast vollständigen Unterdrückung der Aktivität von sensorischen Neuronen, ohne deren Überleben zu beeinträchtigen. Es wurde gezeigt, dass sensorische Neuronen, die von ihren Gliazellen isoliert wurden, immer noch Aktionspotentiale erzeugen können. Allerdings wurde eine erhöhte Stimulation benötigt, was in einer Verzögerung der Entwicklung des Aktionspotentials resultierte.

Sie zeigt auch, dass die meisten Gliazellen in Ganglien Schwann-Zellen sind, was zu der Hypothese führt, dass diese Zellen für die neuronale Erregbarkeit im PNS essentiell sind.

Sie zeigt auch, dass diese Gliazellen nicht in direktem Kontakt mit DRG-Neuronen stehen müssen, um die neuronale Erregbarkeit zu beeinflussen, sondern dass es ausreicht, wenn sie sich im gleichen Kulturmedium befinden. Darüber hinaus wird in dieser Arbeit eine Herabregulierung spezifischer Gene in sensorischen Neuronen, die ohne Gliazellen gezüchtet wurden, festgestellt, was mit der Hochregulierung derselben Gene in etablierten in vivo Schmerzmodellen korreliert.

Diese Befunde unterstützen die Hypothese, dass Gliazellen eine entscheidende Rolle bei der Erregbarkeit von sensorischen Neuronen spielen und bei der Entstehung von Schmerzen, insbesondere neuropathischen Schmerzen involviert sind.

Acknowledgements

These last four years have been the most challenging in my life so far. Nonentheless, I am proud to be able to present this dissertation, which wouldn't have been possible without the help of other people. First of all, thanks to Noémia-Rita Alves Fernandes and Dr. Patrizia Rizzu for their precious help in the generation of the libraries for the single-cell sequencing. Thanks to Dr. Sara Villa Hernandez for her precious help in analysing the sequencing libraries and Prof. Dr. Franziska Denk (Wolfson centre for age-related diseases at King's College London) for providing useful insight into the single-cell sequencing results. A huge thanks to Prof. Dr. Stephen B. McMahon for his supervision and his useful suggestions during the doctoral period. Thanks to my supervisor, Dr. Paolo Cesare, and the PhD students from the Neuro Microphysiological Systems group at the NMI. Thanks to Julian Schwarz for helping with the German translation of the summary. A warm and huge thank you to my parents, who never stopped supporting me despite the distance. Last, but not least: pursuing a PhD is already tough. Doing that in another country, with a completely new culture and language is possibly even harder. For this, I will never be thankful enough to my boyfriend Knut. Not only for your precious help with data analysis and the layout of this dissertation, but for your constant support every single time I came home overwhelmed from the lab and thought about quitting the program.

Abbreviations

ATP	Adenosine Triphosphate
BF	BrightField
BSA	Bovine Serum Albumin
CNS	Central Nervous System
DAPI	4',6-diamidino-2-phenylindole
DIV	Days in vitro
DMEM	Dulbecco's Modified Eagle Medium
DPBS	Dulbecco's Phosphate-Buffered Saline
DRG	Dorsal Root Ganglia
EC	Extracellular solution
ELISA	Enzyme-Linked Immunosorbent Assay
FACS	Fluorescence-Activated Cell Sorting
GFAP	Glial Fibrillary Acidic Protein
HBSS	Hank's Balanced Salt Solution
ICC	Immunocytochemistry
IF	Immunofluorescence
iPSC	induced Pluripotent Stem Cell
LC/MS	Liquid Chromatography/Mass Spectrometry
MACS	Magnetic-Activated Cell Sorting
MEA	Microelectrode Array
NGF	Nerve Growth Factor
PDMS	Polydimethylsiloxane
PNS	Peripheral Nervous System
PEI	Polyethylenimine
ROI	Region Of Interest
RT	room temperature
S.E.M.	Standard Error of the Mean
Simoa®	Single molecule array
TNF-α	Tumor Necrosis Factor alpha
UV	Ultraviolet

Contents

List of Figures

List of Tables

1 Introduction

1.1 State of the art

Neuropathic pain is defined as pain caused by an injury in the nerves that constitute the somatosensory system. Unlike acute pain, the chronic nature of neuropathic pain gives rise to more challenges for its proper medical treatment [1].
It has been assessed that between 3 and 17% of the general population suffers from chronic pain, placing several burdens on both the economic and health systems [2, 3]. However, as there is a lack of globally accepted criteria for defining neuropathic pain in a patient, it is likely that most patients that show chronic pain symptoms are suffering from neuropathic pain [1]. Patients suffering from neuropathic pain report a lower quality of life, characterized by physical and emotional burdens. They tend to develop sleep disorders, anxiety, and even depression. Furthermore, chronic pain is responsible for more than 200 billion € per year of medical costs only in Europe [4].
As the onset of neuropathic pain cannot be defined precisely, current treatments are focused on treating the symptoms of the disease rather than its origin. NSAIDs routinely used in the management of acute pain conditions are ineffective against neuropathic pain; plus, their side effects related to their prolonged use move the bar even more towards not using them for neuropathic pain as well.
As for many other pathological conditions, pharmacological therapies for treating neuropathic pain can be divided into first, second, and third-line interventions (1.1). Other than the mentioned therapies, recent progress in neuropathic pain research identified novel targets for developing novel therapeutics. These targets include blockers of the sodium channel Nav1.7, angiotensin type II antagonists, and even treatments involving the use of stem cells [5, 6, 7, 8].
It is vital to distinguish neuropathic pain from other chronic pain conditions. In fact, in medical conditions associated with chronic pain, it is usually possible to identify the painful stimuli' source and act on it. For example, in the treatment of rheumatoid arthritis, therapies with monoclonal antibodies against the pro-inflammatory cytokine TNF-α have shown positive effects on pain symptoms caused by the pathology [9].
Most of the research on neuropathic pain has been focused on identifying the changes in the nervous system that lead to the development of such conditions, in parallel with novel therapeutics. It is already known that neuropathies affecting peripheral nerves involve altering the electrophysiological properties of such nerves, caused by damages typical of neuropathic pain

Intervention	Drug	Class
First-line	Amitriptyline	Tryclicic Antidepressant
	Duloxetine	Serotonin-noradrenaline uptake inhibitor
	Pregabalin	Antiepileptic
	Gabapentin	Antiepileptic
Second-line	Lidocaine	Sodium channel blocker
	Capsaicin	Topical treatment
	Tramadol	Serotonin-noradrenaline uptake inhibitor
Third-line	Botulinum toxin A	Neurotoxin
	Oxycodone	Opioid
	Morphine	Opioid

Table 1.1: List of drugs currently prescribed for the treatment of neuropathic pain [1]

conditions. This is likely caused by alterations in ion channels' properties found in neural cells [1]. Recent studies have been exploring a novel target in neuropathic pain: glial cells.
Glial cells have often not been considered in pain research, as they are not involved in the electrophysiological transmission of stimuli as in neuronal cells. Recent studies have been focusing more on glial cells and their possible contribution to the development of neuropathic pain states [10, 11, 12, 13]. However, what has not been clarified yet is how glial cells affect the excitability of sensory neurons and how this may contribute to the development and maintenance of neuropathic pain conditions.

1.2 The somatosensory system: from perception to pain

The somatosensory (from Greek soma, "body") system is an essential component of the nervous system. It allows the perception of different external inputs, or signals, necessary for an organism's survival through specialized receptors distributed in the body. These signals are then converted into electrophysiological signals transmitted to the central nervous system for processing [14].

1.2.1 Overview of the somatosensory system

The somatosensory systems' significant functions can be summarized into three categories: proprioception, exteroception, and interoception.
Proprioception (from Latin *proprius*, "one's own") consists in the ability to pure sensing the own body. It is achieved thanks to receptors' presence in muscles, joints, and skins, which allow the individual to be aware of his body's movements [14].
Exteroception groups all the functions that are deputy for the interaction with the external world. It includes sensations like touch, heat, cold, but also pain. It also includes more sophisticated versions of the mentioned senses; for example, the pure touch is contemplated in this category and variations that required some movements, like grabbing an object with the hand or pressing a button [14].
Interoception is similar to exteroception, with the difference that the functions are directed towards the sensing of the internal organs inside the body. Even if these receptors are not actively transmitting the signals perceived to generate a conscious sensation, they are nevertheless responsible for regulating crucial physiological processes. Their essential role makes these receptors accountable for receiving signals in case of malfunction of these organs. The conveying of these signals into painful sensations is crucial for one individual's survival [14].

1.2.2 Structure and function of DRG neurons

The somatosensory systems' three primary functions share one crucial feature: they involve a specific sensory neuron class called DRG (Figure 1.1, C).
DRG neurons are responsible for conveying the information perceived by organ systems that possess somatosensory properties (skin, muscles, joints, viscera). The convey of the information is performed in two steps: first, the neurons need to transform the stimuli into electrical signals. Second, these electrical signals need to be transmitted to the central nervous system for processing [14].
Dorsal root ganglion neurons belong to a family of bipolar cells, classified as pseudo-unipolar cells (Figure 1.1). Their axon possesses two branches: one is projected to the periphery, with its terminals innervating the already mentioned organs like skin and muscles. These terminals express different receptors for the different kinds of stimuli that they can receive.

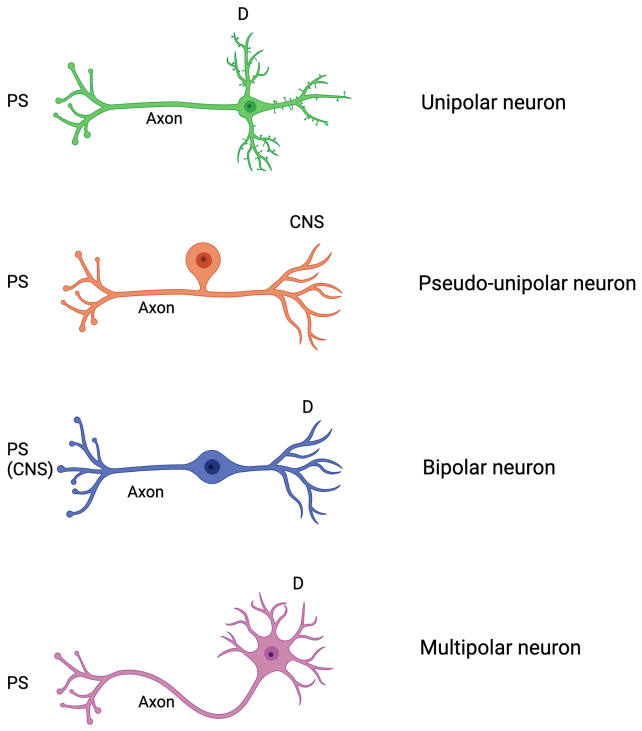

Figure 1.1: Comparison between different types of neurons (created with BioRender.com).

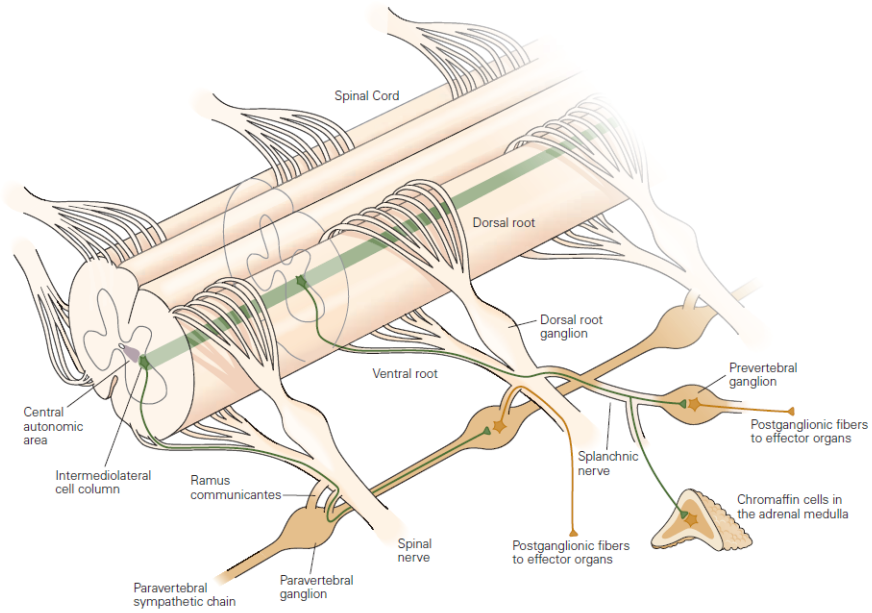

Figure 1.2: The spinal cord's anatomy and its relationship with DRG (modified from [14]).

The second branch is projected to the spinal cord and conveys the signals from the periphery (that have been converted into electrical signals) to the central nervous system (Figure 1.3) [14].

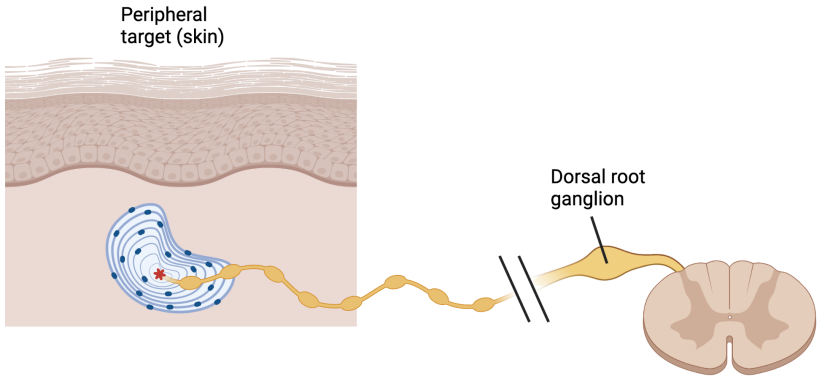

Figure 1.3: Structure of dorsal root ganglion neurons (created with BioRender.com).

Every neuron in a dorsal root ganglion expresses a series of receptors on their peripheral terminations, specific for a particular type of stimulus (described in the previous section).
This peculiar conformation for dorsal root ganglion neurons generates a single line transmission, where the stimuli detected by the peripheral terminals are simply transmitted to the spinal cord [14]. Axons with this characteristic are denominated primary afferent fibers; they are grouped in relation to a particular section of the body that they innervate, generating the peripheral nerves [14].

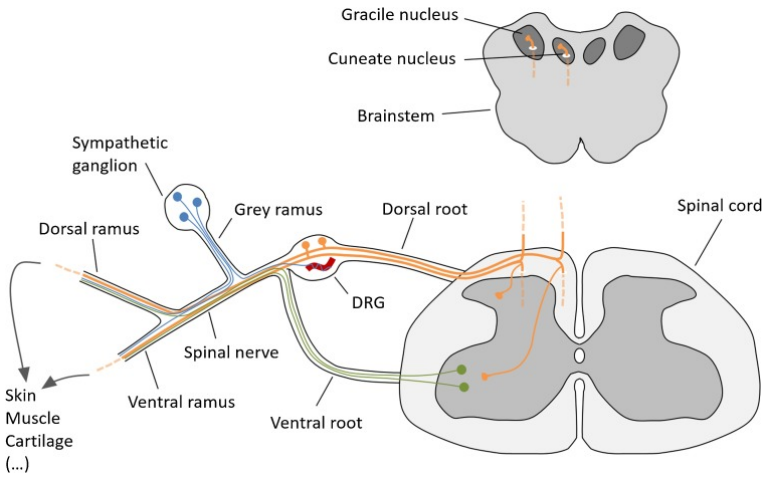

Figure 1.4: Anatomy of a dorsal root ganglion in relation with the spinal cord and the peripheral target [15].

As mentioned above, each dorsal root ganglion contains neurons specializing in the type of stimulus they can detect and convey. They include mechanoreceptors, thermal receptors, nociceptors, and chemoreceptors. Depending on their nature, their axons possess different characteristics. For example, mechanoreceptors have large-diameter, myelinated axons, able to conduct fast action potentials. On the other hand, the remaining types of sensory neurons are characterized by small-diameter and unmyelinated axons, which transmit action potentials slower than their counterparts. The ability to conduct action potential faster or slower in relation to the axon's diameter depends on two factors. First of all, the velocity of action potential's conduction depends on the axon's diameter; this is due to the lower resistance to the flow of current inside the axon. Therefore, larger axons are capable of conducting action potentials faster than smaller axons. Secondly, in larger axons, the nodes of Ranvier are broadly spaced along their lengths; this helps in frequently regenerating the action potential along the axon length [14].

The activation of a specific type of sensory neurons through an appropriate stimulus leads to the membrane's depolarization at the peripheral terminal. Suppose the stimulation can depolarize the membrane sufficiently to reach the threshold for the activation. In that case, an action potential is generated and transmitted along the axon of the sensory neuron [14]. The depolarization of the membrane driven by the transduction into an electrical signal is also called generator potential, and it can be initiated in three different ways [16].
The first mechanism is also the most straightforward. It engages the opening of an ion channel, which permeability characteristics allow a change in the cell's equilibrium potential towards the threshold necessary for generating the action potential [16]. The non-selective ligand-activated ion channel TRPV1 represents an example.
The second mechanism requires closing an ion channel typically responsible for a hyperpolarizing current [16]. For these mechanisms, the only channels that possess such characteristics are K+ channels.
The third mechanism implicates the combination of two conditions: a first ion channel that can switch the membrane potential towards depolarization, and a second ion channel, typically voltage-gated, able to furtherly depolarize the membrane until the threshold necessary for the generation of an action potential is reached.

1.2.3 Overview of ion channels

Ion channels in neuronal cells consist of membrane proteins characterized by specific properties. First of all, the flow of ions through these channels is passive, meanings that it does not require any consumption of energy. Secondly, these ions' flow is determined and driven by electrical properties in terms of membrane potential and ion charge. In some cases, these ions' flow can be blocked, unintentionally or voluntarily [17]. For example, voltage-gated sodium channels can be blocked by tetrodotoxin (TTX), a lethal molecule found in pufferfish that can be swallowed unintentionally when pufferfish is not correctly prepared. On the other hand, the same ion channels can be blocked by lidocaine, a local anesthetic routinely used in dentistry and small interventions.
Ion channels can be classified into two main classes, depending on how the ion flow is regulated. In non-gated channels, the channel itself is in its open state most of the time, although they technically possess a closed state as well. For this property, they are also known as leak channels. Ion channels belonging to this family are responsible for maintaining the membrane resting potential [17]. On the other side, gated channels are made of allosteric proteins, thus existing in

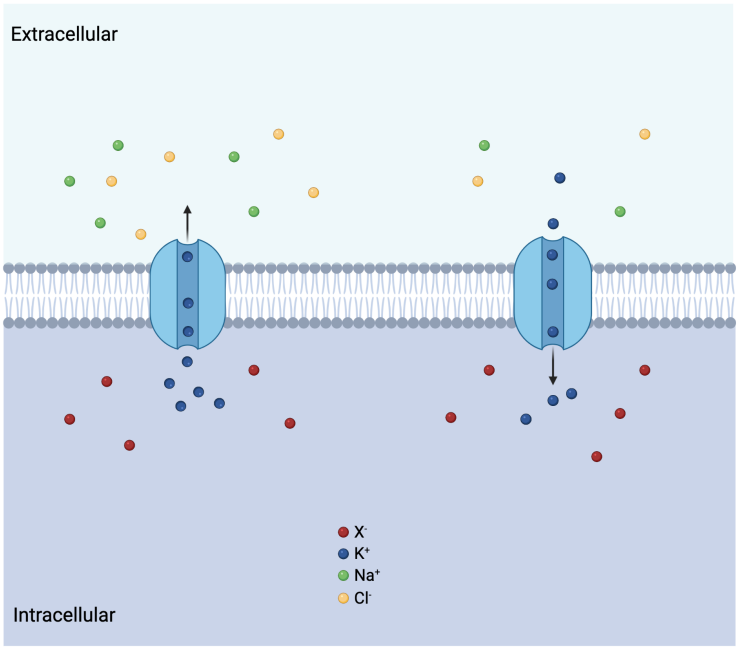

Figure 1.5: Example of a potassium non-gated ion channel (created with BioRender.com).

more than one conformation (usually open and closed). Typically, these channels are in their closed state and can open in response to stimulation [17]. Gated channels can be open by two different conditions: a change in the membrane potential (voltage-gated) or a molecule's binding (ligand-gated).

Voltage-gated ion channels exist in three different conformations: resting, active, and refractory. In the resting state, the channel is closed, but it can be activated by a change in the membrane potential (Figure 1.6, C). In the active state, the channel is open and allowing ions to flow (Figure 1.6, D). In the refractory state, the channel is inactivated, meaning that even though the activation gate is open, a second gate called the inactivation gate is responsible for blocking the access to the channel, thus preventing the ions flow (Figure 1.6, E). It is vital to notice that, to go back into their active state, it is first necessary to de-activate the ion channel by opening the inactivation gate and closing the activation gate, bringing the channel back into the resting state [17].

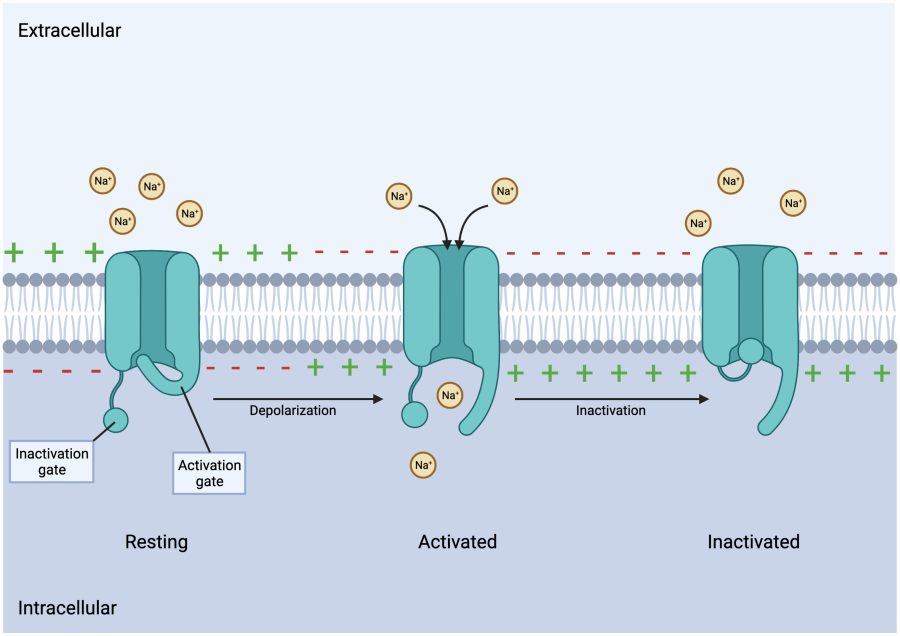

Figure 1.6: The three states of the voltage-gated channels, here in an example represented by a sodium channel (created with BioRender.com).

The voltage-gated sodium channel family represents the most known voltage-gated ion channel. This ion channel is constituted by a single polypeptide chain organized in four domains. Each of these domains possesses six hydrophobic alpha-helix regions that cross the neuron's cell membrane (Figure 1.7, A). These four domains constitute together the porous channel across the membrane that allows the ions to flow. The opening and closing of the channels are regulated by a conformational change in one of the four domains' alpha-helix regions (Figure 1.7, B). Calcium channels represent another family of voltage-gated ion channels. The molecular structure of these channels is similar to that of sodium channels (see Figure 1.7). The flow of calcium ions inside neuronal cells results in neurotransmitters' release from the presynaptic nerve terminals [17].

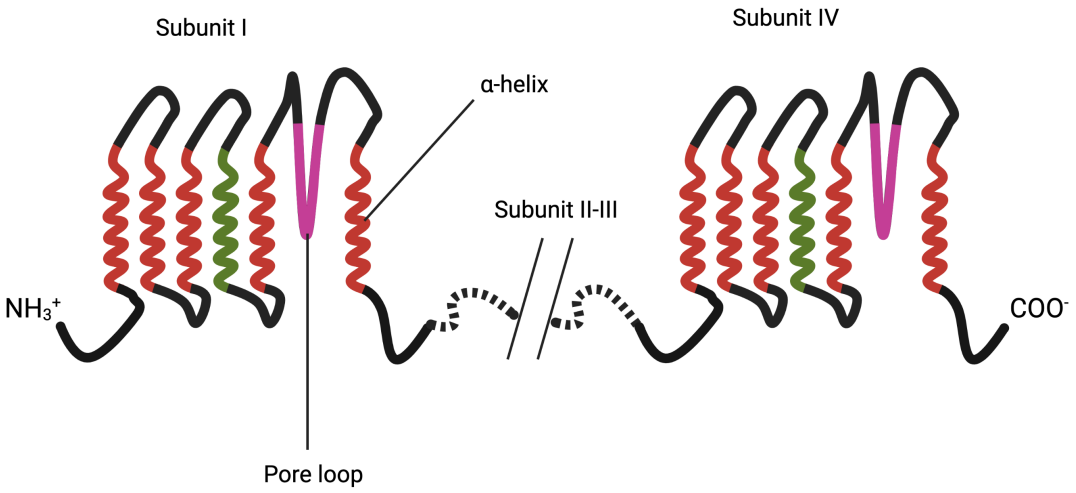

Figure 1.7: Structure of voltage-gated sodium channels (created with BioRender.com).

Potassium channels represent the third family of voltage-gated ion channels. Also, their structure is similar to that found in the sodium channel, with one significant difference: instead of being constituted by a long polypeptide chain that suddenly organizes into four domains, the four domains are formed by four separated chains, called subunits [17]. These subunits are also organized in six alpha-helix transmembrane domains, with a segment acting as an activation gate for the ion channel [17].

Differently from the voltage-gated, ligand-gated ion channels are activated by binding a molecule, such as neurotransmitters or hormones. One of these molecules' binding induces a conformational change in the ion channel structure that turns into its opening, allowing the ions to flow [17].

Ligand-gated ion channels are divided into two categories: directly and indirectly gated channels. The channels belonging to the first category are also known as ionotropic receptors. Here, the molecule binding site is part of the channel itself, and the consequent electrical response is fast, lasting few milliseconds (Figure 1.8, top) [17].

In indirectly gated channels, the binding site for the transmitter is separated from the ion channel itself. These channels are also known as metabotropic receptors, and they are usually associated with G-proteins that activate an intracellular signal transduction cascade that turns into either direct activation of the same channel or in the modulation of a protein kinase that lately activates the channel through phosphorylation (Figure 1.8, bottom) [17].

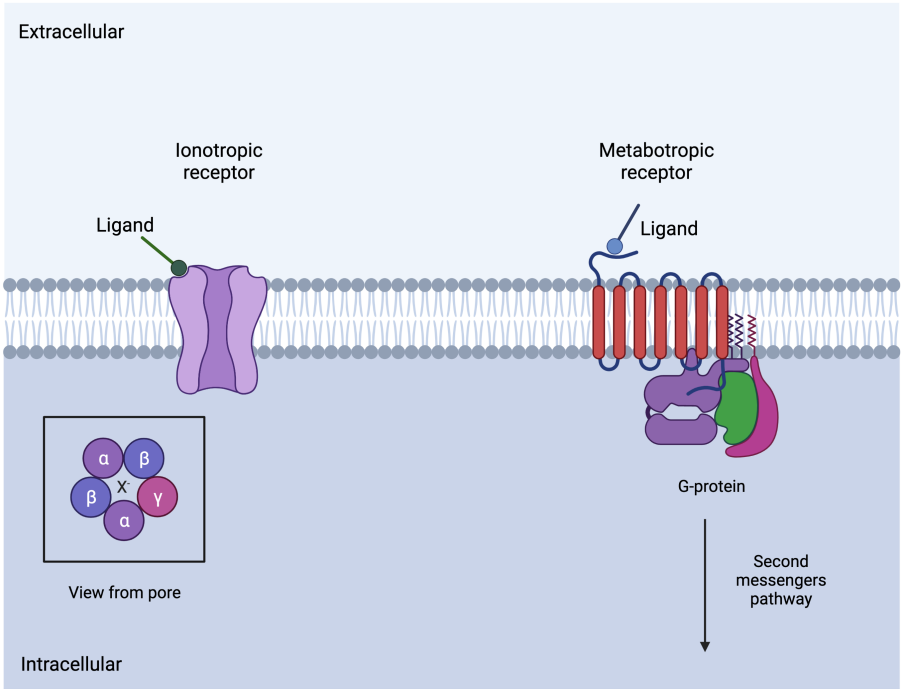

Figure 1.8: Differences between ionotropic (top) and metabotropic (bottom) ligand-gated ion channels (created with BioRender.com).

1.2.4 Nociception and pain

The perception of pain is associated with actual or potential damage in the tissues of an individual [14]. Even though pain's perception provides unpleasant sensations, it plays a vital role in preserving an organism with its protective function [14]. For example, the pain signals released by a sprained ankle will prevent us from walking over our injured limb, thus helping our healing and recovery process.

One of the most exciting pain features is that the same noxious stimulus can elicit different responses between different individuals: what is considered painful from one specific individual may be tolerable by another. At the same time, what is not regarded as painful may elicit an over-reaction to pain in some individuals. This is explained by the fact that the mechanisms that constitute the overall perception of pain are not limited to the pure noxious stimulus at the peripheral level and to a series of mechanisms that involve the central nervous system as well [14].

Pain can be classified as acute, persistent, or chronic, depending on its duration. Acute pain can be localized to a specific part of the body, and usually, it can resolve with small interventions from the patient. For example, a headache caused by a lack of sleep at night can generally be resolved by taking a simple over-the-counter painkiller. Persistent pain is the reason why individuals look for medical assistance. Thinking about the example of the sprained ankle above: if the pain does not resolve within few days, there may be some damages in the joint structure, and a visit to an orthopedic may be useful to find the physiological cause of the pain. At the same time, a headache that turns into a migraine could benefit from a specialized consultation. Differently from persistent pain, which has a medical purpose by "telling" the individuals that there is something off in the body (a broken ligament in the ankle), chronic pain has no medical purpose other than creating a constant and unpleasant sensation that affects the individual's existence negatively [14].

The somatosensory system deputy components for pain perception are called nociceptors (from Latin *nocere*, "to injure"). They respond to noxious stimuli, defined as stimuli that reduce any tissue damage [18].

There are different ways in which nociceptors have been classified over the years, and even nowadays, there is still some confusion regarding their classification. One of the classification systems used is based on the noxious stimulus characteristics that activate them: thermal, mechanical, polymodal, and silent.

Thermal nociceptors respond to extreme temperatures, usually higher than 45°C or lower than 5°C. They have a small diameter, myelinated Aδ axons, thus able to conduct action potential fast.

Too intense pressure stimuli activate mechanical nociceptors. As in the case of thermal nociceptors, the axons of mechanical nociceptors are also of the Aδ family, able to conduct action potential fast.

As stated in their name, polymodal nociceptors can be activated by different stimuli classified as high-intensity chemical, mechanical or thermal. Differently from the two previous classes, their axons are unmyelinated C fibers, and therefore their conduction speed is slower. They are mainly responsible for the secondary, persistent pain that follows a first acute and sharper pain. For example, suppose we burn our finger by accidentally touching a pot full of boiling water. In that case, we immediately feel a painful sensation transmitted by the Aδ of thermal nociceptors (first pain). Subsequently, a sense of persistent and pulsing pain arises, with lower intensity than the first pain caused by touching the pot (second pain) (Figure 1.9) [14].

The three classes of nociceptors just described are distributed evenly in both skin and deep

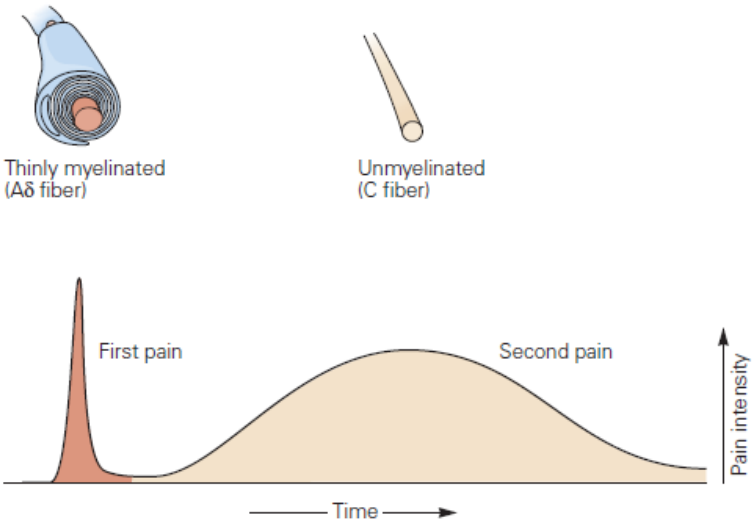

Figure 1.9: Characteristics of first and second pain in relation to the type of axons involved, pain intensity and duration (modified from [14])

tissues, and they are often co-activated, as shown in the example of the hot pot.

The fourth category, corresponding to silent nociceptors, is found exclusively in the viscera. Unlike the other three types, these receptors are not activated by noxious stimuli but from inflammatory conditions and different chemical agents capable of reducing the threshold necessary for their activation and firing of action potentials [14].

The mechanisms with which nociception is achieved are relatively straightforward: the nerve endings of afferent axons of DRG are depolarized by noxious stimuli previously described. This leads to the generation of action potentials transmitted to the spinal cord by these neurons' central branches. To achieve this, it is necessary to convert the signal generated by the noxious stimuli into an action potential. This involves specific receptors in the neurons' nerve ending's cellular membrane represented by ion channels [14].

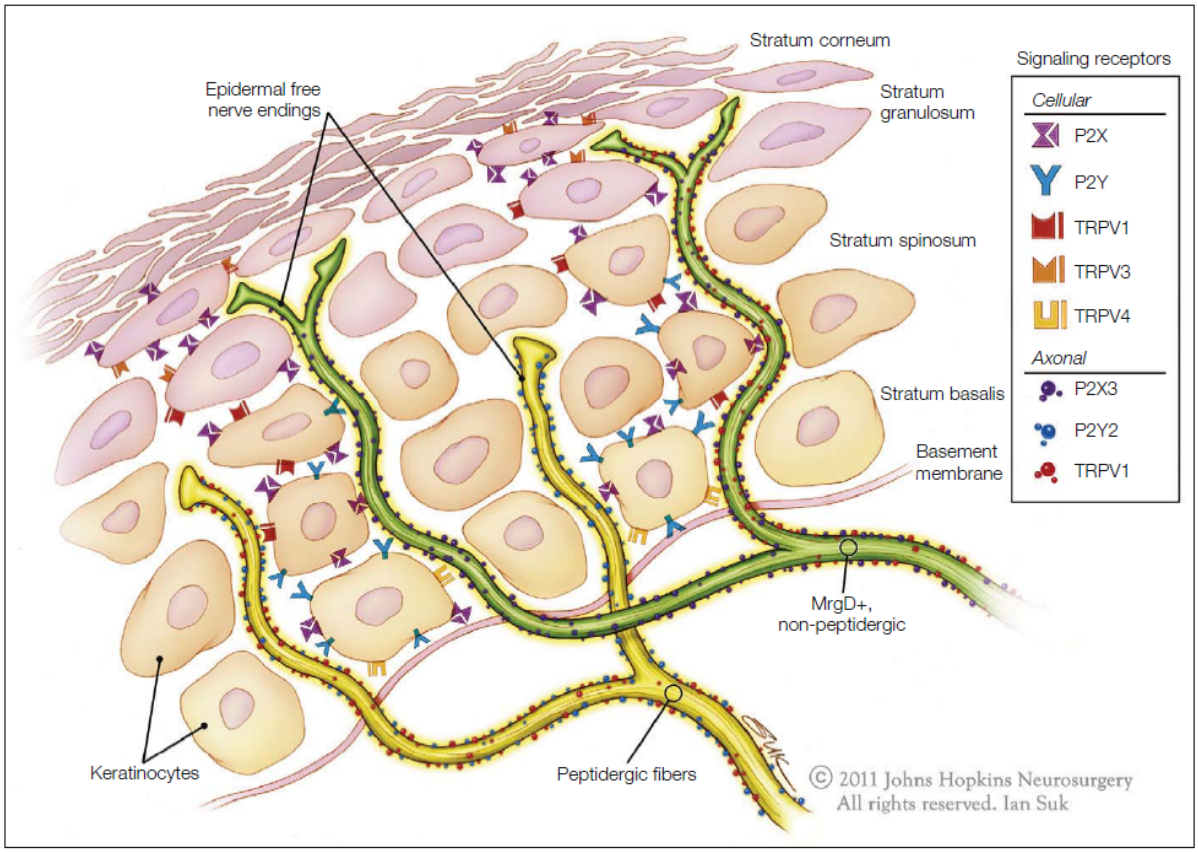

Figure 1.10: Representation of unmyelinated C-fibers nerve endings in the epidermis and expressed signalling receptors [16]

One of these receptors' largest families is represented by the transient receptor potential ion channels (TRP). Among these receptors, the TRPV1 is probably the most known; the V stands for "vanilloid," as this ligand-gated ion channel is activated by molecules that belong to the vanilloid family. Nociceptors express this channel, and one of its activators is capsaicin, the main component of hot peppers that gives them their characteristic pungent taste. As thermal stimuli also activate TRPV1, this channel is ordinarily responsible for transducing the signals from painful heat stimulation [14]. Studies have shown that inflammatory processes induce an increase in the mRNA of TRPV1, resulting in an increased sensitization of nociceptors expressing the receptor [19].
Other members of the TRP ion channels family that are found in nociceptors include TRPV2, activated by too high temperatures (although some studies could not confirm this [16]), and TRPM8, which is activated by low temperatures and molecules such as menthol, which explains the cooling sensation evoked by it (Figure 1.11).

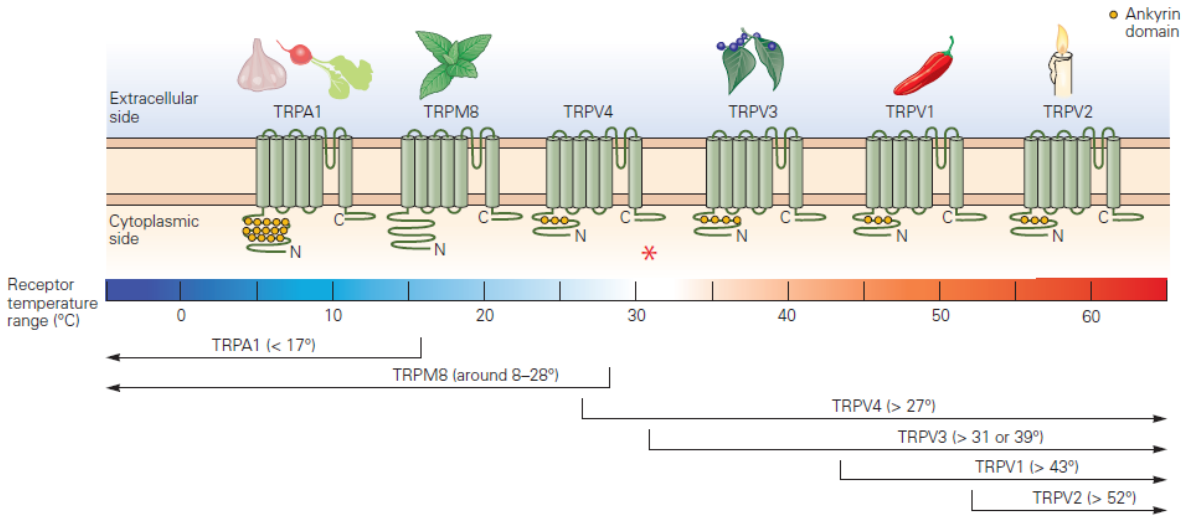

Figure 1.11: Overview of the TRP receptors found in the cellular membrane of DRGs and their corresponding sensitivity to different temperatures. Some of their activating agonists are also displayed (modified from [14]).

However, TRP ion channels are not the only family found on the nerve endings of nociceptors. Another important family of ion channels is represented by sodium channels, of which the Nav1.7 plays a key role. Differently from the previously described TRP channels, Nav1.7 is a voltage-gated ion channel, activated by a change in the membrane voltage. Studies have shown that a family of mutations in this channel leads to its inactivation, and therefore insensitivity to pain. Even though the possibility of not feeling any pain may be appealing, it still has an essential role in defining the presence of damage.

The inability to sense any of these damages could lead to permanent damages. On the other hand, mutations that modify this channel's activation kinetics develop in conditions characterized by persistent pain in a different part of the body [14].
Nociceptors also express the ionotropic purinergic receptor PTX3, which ATP activates following tissue damage [14].
Finally, they also express Mas-related G protein-coupled receptor (Mrg); these receptors are activated by peptide ligands, with the scope of sensitizing the nociceptors to other chemicals [14]. The bradykinin receptor represents an example: the signal transduction that follows the binding of bradykinin to its receptor leads to the sensitization and subsequent opening of the TRPV1 receptor as well, followed by Ca2+ influx (Figure 1.12).

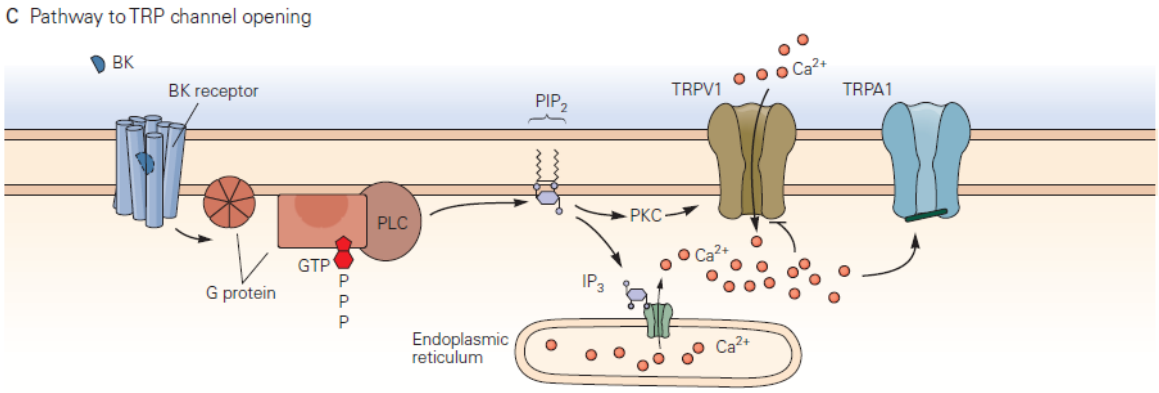

Figure 1.12: Mechanism of action of bradykinin (modified from [14])

So far it has been clarified the physiological role and function of nociceptors. However, several pathological conditions are associated with the uncontrolled activation of this class of neurons [14]. For example, allodynia is characterized by pain evoked by stimuli that are usually considered hurtles. However, individuals suffering from allodynia do not feel any pain if there is no stimulation. Sore muscles give an example after an intense workout: we may feel pain in our legs if we walk or climb the stairs, but as soon as we lay down again in bed or sit, the pain is not perceived anymore.
In contrast to allodynia, hyperalgesia is characterized by a highly intensive response to noxious stimuli; individuals affected by such a condition feel pain even without such stimulation [14]. In this condition, a cocktail of chemicals released by nearby damaged cells contributes to its onset. This cocktail includes the already mentioned bradykinin and ATP and NGF, substance P, histamine, acetylcholine, prostaglandins, and serotonin [16]. Even though different cell types typically release these molecules, together are capable of lowering the threshold necessary for the activation of nociceptors.

Other than a consequence of a lowered threshold, hyperalgesia can be a consequence of different mechanisms. For example, inflammation in a specific area can increase the response due to a stimulus that overcomes the activation threshold [16].
A third mechanism is the consequence of the expansion of the receptive field of nociceptors following tissue injury. This expansion leads to the activation of many fibers in the injured tissue, even though the stimulus applied is of the same entity [16]. In particular, NGF is shown to be active in inflammatory pain states. For these reasons, recent studies have been focusing on studying this neurotrophin as a target for possible pain therapies [20, 21, 22, 23]. These studies lead to the discovery of tanezumab, the first monoclonal antibody for treating pain [24], currently under clinical trials.
This type of persistent pain can, in turn, be classified into two types: nociceptive and neuropathic pain. The nociceptors cause nociceptive pain in the skin that activates in response to injury and is usually characterized by a local inflammatory state. For example, a sprained ankle produces a mild form of nociceptive pain, while tumors and arthritis generate a more severe form. Neuropathic pain is caused by an injury that occurred directly on nerves in the nervous system (central or peripheral); because of the particular body region it affects, this condition is characterized by a sensation of burning in the nerves.

1.2.5 Pain mediators

Until now, the role of nociceptors in the development of painful conditions should be clear. What has not been explained and clarified yet is the types and nature of the chemical mediators involved in painful sensations.
These mediators belong to different classes and can be released in different conditions and by other cell types [16].
For example, bradykinin has been found in injured tissues and the exudates typical of inflammatory processes. It has been found that it also acts on peripheral nerve terminals by sensitizing them to typically normal entity stimuli [25]. This sensitization occurs by activation of the bradykinin receptors, which subsequently start a cascade that involves the activation of phospholipase C and protein kinase C, ending with the modulation of TRPV1 [16, 26].
ATP has also been found at higher levels in inflamed tissues, and therefore its role in nociception has been proposed and investigated. Studies on human models showed that the development of pain induced by the presence of ATP depends on the presence of capsaicin-sensitive neurons [27].
It is well known that cytokines constitute essential mediators in inflammatory processes; therefore, it is reasonable to speculate a possible role in nociception, as pain is one of the marks of ongoing inflammation. For example, TNF-α is typically found at the level of joints in patients with rheumatoid arthritis, and therapies involving the use of monoclonal antibodies against these cytokines have been proved effective and routinely administered for the treatment of this pathology

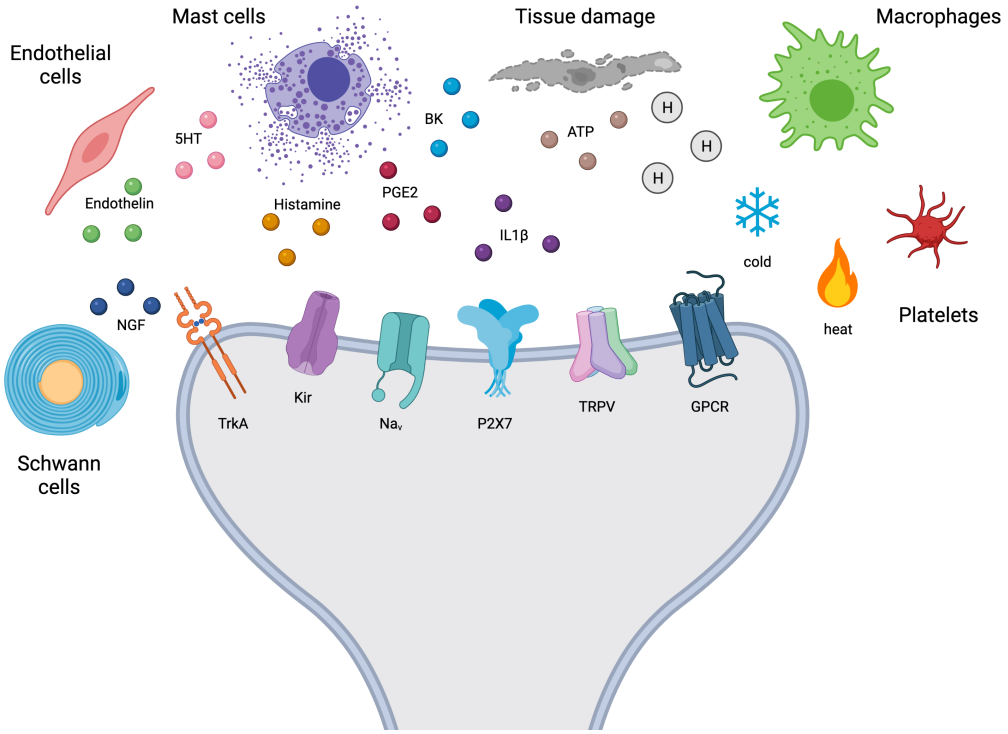

Figure 1.13: Overview of chemical mediators involved in pain mechanisms (created with BioRender.com).

[9]. On the other hand, IL-6 has been demonstrated to sensitize nociceptors when applied together with its soluble receptor [28].
The effect of cytokines on nociceptor excitability occurs through different mechanisms. They can directly modify the properties of ion channels or indirectly by inducing the release of other inflammatory mediators, like prostaglandins, neurotrophins, and the already mentioned ATP. They can also sensitize sensory neurons in the long term by influencing gene transcription [16].
Neurotrophins represent another category of pain mediators that has gained particular attention in recent years. In particular, NGF has been found released by different types of glial cells following stimulation from pro-inflammatory cytokines [16]. It has been found that NGF is also capable of sensitizing nociceptors by modulating the activity of different ion channels [16]. For its properties, research has recently been focusing on targeting NGF in the development of novel pain therapeutics [20, 24].

1.3 Glial cells in the peripheral nervous system

Glial cells play an essential role, both in the central and peripheral nervous systems. Although they are not excitable (thus unable to generate or propagate action potentials), they are responsible for supporting neurons and maintaining their vital functions. For these reasons, glial cells are present in higher numbers compared to neurons [17].
Glial cells have been widely studied in the central nervous system; however, their counterparts in the peripheral nervous system have sparked interest among researchers only recently. Even though it may come naturally to think that one specific glial cell has the same functions whenever considering the "central" or the "peripheral" version, some of the peripheral counterparts possess some unique features absent in their central partners. There are two major types of glial cells in the peripheral nervous system: Schwann cells, whose counterpart in the central nervous system is represented by oligodendrocytes, and satellite glial cells, less known, whose counterpart is believed to be astrocytes.

1.3.1 Schwann cells

Just like their counterpart in the central nervous system, Schwann cells are mainly responsible for wrapping the neuron's axon with a myelin sheath.

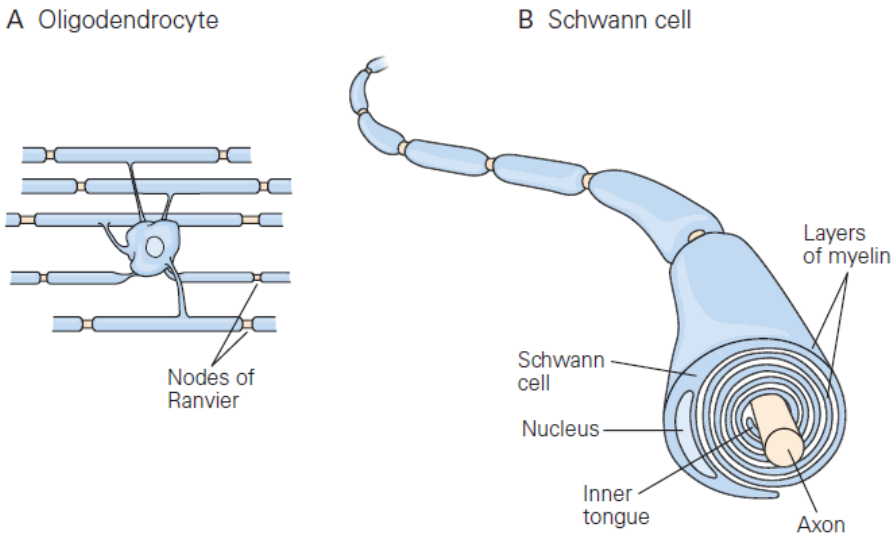

Figure 1.14: Difference between oligodendrocytes in the CND (A) and Schwann cells in the PNS (B) (modified from [14]).

However, Schwann cells are involved in other crucial functions. First of all, they support neurons by keeping them in the right position and protecting them from physical damage. They also support neurons by providing nutrients and oxygen, as the neurons' primary function is to convey information rather than find their way to survive. Furthermore, Schwann cells can help in the

case of minor nerve damages.
Another critical feature of Schwann cells is provided by evidence of expression of several ion channels, including the ligand-gated ion channel P2X, regulated by ATP [29]. These features suggest a possible active role of Schwann cells in regulating the electrical activity of nearby neurons.
From a developmental point of view, Schwann cells are derived from the neural crest. During embryonic development, the so-called Schwann cell precursors migrate and localize along the axons of the neurons. These cells cannot still survive without axons but could potentially become Schwann cells in the future [30]. For this reason, it has been proposed the role of Schwann cells in guiding the axons in positioning themselves in the right positions and towards their targets [31]. These cells also express markers that are routinely used for ICC, like p75 (receptor for NGF), L1, and N-CAM (molecules necessary for cell adhesion [32]. However, they still lack the widely used marker S100, as its expression starts later with development [33].

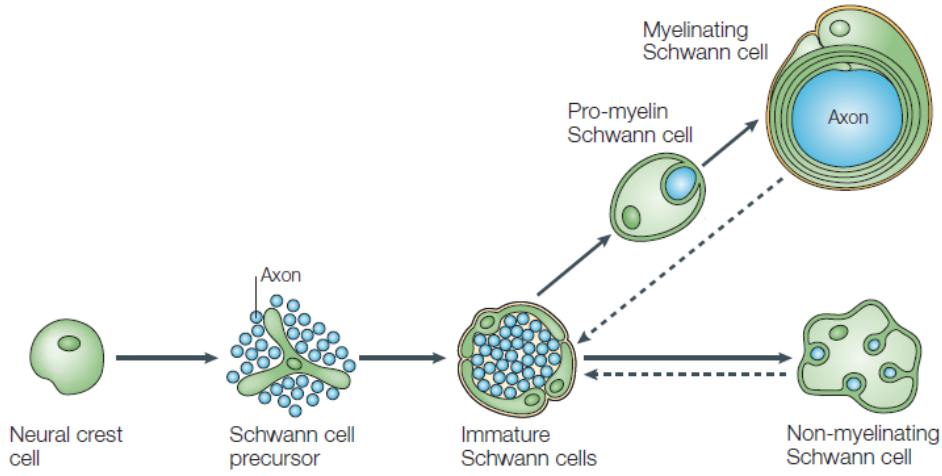

Figure 1.15: Development of Schwann cells (modified from [30]).

As the proceeding of development, Schwann cells enter the so-called "immature Schwann cells" state, where they start forming a basal lamina and become able to survive without the presence and assistance of neuronal axons (Figure 1.15) [30].
At this point, Schwann cells come in front of a differentiation crossroad: those that are associated with large diameter axons will differentiate into myelinating Schwann cells. They will end up wrapping the axons with the myelin sheath [32].
Those Schwann cells that are still associated with small diameter axons will differentiate into non-myelinating Schwann cells. One could imagine that these cells will thoroughly degenerate and die; however, they will give origin to the so-called Remak's bundle [34].

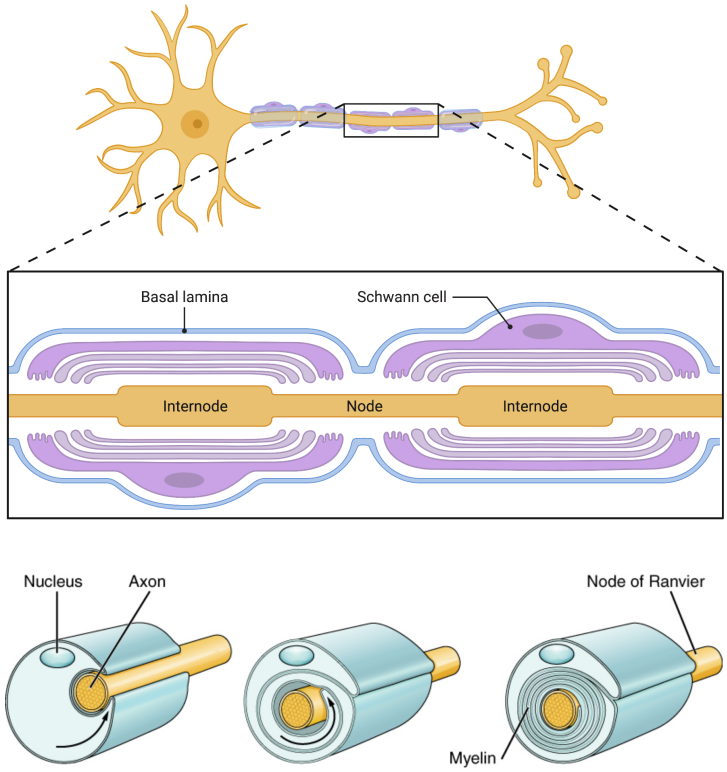

Figure 1.16: Schwann cells myelinating peripheral nerves (created with BioRender.com; created by CFCF, distributed under a CC-BY-SA 3.0 license.).

Different from myelinating Schwann cells, where one specific Schwann cell wraps around only one axon, one Remak's bundle embeds several small-diameter axons at the same time. For this feature, Remak's bundle may play a role in maintaining small axons' structure in the peripheral nervous system [34].

1.3.2 Satellite Glial Cells

Satellite Glial Cells (SGCs) possess a unique morphological characteristic: they wrap around the cell body of sensory neurons in the peripheral nervous system, leaving a gap of 20 nm, which resembles that found in the synaptic cleft. For this reason, interactions between neurons and SGCs raised interest in peripheral glial cell research [35, 36].

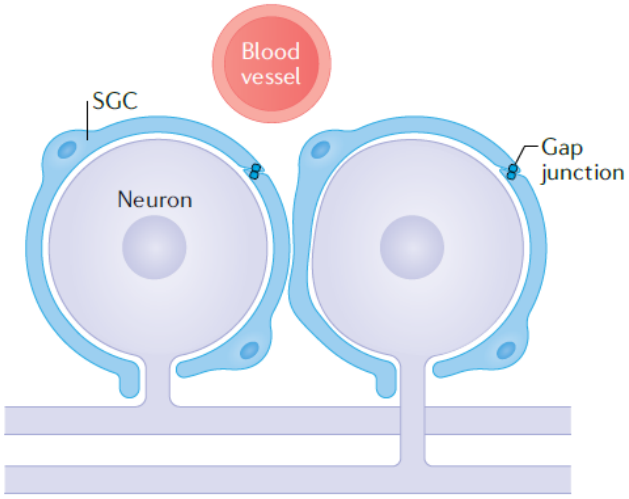

Figure 1.17: Structure of SGCs in relation to DRG neurons (modified from [11]).

As for Schwann cells, SGCs have their counterpart in the central nervous system; in this case, it is represented by astrocytes. For this reason, research on these peculiar cells has been conducted basing on the characteristics of astrocytes. However, there are two main differences between astrocytes and SGCs when we compare their interaction with neurons. Astrocytes do not overlap in the central nervous system, and one single astrocyte can contact several neurons simultaneously; on the other hand, SGCs can overlap on top of each other they wrap around the cell body. For this reason, one SGCs can generate contact with only one neuron at a time [11]. These features allow SGCs to regulate the neuronal cell body's homeostasis, as Schwann cells can support neurons at the axonal level. It has also been proposed that SGCs possess plasticity properties, thus being able to generate new Schwann cells and even neurons following peripheral nerve damage [37, 38].

Like Schwann cells, SGCs originally developed from the neural crest; however, their exact nature has not yet been deeply studied. It has been found that SGCs express sox2, a typical stem cell marker; this supports the plasticity hypothesis of SGCs [38]. Furthermore, high levels of the transcription factor sox10, which has a vital role in cell differentiation, have been found in SGCs that later developed into oligodendrocytes-like cells [39]. Despite the same origin, SGCs have not been characterized as Schwann cells. However, it is reasonable to think that they may have similar developmental stages. It has been encountered that mutations in the already mentioned sox10 expression in Schwann cells and SGCs turn into an interruption in the developmental process in both cell types [39, 40]. Furthermore, SGCs cultured in the absence of neurons show the typical double spindled morphology of Schwann cells; this feature is furtherly confirmed by the expression of markers encountered in Schwann cells, such as GFAP and S100 [41]. Together with the already mentioned plasticity, these findings support the idea that SCGs represent a source of multipotent cells that can develop into neuronal or glial cells following nerve injury in the peripheral nervous system [38].

Provided the significant role of SGCs in maintaining neuronal functionality in healthy conditions, it is reasonable to speculate a possible role in diseases, including pain states. It has been found that SGCs express different receptors, including the ATP receptor P2X. Given the critical role of ATP in pain models, the fact that SGCs express ATP receptor suggests their possible contribution to pain states [11]. Furthermore, it has been shown that SGCs releases molecules that have been associated with pain states, including the already mentioned ATP, but also TNF and IL-1β [42]. For this reason, studies on pain models that initially focused exclusively on studying the neuronal behavior and possible neuronal targets for pain management started focusing more on SGCs and their role in neuronal excitability. SGCs have been studied as a potential target for novel pain therapeutics rather than neurons [12, 43], thanks also to the findings that their astroglial counterpart in the CNS has been demonstrated crucial for hyperalgesia [42, 44, 45].
First studies conducted on SGCs to exploit their possible contribution to pain states have found that SGCs express higher levels of GFAP following inflammation or nerve damage, as it can be found in astrocytes during inflammatory conditions [11].
Despite the absence of voltage-gated ion channels for Na+ and Ca2+ (which turns into the inability to generate action potentials), SGCs express K+ channels. It has been shown that some of these K+ channels' standard functionality is reduced or even suppressed after an injury; this leads to a higher release of ATP from SGCs, which increases the excitability of the associated neurons [11]. These findings correlate with what has been found in astrocytes in the CNS, where loss or gain of function mutations in K+ channels affects neurons' excitability [11].
Gap junctions between SGCs and the neuronal body have been studied as well, and it has been found that there is an increase in the coupling between neurons and SGCs during pain state models [11]. Because of these findings, it has been suggested that these gap junctions also play an active role in the development of pain states. For this reason, recent pain models have been

focusing on the development of pain therapeutics directed towards blocking these gap junctions [10, 46, 47].

2 | Materials and Methods

2.1 Preparation of MEAs and glass coverslips for cells seeding

The day before the planned seeding of the cells, coating of the substrate for the seeding was performed. The protocol for the coating changes slightly according to the seeding substrate chosen.

2.1.1 Preparation of PDMS

PDMS was used to produce inserts and microfluidics chips (MFC) necessary for plating the cells. PDMS is prepared by weighting Silicone elastomer and curing agent in a 10:1 ratio and mixing them at 2000 rpm for 5 minutes (SpeedMixer DAC 150.1 FVZ-K, FlackTec Inc., USA). The mixed solution was poured inside a clean 150mm Petri dish until the weight of 59g was reached and let partially polymerize over-night on a flat surface. After the first baking for 12 hours at 40°C, the PDMS mold was carefully cut out from the Petri dish and baked a second time for 13 hours at 100°C. Microfluidics chips were prepared via soft lithography (Figure 2.1). A master was fabricated by negative photolithography [48], cleaned with propan-2-ol, and placed inside the Petri dish before pouring the PDMS solution. After the first baking, the master was removed from the PDMS mold so that the second baking would not damage it.

2.1.2 Preparation and cleaning of PDMS inserts and MFC

To guarantee the seeding of the cells on top of the electrodes, special inserts made of PDMS were used. PDMS inserts were prepared by punching PDMS with a 3-mm biopsy puncher; MFCs were prepared by cutting out the desired number of MFC from the PDMS mold and punching the cells reservoir with a 2-mm biopsy puncher. PDMS inserts and MFC were rinsed with running water and Milliq water and then cleaned with cold propan-2-ol in an ultrasonic bath for 5 minutes. Cleaned inserts were rinsed from the alcohol with Milliq water and let dry in a sterile hood.

2.1.3 Preparation of MEA

MEAs were cleaned for 2 hours with 10% tergazyme solution, then over-night with Milliq water. After air-drying under the hood, MEAs were plasma-cleaned for 2 minutes and coated with 0.075% PEI solution for 1 hour. MEAs were then rinsed 4x with Milliq sterile water and let dry in a sterile hood. Each MEAs was placed in a 100mm Petri dish.

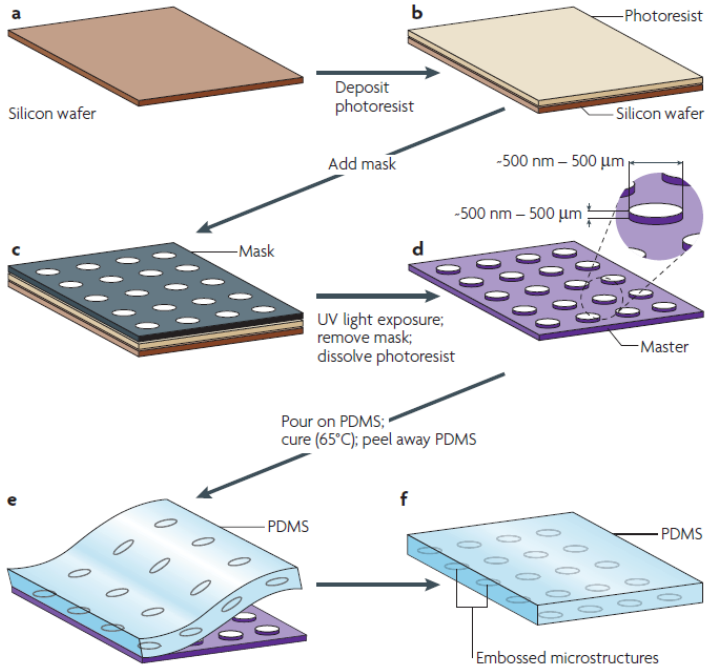

Figure 2.1: Production of the master and generation of PDMS mold for microfluidics via soft-lithography (modified from [48]).

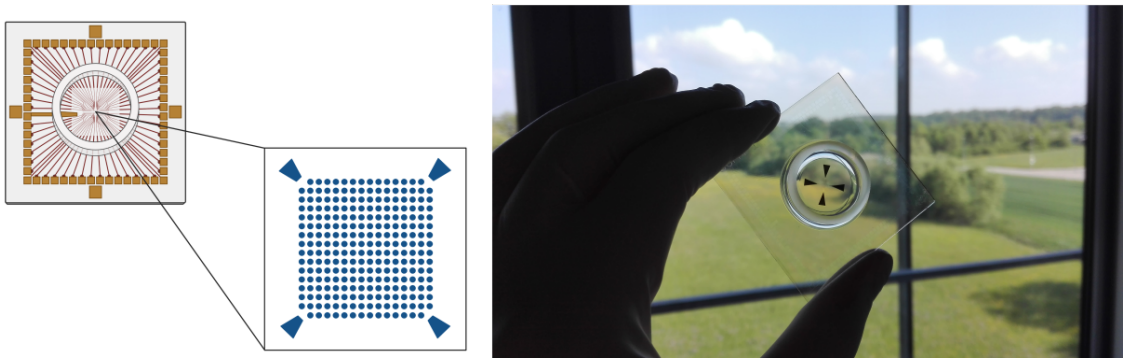

Figure 2.2: Left: schematic representation of an open-electrodes MEA with 252 electrodes (created with BioRender.com). Right: MEA with 252 electrodes used in Neuro-Microphysiological Systems laboratory.

PDMS inserts were sterilized with UV-light for 3 minutes. Under a microscope placed inside a sterile hood, inserts were attached on top of the electrodes for each MEA with a pair of sterile forceps. Inserts were filled with 20mg/ml laminin solution, and the MEAs were kept in the fridge o/n, sealed with parafilm and with a water reservoir, to prevent laminin evaporation.

2.1.4 Preparation of MFC-MEA

MEAs for MFC chips and PDMS MFC were cleaned as already described above. MEAs were plasma-cleaned for 5 minutes, and MFCs were UV-sterilized for 3 minutes and aligned on top of the MEA with a Fineplacer® lambda (Finetech GmbH, Germany) (Figure 2.4).

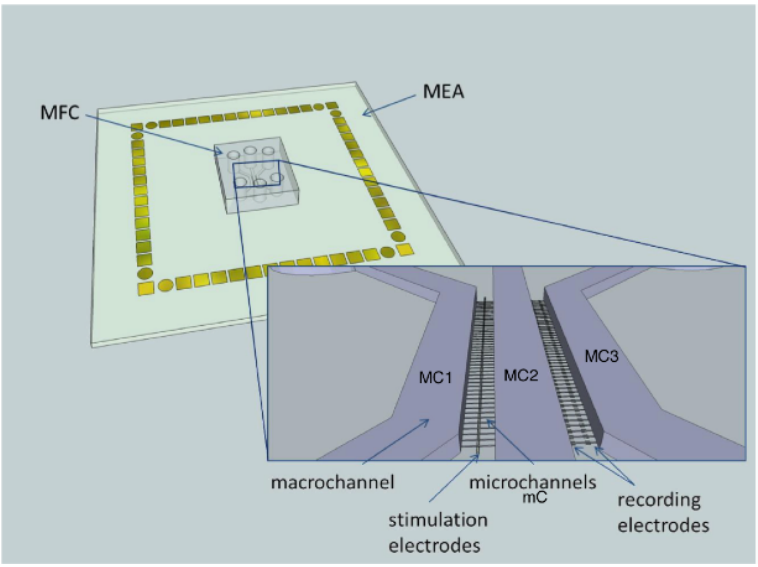

Figure 2.3: Representation of a PDMS-MF chip (modified from [49]).

MFC-MEA were plasma-cleaned one more time for 2 minutes. MFC-MEAs were coated with PEI solution for 1 hour by filling the three macrochannels under a microscope in sterility conditions. PEI was removed, and MFC-MEAs were washed with sterile Milliq water as following:

1. Removal of half PEI solution from each channel and replacement with water, twice; in this way, PEI is wholly removed from the macrochannels;

2. Removal of half PEI solution from the two external macrochannels; in this way, the pressure applied from the central macrochannel still filled with water pushes the PEI solution in the microchannels towards the external macrochannels;

3. Removal of half water/PEI solution from each channel and replacement with water, twice; in this way, the PEI once contained in the microchannels and now in the macrochannels is wholly removed, and the MFC-MEA are cleaned from PEI solution.

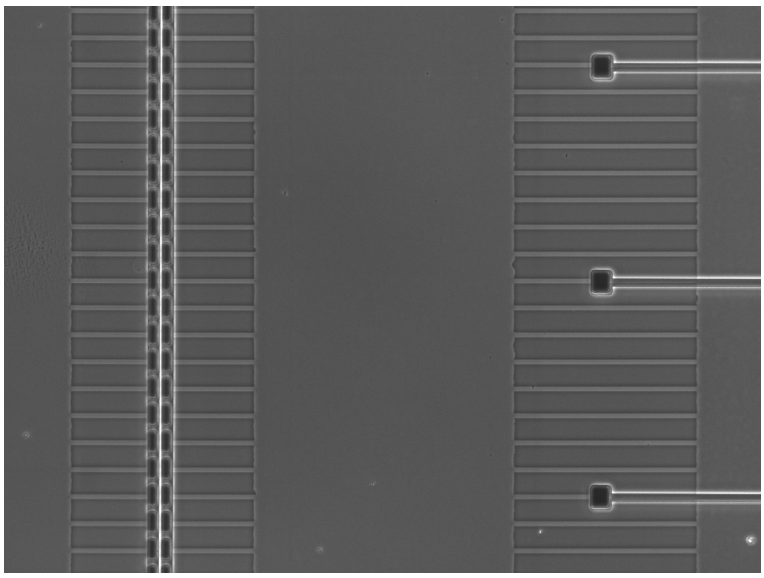

Figure 2.4: MFC with PDMS microchannels. The alignment yield to the overlapping of the microchannels on the electrodes, making electrical stimulation possible whenever a neurite grows inside the stimulation microchannels (left), and recording possible from the recording electrodes with at least one neurite on top of them (right).

MFC-MEA were coated with laminin following the same scheme used for the PEI coating:

1. Removal of half water from each channel and replacement with laminin solution, twice;

2. Removal of half laminin solution from the two external macrochannels; in this way, the pressure applied from the central macrochannel pushes the laminin solution in the microchannels towards the external macrochannels, replacing the water previously in the microchannels;

3. Removal of half laminin/water solution from each channel and replacement with laminin solution, twice; in this way, the water once contained in the microchannels and now in the macrochannels is wholly removed, and the MFC-MEA are coated with laminin both in the macrochannels and inside the microchannels as well.

2.1.5 Preparation of glass coverslips

24-mm glass coverslips were cleaned with propan-2-ol and let air-dry inside a laminar flow hood. Coverslips were placed inside a 60mm Petri dish and plasma-cleaned for 2 minutes. Each Petri dish was filled with PEI solution to cover the coverslips completely, for 1 hour. The PEI solution was removed, the Petri dish was rinsed four times with sterile Milli-Q water, and each coverslip was placed diagonally inside a well in a 24-well plate. PDMS inserts were cleaned and sterilized

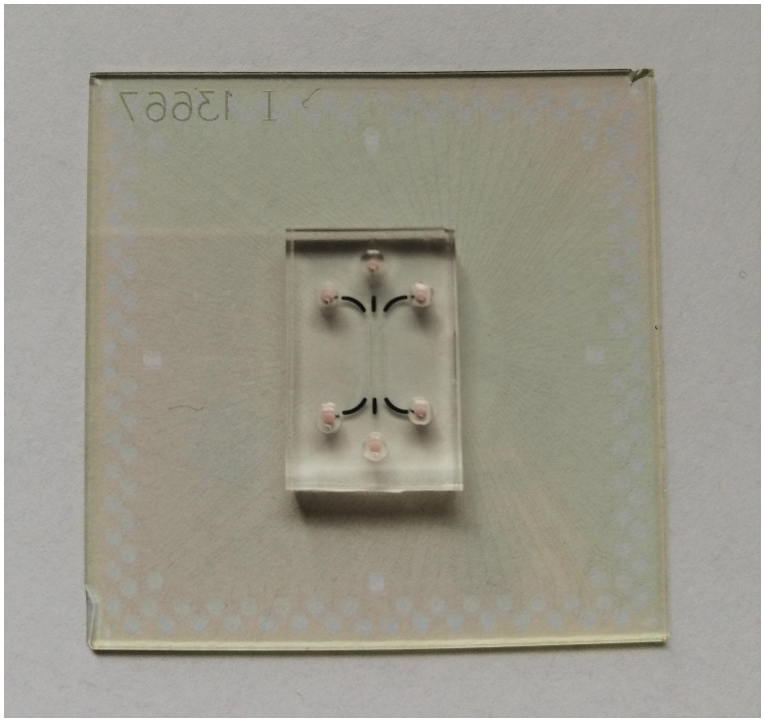

Figure 2.5: PDMS-MFC used by Neuro-Microphysiological Systems group.

as previously described. Each insert was attached to a coverslip with a pair of sterile forceps under a microscope in sterility conditions. Inserts were filled with 20mg/ml laminin solution, and the MEAs were kept in the fridge over-night, sealed with parafilm, and with a water reservoir, to prevent laminin evaporation.

2.2 Cells preparation

2.2.1 Primary DRG preparation

This protocol has been adapted from a previously published one [50]. Wild-type Swiss mice (Janvier Labs) were kept in the institute animal facility in specific boxes (GM500 Mouse IVC Green Line, Tecniplast, Italy), under controlled temperature and light-dark cycles of 12 hours, with food and water ad libitum. Postnatal (P) mice between 13 and 16 days were chosen for the experiments due to the ease of cleaning their tissues; this allowed several mice's employment for one single experiment, when a large number of cells was required, without excessively increasing the time dedicated to the dissection. As mice are breastfed until they reach 21 days, they were kept with their mother until the preparation day, when they were sacrificed with CO2. After disinfecting them with 70% ethanol, they were placed under the preparation hood with their dorsal side facing up and decapitated.

With a pair of dissection scissors (14070-12, Fine Science Tools, Germany), a first cut was made between the tail and the anus. The skin was then cut above the tail and along the central axis to expose the underlying tissues. The cut previously made between the tail and the anus continued along the vertebral column's two sides up to the head. The exposed vertebral column was removed by cutting the neck and the tail and placed in a 100mm Petri dish filled with cold HBSS without calcium and magnesium (Figure 2.6, a-e). By securing it with a pair of forceps (06 100 003, Fine Science Tools, Germany), the vertebral column was cleaned of flesh residues, and the vertebrae were exposed. With a scalpel mounting a sterile No. 15 surgical blade (Swann-Norton, England), the vertebral column was cut along its longitudinal axis (Figure 2.6, f-h). With a pair of dissection forceps (No. 5, Fine Science Tools, Germany), the spinal cord was carefully pulled away, and the ganglia were collected from both halves (Figure 2.6, i-m).

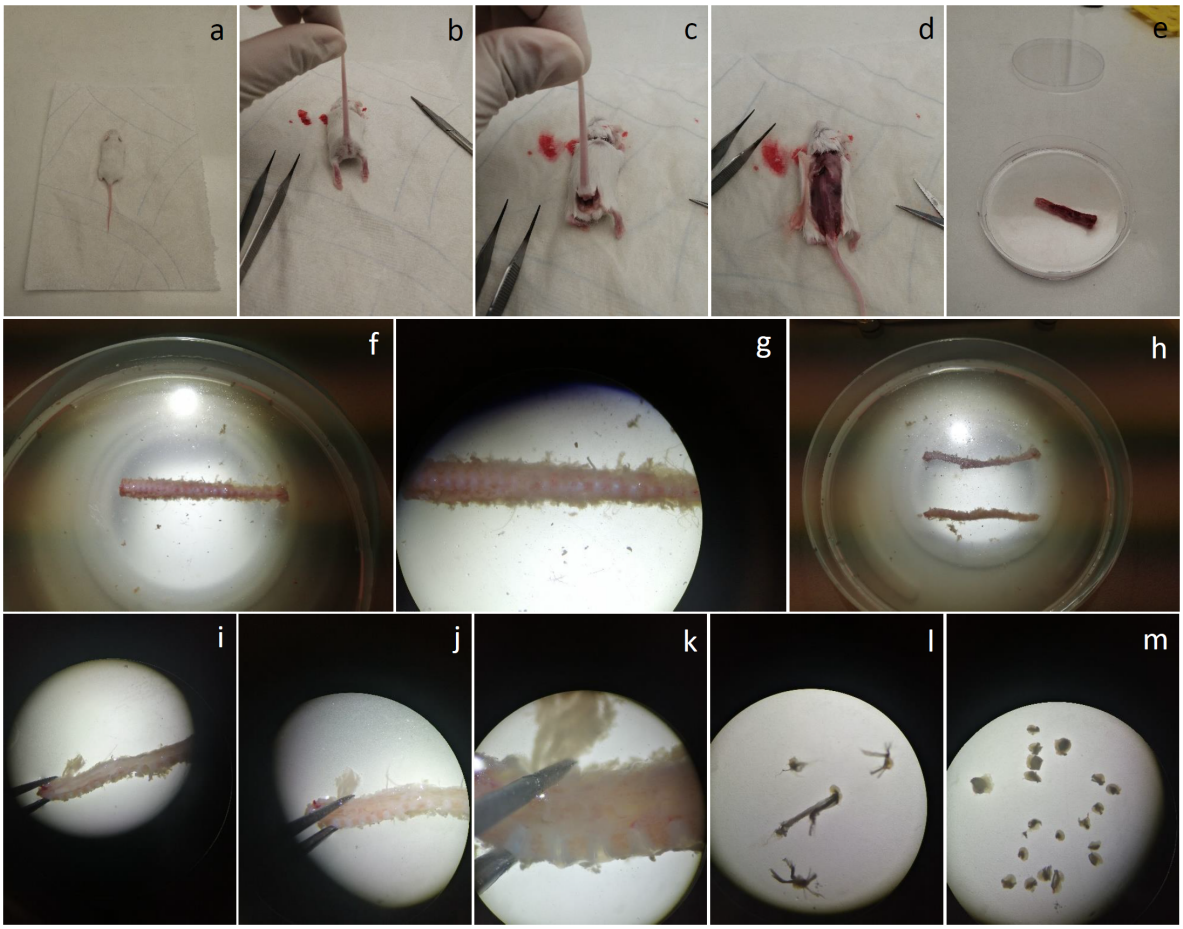

Figure 2.6: Illusrrated protocol for the preparation of primary mouse DRG neurons.

Cleaned ganglia were incubated with the enzymatic solution collagenase-dispase (CD) at 37°C for 40 minutes. CD solution was removed without touching the ganglia and replaced with the

enzymatic solution dispase (D) at 37°C for 40 minutes. After removing solution D, the ganglia were manually dissociated with DNAse solution. To remove dead cells and debris, thus increasing the cell suspension's viability, gradient centrifugation was performed (Figure 2.7).

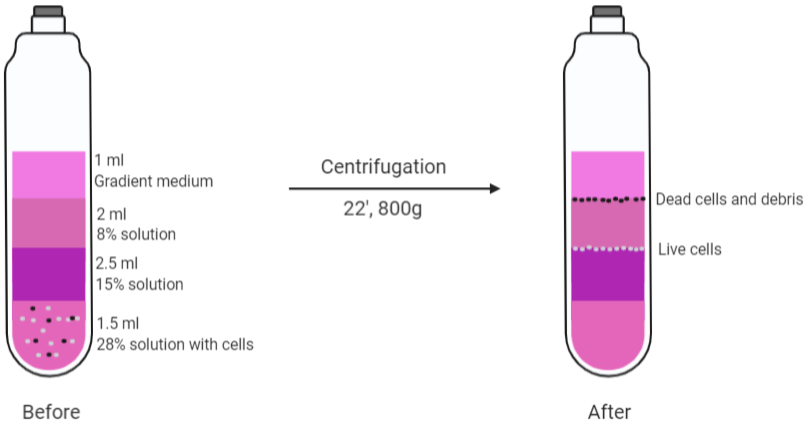

Figure 2.7: Representation of how the gradient centrifugation works. The gradient is generated by underlying the different solutions with the help of a spinal needle. The needle is inserted into the vial until it touches the bottom and the solution is slowly plugged with a syringe. The order in which the solutions are applied is the following: gradient medium, 8%, 15%, 28% with cells.

If pure sensory neurons were needed, neuron isolation was performed following the manufacturer's indication for the Neuron Isolation Kit (Miltenyi Biotec, Germany). According to the desired experimental output, purified and non-purified sensory neurons were then seeded on the appropriate substrate. The day following the cells' seeding, PDMS inserts were carefully removed with sterile curved forceps, and Neurobasal-A medium modified for DRG cultures was added to the cell cultures. The cultures were regularly checked with a phase-contrast microscope (Evos FL, Invitrogen, Germany).

2.2.2 Immortalized mouse Schwann cells (IMS32)

Immortalized mouse Schwann Cells IMS32 were purchased from Applied Biological Materials Inc. (Richmond BC, Canada) and stored at -195°C in liquid nitrogen immediately upon arrival in the institute. Cells were thawed and seeded on a pre-coated T25 culture flask. Once cells reached 90% confluency, cells were detached and subcultured according to the provided protocols. At subculture P4, part of the cells was frozen and stored in liquid nitrogen in Recovery ™ Cell Culture Freezing Medium (12648-010, Thermo Fisher, Germany) for future studies.

2.3 Activity recording

2.3.1 Recording of MEA with chemical stimulation

DRG neurons' activity was recorded after 3 hours, one, three, or six DIV. Recordings were performed by alternating samples of the two conditions. For recordings after 3 hours in vitro, cells were left in the inserts for 2 hours; inserts were then removed, the medium was added, and the MEA were kept in the incubator for at least 30' before the first recording. For recordings after 12 hours, inserts were removed the following day of the plating, the medium was added, and MEA were kept in the incubator for at least 30 minutes before the first recording. For recordings after three days, inserts were removed the following day of the preparation. For the recordings, MEA2100-System (Multichannel Systems MCS GmbH, Germany) controlled by an interface board (MCS-IFB 3.0 Multiboot, Multichannel Systems MCS GmbH, Germany) and connected via USB to a PC, was used. The temperature was controlled (TC02, Multichannel Systems MCS GmbH, Germany) and set to 30°C to avoid the cells' thermal stimulation. Recordings were acquired using MC Rack v. 4.6.2 (Multichannel Systems MCS GmbH, Germany). At the beginning of the recording, each sample was washed from culture medium with 4mM glucose in EC at RT and equilibrated for 10 minutes in the recording system. Each agonist solution was prepared by diluting the relative agonist stock solution in 4mM glucose EC to a concentration twice as high as the final one to be applied to the cells. To not leave the cells dry, the recording protocol followed a scheme based on the first removal of half of the EC contained in the MEA and then replacement with either new EC (control) or agonist solution (chemical stimulation). Each agonist was applied after 30 seconds from the beginning of the recordings to identify any spontaneously active electrode. The activity was recorded for 2, 3, or 5 minutes, depending on the nature of the agonist used.

2.3.2 Calcium imaging

Calcium imaging experiments were performed on MEA simultaneously with chemical stimulation recordings. Samples were incubated with 1µM Cal-520 solution for 30 minutes at 37°C and then washed with pre-heated DPBS without calcium and magnesium three times, 5 minutes each, at RT and in the dark. For these experiments, the equilibration step was not performed. Images were taken with an inverted microscope (Eclipse Ti2-E, Nikon Instruments Europe), mounting a 20X objective (S Plan Fluor ELWD Ph1 ADM, Nikon Instruments Europe). NIS-Elements (Nikon Instruments Europe) was used as a user interface for the acquisition. To record the electrical activity on the MEA and the imaging simultaneously, a specific triggering for the recording was used. In this way, even if the imaging and the electrical recording are saved with two different software in two separate files, it is possible to overlap the electrical trace with the imaging video thanks to the triggering's time intervals.

2.3.3 Recording of MFC-MEA with electrical stimulation

The activity was recorded after three DIV. To avoid evaporation of the medium, a special incubation chamber was used. The chamber keeps the same temperature, humidity, and CO2 pressure values as those used in the incubator. Cells were equilibrated for 10 minutes in the incubation chamber to verify that the chamber does not generate any noise in the electrical traces. A specific stimulation protocol was used: cells were stimulated from 100 to 500 mV, with steps of 10 mV; each step was repeated four times.

2.4 Imaging

2.4.1 Imaging for glia experiments

After the recording of the MEA was completed, cells were washed with fresh EC to remove the agonist traces. For staining the neurons, cells were incubated with 250nM NeuroFluor™ NeuO (01801, Stemcell, Germany) in Neurobasal-A medium for 1 hour at 37°C in the dark. After washing the neuronal staining solution, cells were left for 2 hours at RT in the dark. For staining the cell nuclei, cells were incubated with Hoechst 33342 (Molecular Probes™ NucBlue Live ReadyProbes™ Reagenz, R37605, Thermo Fisher, Germany) for 15 minutes at RT in the dark. After washing the nuclei staining solution, pictures were taken with an inverted microscope (Eclipse Ti2-E, Nikon Instruments Europe), mounting a 20X objective (S Plan Fluor ELWD Ph1 ADM, Nikon Instruments Europe), with an extra magnification of 1.5X. NIS-Elements (Nikon Instruments Europe) was used as a user interface for the acquisition.

2.4.2 ICC

ICC was performed after 1, 3, or 8 DIV. Each washing step consists of washing the cells three times with washing buffer. Cells were fixed with PFA solution for 20 minutes at 37°C and washed. Cells were then permeabilized for 10 minutes at RT and washed again. After incubation for 45 minutes at RT with blocking buffer, cells were incubated with primary antibodies for 2 hours at RT. Primary antibodies were washed, and cells were incubated with secondary antibodies for 45 minutes at RT in the dark. After washing the secondary antibodies, cells were kept for 20 minutes in the dark at RT. Cells were mounted on a clean glass slip with a mounting medium containing DAPI for staining the nuclei and dried for 1 hour at RT in the dark on a horizontal surface. Samples were stored at four °C in the dark before imaging. Images were taken using a confocal microscope (Axio Observer, Carl Zeiss GmbH, Germany), mounting 20X objective (Plan-Apochromat 20X/0.8 M27, Carl Zeiss GmbH, Germany). To increase the image area without affecting the resolution, images were taken with tiles and z-stack functions simultaneously, and both were provided with the image acquisition software (Zen Blue Edition,

Carl Zeiss GmbH, Germany). The final image was created by merging the tiles and drawing the projection of the z-stack through the image analysis software (Zen Black edition, Carl Zeiss GmbH, Germany).

2.5 Single-cell sequencing

2.5.1 Sample preparation

Non-purified and purified DRG neurons were prepared according to the previously described protocol and plated on a 24-well plate previously coated. The concentration of cells seeded was proportional to the concentration usually seeded on MEA. The day following the plating, the plates were brought to the Deutsches Zentrum für Neurodegenerative Erkrankungen e.V. (DZNE) in Tübingen and kept in the incubator located in the institute. Three days after the seeding, cells were detached in loco with Trypsin-EDTA 0.25%, centrifuged, counted, and diluted according to the desired number of cells to capture.

2.5.2 Data analysis

Data obtained at DZNE were analyzed within a collaboration by King's College in London

2.6 Data collection and analysis

2.6.1 Recording with MEA

Original recordings generated in MC Rack were analyzed with Neuroexplorer 5 (Nex Technologies, Madison, AL). Spikes were detected using specific parameters previously defined [51]. For the band-pass filter, the filter order was 4; filtering was done from 60 Hz to 6000 Hz. For the threshold value type, the number of median sigma was chosen. The custom threshold was -5, and the threshold crossing type was set to "Auto". Segments were included 0.2 milliseconds before and one millisecond after the threshold, with a minimum time between spikes of 0.001 seconds. For the detection of bursts, an algorithm based on Poisson surprise was chosen [52]. The minimum duration of the burst was set at 0 seconds, while the minimum surprise and the minimum number of spikes in a burst were defined for each agonist used, based on simulations summarized in Table 1. Briefly, for each agonist, 3 MEAs corresponding to non-purified DRG neurons experiment were chosen. The original MC Rack recording file was visualized, and the electrodes with an apparent response to the agonist were counted. For each MEA, the total number of responding electrodes (and the resulting percentage) was noted (leftmost column). Different parameters for the minimum surprise and the minimum number of spikes in burst were tried for each experiment. The resulting number of responding electrodes (with at least one

burst) were noted. For each MEA, the combination of minimum surprise and the minimum number of spikes that gave the most similar results to those obtained by visualizing the original recording file was noted (highlighted in yellow). When the parameters were tested for all three experiments, they were chosen by taking the average of the three combinations of values for the three experiments. The minimum surprise was set on 3 for all agonists, while the minimum number of spikes differed according to the agonist used: 5 for capsaicin; 7 for αβ-ATP; 6 for veratridine; 3 for bradykinin.

αβ-ATP Experiment date: 19/07/2019

No. MEA	Poisson surprise	Min. spikes 3	4	5	6	7	8	9
18525	2	41%	34%	30%	28%	26%	24%	22%
72	3	40%	34%	31%	28%	26%	24%	22%
29%	4	39%	34%	30%	28%	26%	24%	22%
18530	2	37%	30%	25%	23%	20%	18%	16%
47	3	36%	31%	25%	23%	20%	18%	16%
19%	4	35%	30%	25%	23%	20%	18%	16%
18541	2	44%	36%	30%	26%	24%	21%	19%
50	3	42%	36%	31%	26%	24%	21%	19%
20%	4	42%	36%	31%	26%	24%	21%	19%

capsaicin Experiment date: 18/10/2018

No. MEA	Poisson surprise	Min. spikes 3	4	5	6	7
2816	2	19%	16%	13%	12%	11%
16	3	17%	16%	13%	12%	11%
13%	4	17%	15%	13%	12%	11%
2774	2	14%	12%	12%	12%	10%
14	3	14%	12%	12%	12%	10%
12%	4	14%	12%	12%	12%	10%
2822	2	20%	17%	17%	13%	12%
15	3	20%	17%	17%	13%	12%
12%	4	18%	17%	16%	12%	11%

veratridine Experiment date: 28/09/2018

No. MEA	Poisson surprise	Min. spikes 3	4	5	6	7	8	9
8336	2	29%	23%	17%	13%	11%	9%	8%
24	3	25%	22%	17%	13%	11%	9%	8%
10%	4	25%	22%	17%	13%	11%	9%	8%
6996	2	29%	21%	17%	13%	9%	7%	5%
42	3	26%	21%	16%	13%	9%	7%	5%
17%	4	25%	21%	16%	13%	9%	7%	5%
13162	2	40%	30%	24%	18%	15%	14%	11%
28	3	35%	30%	24%	18%	15%	14%	11%
11%	4	33%	28%	23%	17%	15%	13%	11%

bradykinin Experiment date: 27/03/2020

No. MEA	Poisson surprise	Min. spikes 3	4	5	6	7	8	9	10	11	12	13	14	15
18527	2	14%	11%	10%	10%	9%	8%	8%	7%	6%	6%	6%	6%	6%
18	3	11%	11%	10%	10%	9%	8%	8%	7%	6%	6%	6%	6%	6%
7%	4	11%	10%	9%	9%	8%	7%	7%	7%	6%	6%	6%	6%	6%
18541	2	13%	9%	8%	8%	8%	7%	6%	5%	5%	4%	4%	4%	4%
18	3	11%	9%	8%	8%	8%	7%	6%	5%	5%	4%	4%	4%	4%
7%	4	8%	8%	8%	8%	8%	6%	6%	5%	5%	4%	4%	4%	4%
13164	2	9%	7%	6%	5%	4%	4%	3%	3%	3%	3%	3%	3%	2%
6	3	6%	5%	5%	5%	4%	4%	3%	3%	3%	3%	3%	3%	2%
2%	4	7%	6%	6%	5%	4%	4%	3%	3%	3%	3%	3%	3%	2%

Table 2.1: Determination of the different agonists' analysis parameters based on simulations with MC Rack and Neuroexplorer 5.

Data collected with Neuroexplorer 5 were normalized as following [53]: for each MEA recorded, each electrode with at least one DRG neuron on top was counted as "active electrode"; all the electrodes that resulted in "responding electrodes" from Neuroexplorer analysis were counted as

responding DRG (Figure 2.8). The number of not responding DRG (DRG_{nr}) was calculated as

$$DRG_{nr} = elec_{DRG} - DRG_r,$$

where $elec_{DRG}$ is the number of electrodes with at least one DRG neuron on top and DRG_r is the number of responding electrodes.

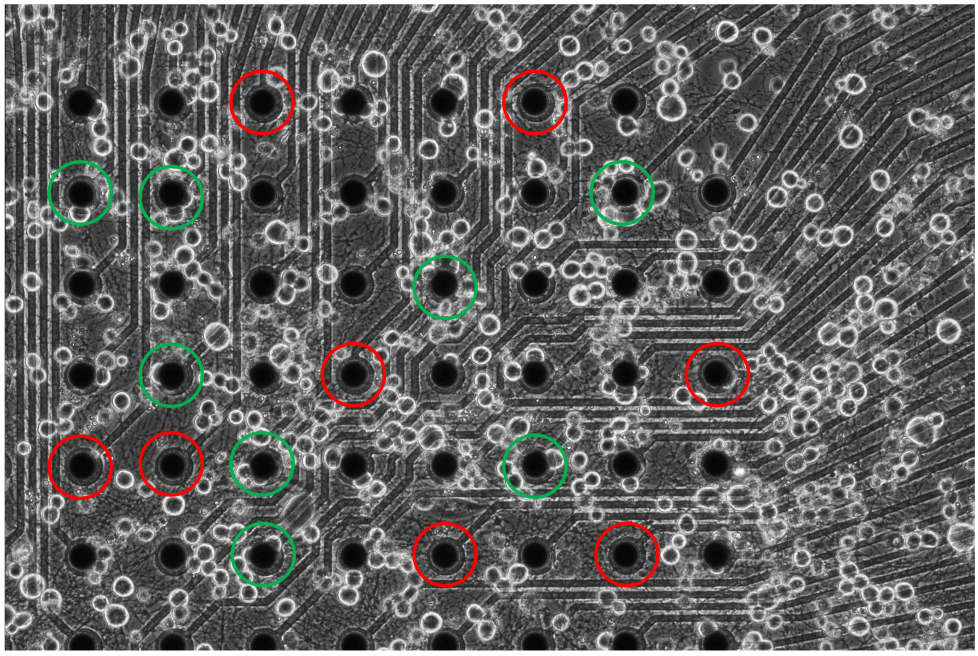

Figure 2.8: Example of how DRG are counted. Red circles represent some of the electrodes without any DRG on top. Therefore, they are not counted; green circles represent some of the electrodes with at least one DRG on top, and therefore counted as "active electrodes".

As DRG neurons don't organize themselves into a neural network, and as the main interest was the analysis of "all-or-nothing" responses, each DRGnr was associated with the same number of "0s" (not responding), and each DRGr was associated with the same number of "1s" (responding). The percentage of responding DRG neurons for a given agonist was calculated by calculating the mean of all responding and not responding DRG; the mean would assume a value between 0 (0% responding DRG) and 1 (100% responding DRG). For better visualization, all plots have been created with the percentage notation. Calcium-imaging experiments were analyzed similarly; in this case, DRGr corresponds to the number of electrodes with at least one DRG neuron on top that responded to the agonist by increasing the intracellular fluorescence, corresponding to an increase in the intracellular calcium concentration.

2.6.2 Recording with MFC-MEA

For MFC-MEA experiments, data were collected with MC Rack and analyzed. Each MFC-MEA was checked. The number of closed recording electrodes that are correctly aligned on top of a microchannel (thus recording an eventual electrical response) was counted (Figure 2.9). As each MEA has 16 recording electrodes, this number can be a maximum of 16.

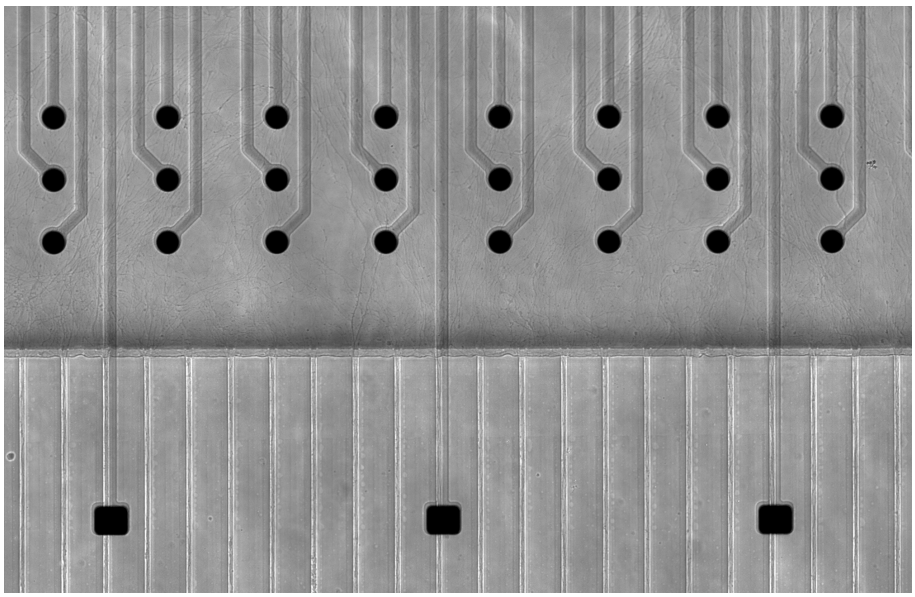

Figure 2.9: Example of MFC-MEA recording electrodes aligned with the microchannels.

All the correctly aligned recording electrodes for a condition from different MFC-MEA (purified or non-purified DRG) were grouped. Remembering that each voltage was applied four times for each sample, the number of closed responding electrodes was counted for each of these applications. So, for each sample, there were four values for each voltage. In the example below, there are 15 aligned electrodes. With each electrode stimulated 4 times, the maximum number of responses is 60.

Stimulation	Responding electrodes
1	10
2	11
3	10
4	9
Total	**40**

The total number of responding electrodes for this stimulation is 40, which corresponds to 66% (40/60). All the values for a single voltage from all the samples for the same condition (purified or non-purified DRG) were grouped.

	MEA 1	MEA 2	MEA 3	MEA 4	**Total**
Aligned electrodes	16	15	16	14	**61**
Responding electrodes	12	11	13	12	**48**
Share of responding electrodes	75%	73.33%	81.25%	85.71%	**79%**

The probability of observing a response for a specific voltage applied is calculated by taking the total number of responding electrodes for a particular condition and voltage and dividing it by the total number of recording electrodes able to detect a response (those located inside the microchannels) for that specific condition.

2.6.3 Cells counting for data analysis in glia experiments

A region of interest (ROI) was created and used to define all the samples' same area. Inside the area, the neurons stained with NeuroFluor ™ NeuO, and the nuclei stained with Hoechst 33342 were counted using the NIS-Elements analysis software (Nikon Instruments Europe) (Figure 2.10). The number of glial cells for each sample was calculated by subtracting the number of neurons counted from the number of nuclei counted, corresponding to the total number of cells.

2.6.4 IMS32 experiments

For the experiments with co-cultures of DRG neurons and IMS32, it was impossible to perform the normalization of the data due to the cultures' characteristics; therefore, data were analyzed merely considering the number of responding electrodes. The number of not responding electrodes was calculated by subtracting the number of responding electrodes from the total number of electrodes.

2.6.5 Data analysis

Data were analyzed with GraphPad Prism 8 (GraphPad Software, LLC, San Diego, CA). For the visualization of some data graphs (3D histograms), Sigmaplot 10 (Systat Software, Inc, San Jose, CA) was used.

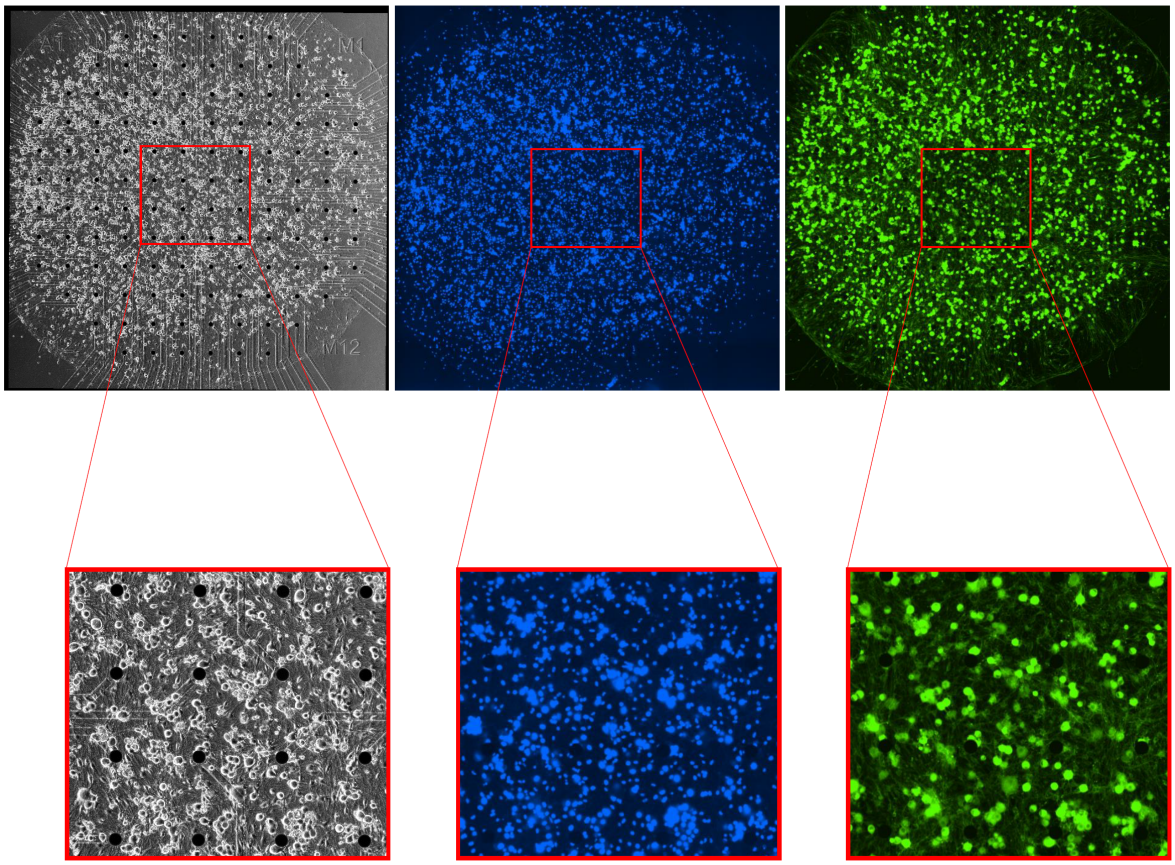

Figure 2.10: Example of a DRG neurons culture stained for cell counting. Left picture: brightfield; middle picture: neurons stained with Neurofluor™ NeuO; right photo: nuclei stained with Hoechst 33342.

3 | Results

3.1 Preliminary electrophysiological studies on sensory neurons

There are several techniques to measure the electrophysiological characteristics of neurons. The golden standard is represented by patch-clamp; it allows obtaining different neurons' information, including the membrane voltage and the ionic currents. However, more recent techniques involving microelectrode arrays (MEA) provide a significant advantage compared to patch-clamp: high throughput. In fact, for cell culture, it is possible to patch only one cell at a time. Therefore once an agonist is applied to the culture as stimulation, we can record the activity only from the patched cell, thus missing the remaining cells' information. On the other hand, even if MEAs do not offer information regarding membrane voltage and ionic currents, they allow us to record the activity coming from 252 electrodes – and therefore, potentially from 252 neurons – at the same time. As the main interest was capturing whether a DRG neuron could respond to a specific agonist rather than recording its pure electrophysiological features, it was decided to exploit the MEAs technology.

In physiological conditions, DRG neurons are surrounded by different types of non-neuronal cells that support their survival and activity (see also Introduction). It is also known that the non-neuronal cells' dysfunction alters DRG neurons' excitability in chronic pain conditions [54]. Before studying in detail possible mediators released by non-neuronal cells and possibly involved in the hyperexcitability of DRG neurons that characterize chronic pain states, it was decided to research both DRG neurons in the two most specific possible conditions: in the presence and absence of glial cells. The preparation of primary mouse DRG neurons leads to obtaining a mixed culture of neurons and non-neuronal cells (non-purified DRG). Therefore, it was necessary to remove the non-neuronal cell fraction to get DRG neuron culture (purified DRGs). For this purpose, a commercial kit specific for removing non-neuronal cells was used (Neuron Isolation Kit, Miltenyi GmbH). This kit allows the complete removal of non-neuronal cells, leading to pure DRG neurons culture (Figure 3.1, right).

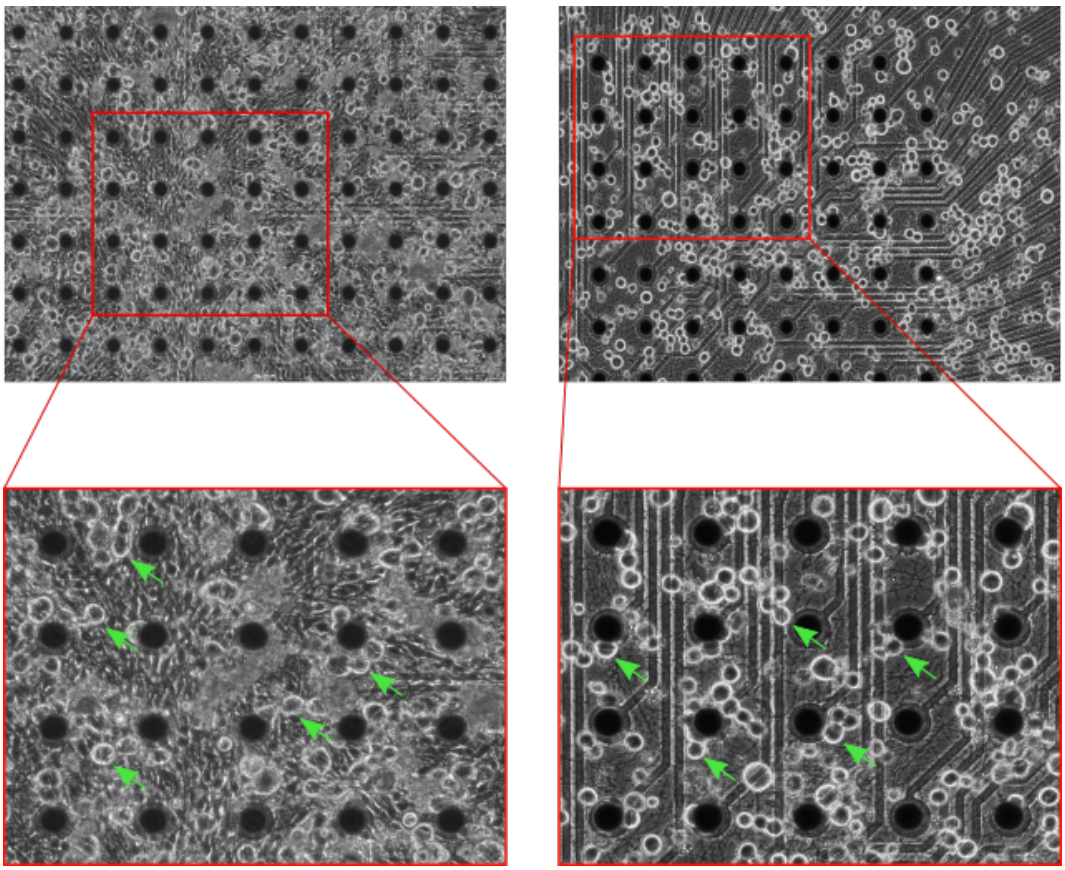

Figure 3.1: Comparison between non-purified DRGs (left) and purified DRGs obtained with neuron isolation kit (right). Green arrows indicate DRG neurons.

The chosen open-electrodes MEA system allows performing recordings in response to an agonist's application. For this purpose, it was decided to use the agonist capsaicin, which gives a fast and clear response in DRG neurons [55]. The activity was recorded after 3DIV [28].
After 3DIV, a first look at the raster plots already highlights the differences between the two conditions: for non-purified DRGs, we can see responses to capsaicin after its application, represented by all the electrodes showing spikes in the form of bursts (Figure 3.2, top). However, if we look at the traces produced in a purified DRGs culture, almost no spikes can be detected (Figure 3.2, bottom).

Figure 3.2: Example of 3DIV recordings on MEA in response to capsaicin application in non-purified (top) and purified (bottom) DRG neurons. The left-most column lists the different electrodes, and for each electrode, spikes are displayed as black dashes.

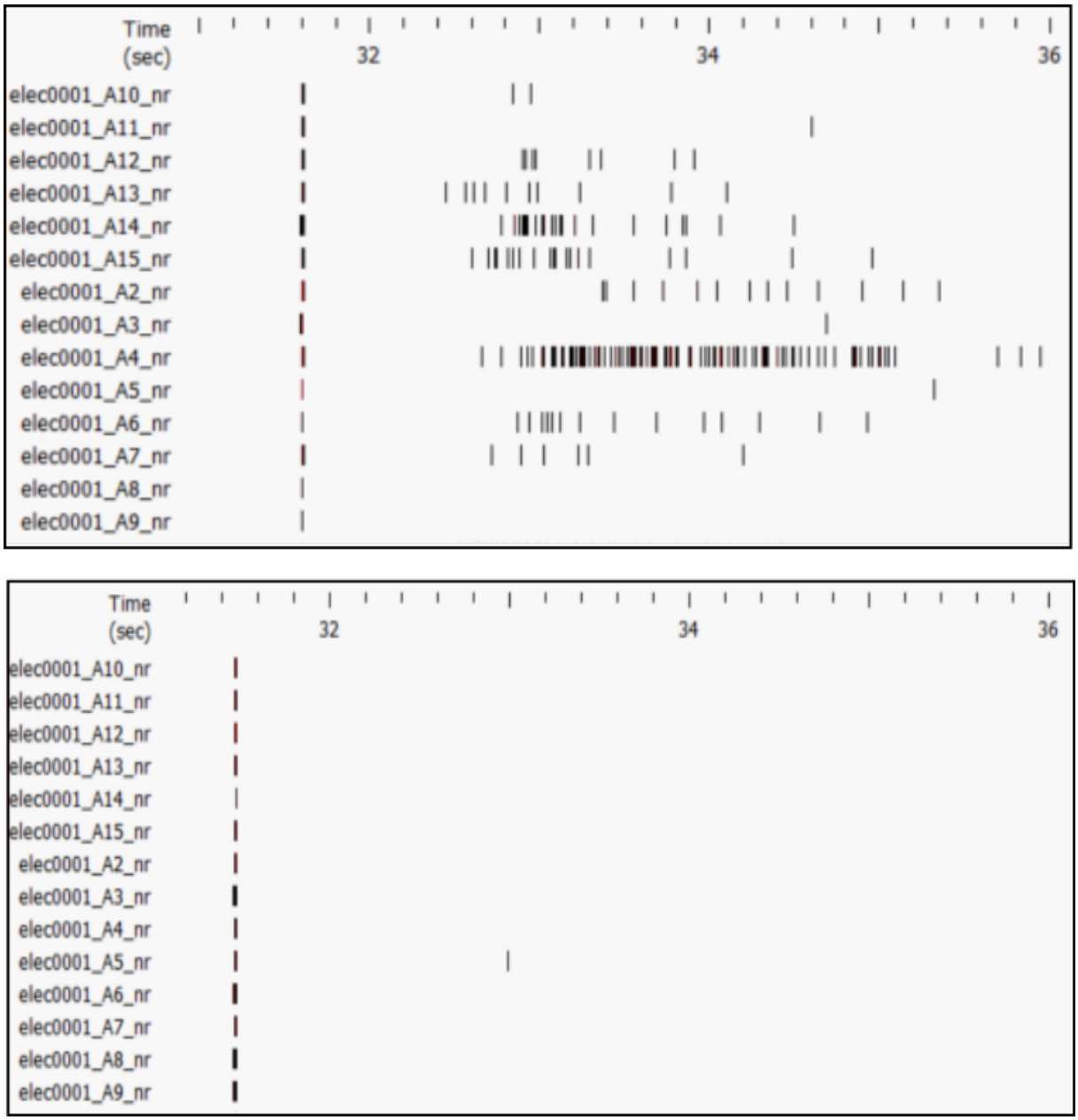

Figure 3.3: The difference between non-purified (top) and purified (bottom) DRGs can be better perceived by highlighting some electrodes from the traces displayed above.

Based on the results obtained after 3DIV, it was decided to perform more recordings. The first recordings emphasized the differences between non-purified and purified DRGs after 3DIV. What was still unclear was when this difference arises; to understand this, two time points for the recordings were added: three hours and one day in vitro. Recording after three hours is the earliest time-point possible, as DRG neurons require at least two hours after their seeding to attach on the surface firmly, plus another 30 minutes after removing the insert for equilibration with the culture medium. We can notice that both purified and non-purified DRGs neurons are already excitable a few hours after the seeding, with the second ones significantly more active (unpaired t-test, $t(2829)=4.895$, $p<0.0001$). We can also notice how non-purified DRGs' excitability increases after 24 hours in culture; this can be detected in purified DRG neurons. However, looking at the data recorded after 72 hours in culture, while the excitability of non-purified DRGs furtherly increases, in the case of purified DRG, it drops dramatically to being almost absent (unpaired t-test, $t(1487)=18.61$, $p<0.0001$) (Figure 3.4).

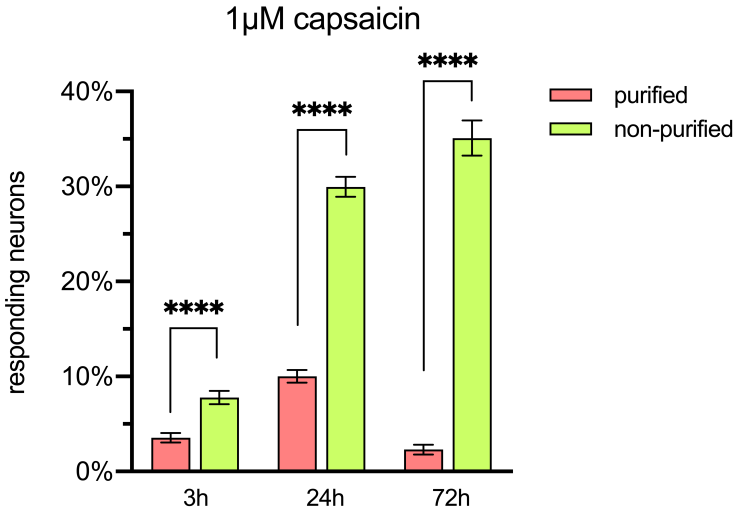

Figure 3.4: Non-purified and purified DRGs response to 1µM capsaicin after 3, 24 and 72 hours in vitro (n = 664 cells, data expressed as mean ± S.E.M., ****p<0.0001).

These differences can be further appreciated if the total number of spikes in a reaction is compared between non-purified and purified DRG neurons (Figure 3.5).
The fact that the excitability of purified DRGs increases a bit after 24 hours in culture could be due to the presence of a sort of "memory" in the neurons themselves: after their dissociation and seeding, purified DRGs still carry and remember some of their features that were initially present during their physiological conditions. However, after three days in culture, this sort of "memory" is lost due to the absence of non-neuronal cells, and the excitability of purified DRGs dramatically drops to being almost absent.

Time	DRG type	n	mean ± S.E.M.
3h	Purified	1365	3.52 ± 0.50
	Non-purified	1466	7.78 ± 0.70
24h	Purified	1375	8.36± 0.75
	Non-purified	1330	30.68 ± 1.26
72h	Purified	825	2.30 ± 0.52
	Non-purified	664	35.09 ± 1.85

Table 3.1: Sample size and percentages of DRG neurons responding to 1µM capsaicin for the different conditions (data expressed as mean ± S.E.M.; n = number of DRG neurons).

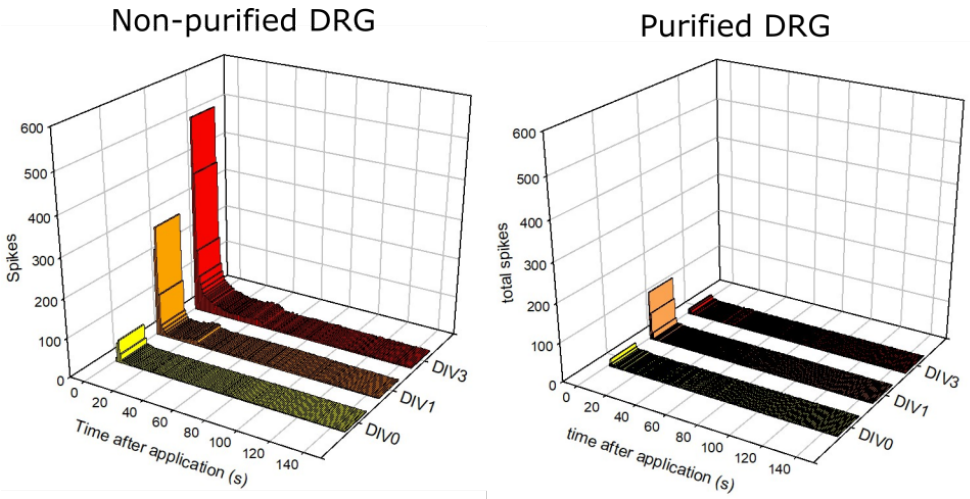

Figure 3.5: 3D representation of the total spikes for non-purified (left) and purified (right) in response to 1µm capsaicin at different time points.

Different hypotheses have been developed to explain this difference in excitability, and each of them was investigated with one or more experiments.

First of all, it was necessary to investigate whether the differences between purified and non-purified DRGs relied only on the number of responding cells or whether they were encountered in other parameters, like the mean frequency in a burst. However, for this specific parameter, no significant difference could be noticed between purified and non-purified DRGs (Figure 3.6).

This leads to the hypothesis that while the mean frequency remains constant between purified and non-purified DRGs, the difference in the percentage of responding neurons can be addressed to a mere loss of cells during the purification process. This could lead somehow to the selection of purified DRG lacking the ability to respond to capsaicin. Although this scenario would be pretty unlikely and unexpected to happen, it was necessary to explore this possibility with further experiments.

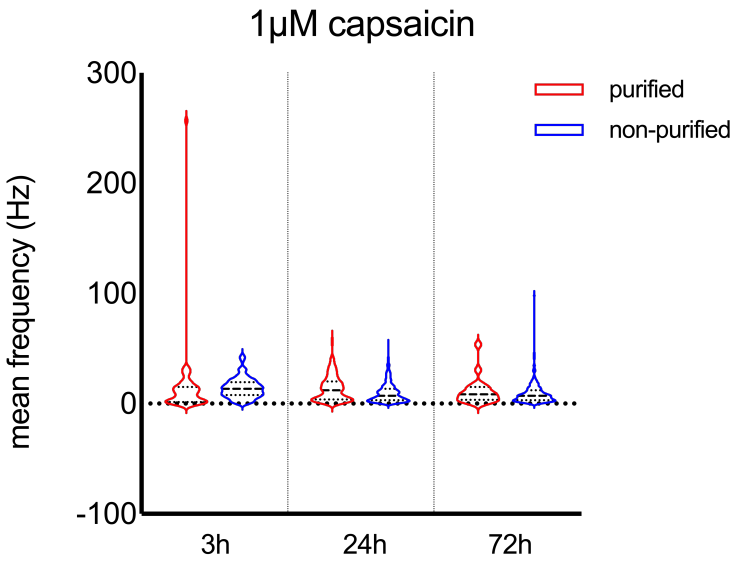

Figure 3.6: Mean frequency in a burst for purified and non-purified DRG neurons for the different time points. Dashed line: median; dotted lines: quartiles.

3.1.1 Lack of TRPV1 capsaicin receptor in purified DRG neurons

The first possible explanation for the lack of excitability in purified DRGs in response to capsaicin application was that for some reasons, the neurons deprived of their corresponding glial cells lack the capsaicin receptor, the ligand-gated ion channel transient receptor potential vanilloid 1 (TRPV1) [56]. Therefore when the agonist is applied, no effect can be observed.
There are different ways to verify this hypothesis. For example, RT-PCR would give information about the level of a specific transcript at one particular time in culture. Simultaneously, ICC could provide information about the location and quantification of the receptor on the cell membrane. However, all these methods do not give information on the functionality aspect. As the main interest was exploring the functionality of DRG neurons, it was decided to perform a faster and easier assay for verifying the presence of the TRPV receptor quickly and, at the same time, its functionality both in purified and non-purified DRG neurons. This assay was represented by calcium imaging.
Calcium ($Ca^{(2+)}$) is an essential second messenger in neurons; as already mentioned in the introduction section, at equilibrium potential, calcium ions are more concentrated on the extracellular side and less concentrated on the intracellular side of the cellular membrane. TRPV1 is a non-selective ligand-gated ion channel; therefore, its activation through the binding of an agonist such as capsaicin leads to the channel's opening and the influx of calcium ions from the extracellular side inside the cell.

The main feature of calcium imaging is the employment of calcium indicators, which can detect calcium ions based on their biochemical properties. There are different families of calcium indicators, and one of them corresponds to chemical calcium indicators. Two distinct portions characterize this group of molecules: the calcium chelating site and the fluorophore. The binding of calcium ions to the calcium chelating site leads to a change in the molecule's conformation, affecting the fluorophore site and modifying the fluorescence emission (Figure 3.7).

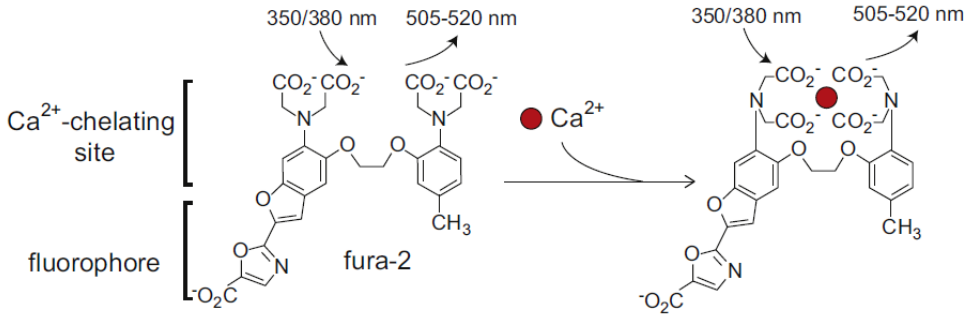

Figure 3.7: Mechanism of action of a chemical calcium indicator (modified from [57]).

For this experiment, the chemical indicator Cal-520® (AM, AAT Bioquest, Sunnyvale, CA) was used.

In the example shown below, representing a non-purified DRGs culture, we can notice that after applying the agonist capsaicin, there is an increase in the intracellular calcium concentration in neuronal cells, characterized by an increase in the fluorescence in the cells. We can also notice that the response's peak, identified by the number of neurons showing an increase in the intracellular fluorescence, coincides for all the cells (Figure 3.8).

The same effect noticed in non-purified DRGs can be detected in purified DRGs (Figure 3.9).

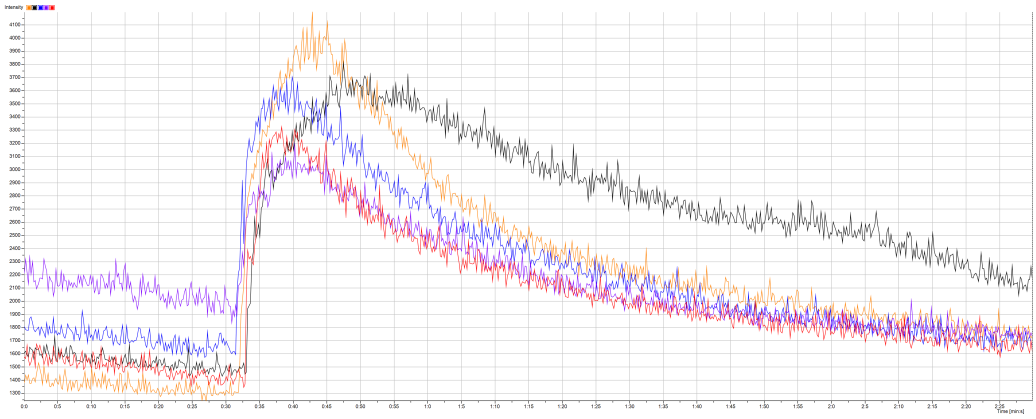

Figure 3.8: Calcium-imaging experiments shows the accumulation of calcium ions in non-purified DRGs (here represented by five sample cells) after drug application. If traces from different cells are overlapped (bottom-right), the peak coincides with different cells.

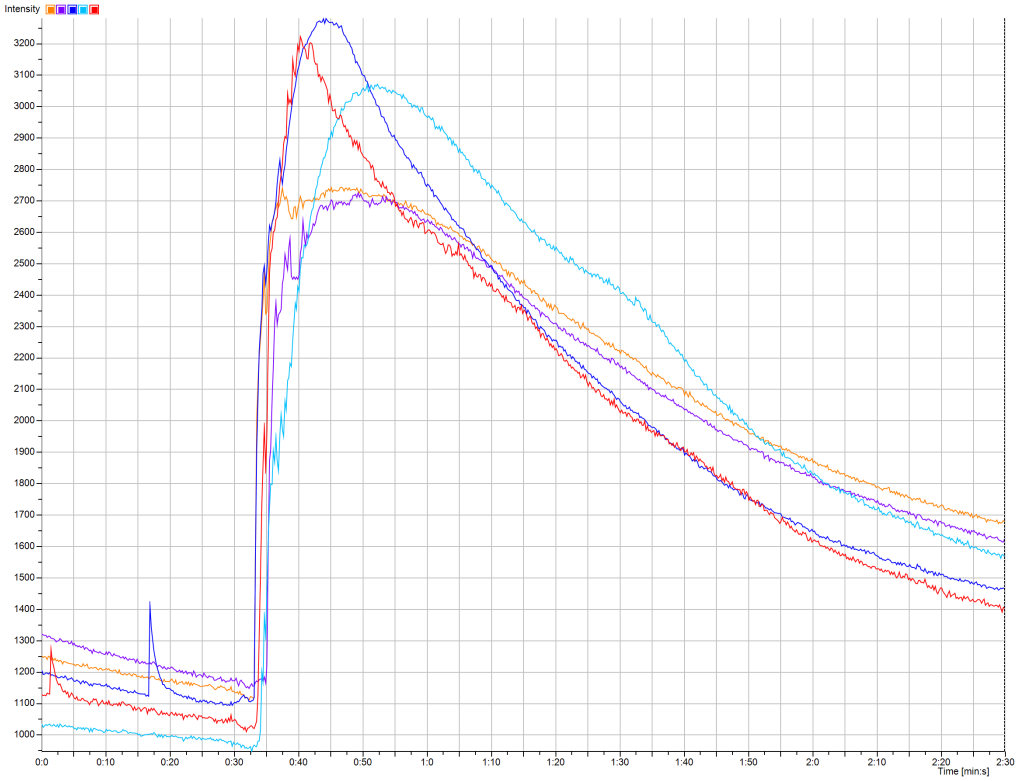

Figure 3.9: Calcium-imaging experiment in purified DRGs also shows the accumulation of calcium ions inside the cells (here also represented by five sample cells) after drug application. If traces from different cells are overlapped (bottom-right), again, the peak occurs at the same time for different cells.

The differences between purified and non-purified DRGs can be quantified similarly to that used for MEA, already described previously. In this way, it is possible to compare the response recorded with the MEA system and those recorded with calcium imaging. By doing so, it can be noticed that there is a significant difference in terms of responding cells for capsaicin (unpaired t-test, $t(929)=14.37$, $p<0.0001$). On the other hand, interesting is the fact that the percentage of responding cells in calcium imaging is comparable to that in the MEA system (unpaired t-test, $t(768)=0.2259$, $p=0.82$).
Calcium-imaging experiments with veratridine also showed a significant difference between veratridine response in MEA and calcium imaging (unpaired t-test, $t(708)=35.01$, $p<0.0001$). Interesting is that for veratridine, the percentage of DRG neurons responding to veratridine by increasing intracellular calcium is above 90% (Figure 3.10).

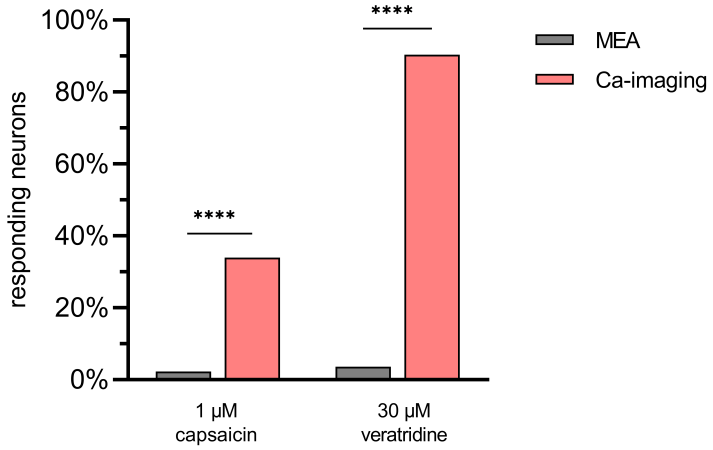

Figure 3.10: Percentage of responding DRG neurons to 1µM capsaicin and 30µM veratridine in calcium imaging and MEA experiments (n = 73 cells, data expressed as mean ± S.E.M., ****$p < 0.0001$).

Agonist	Source	n	mean ± S.E.M.
1µM capsaicin	MEA	825	2.30 ± 0.52
	Ca-imaging	106	33.96 ± 4.62
30µM veratridine	MEA	637	3.65 ± 0.74
	Ca-imaging	73	90.41 ± 3.47

Table 3.2: Percentage of purified DRG neurons responding to 1µM capsaicin and 30µM veratridine on MEA and with calcium-imaging after 3DIV (data expressed as mean ± S.E.M.; n = number of DRG neurons).

Because calcium imaging experiments proved that the capsaicin receptor TRPV1 is still expressed in purified DRGs, it was reasonable to investigate whether the difference in excitability between purified and non-purified DRGs was detectable in response to other agonists that involve different signal transduction pathways. For this purpose, purified and non-purified DRGs activity was also recorded in response to αβATP (ligand-gated ion channel, purinergic receptor, activates kinase/phosphatase signal transduction cascade [58, 59]), veratridine (does not have a peculiar receptor, but acts by altering the state of voltage-sensitive Na+ channels [60, 61]), and bradykinin (G-protein coupled bradykinin receptor, activates kinase/phosphatase signal transduction cascade [62]). Since for capsaicin, the highest difference between purified and non-purified DRGs in terms of excitability was noticed after 3DIV, recordings for the three new agonists were reduced to 3DIV. It can be noticed how the difference in the excitability between the two conditions is also present for the three other agonists used (Figure 3.11).

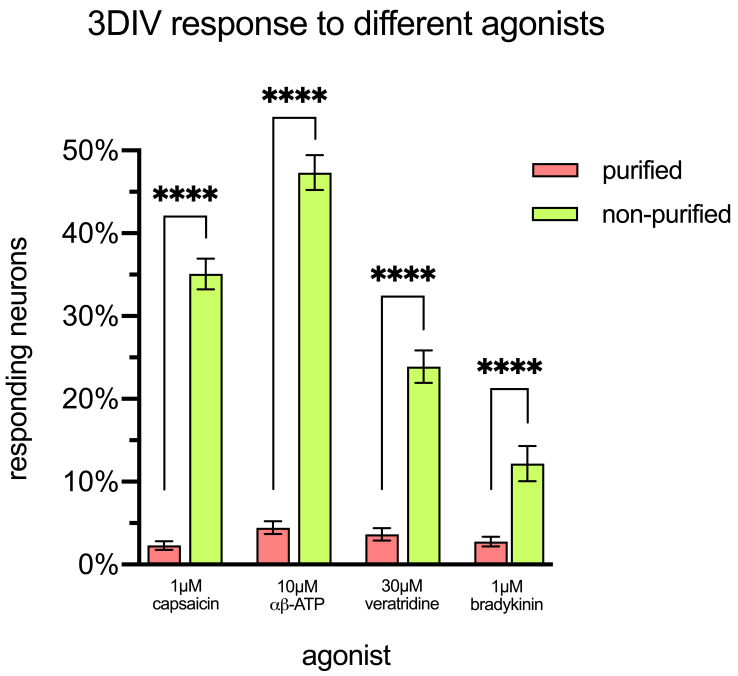

Figure 3.11: Non-purified and purified DRGs response to different agonists after 3DIV (n = 238 cells, data expressed as mean ± S.E.M., ****p < 0.0001).

Agonist	DRG type	n	mean ± S.E.M.
1µM capsaicin	Purified	825	2.30 ± 0.52
	Non-purified	664	35.09 ± 1.85
10µM αβATP	Purified	741	4.45 ± 0.76
	Non-purified	560	47.32 ± 2.11
30µM veratridine	Purified	637	3.65 ± 0.74
	Non-purified	467	23.91 ± 1.97
1µM bradykinin	Purified	795	2.77 ± 0.58
	Non-purified	238	12.18 ± 2.12

Table 3.3: Percentage of responding DRG neurons for the different agonists after 3DIV (data expressed as mean ± S.E.M.; n = number of DRG neurons).

Also for the other three agonists used, there was no clear correlation between the percentage of responding DRG neurons, and the mean frequency in a burst (Figure 3.12)

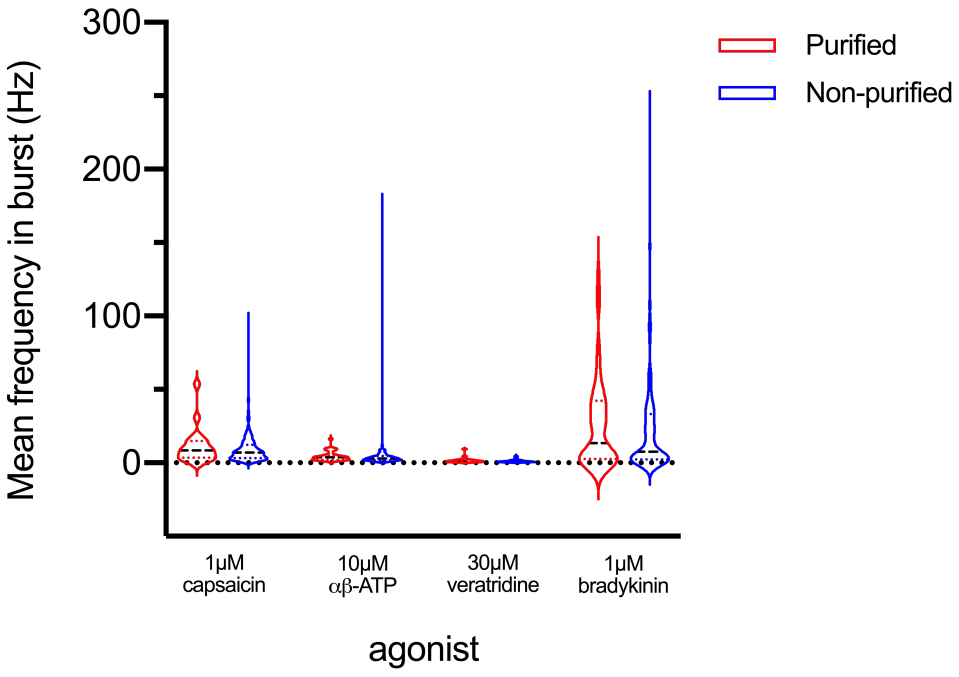

Figure 3.12: Mean frequency in a burst for each agonist and condition (black lines: median; red and blue lines: quartiles).

Furthermore, let's compare the mean frequency in burst with the percentage of DRG neurons responding to a determined agonist. There seems to be no correlation between the two values, meaning that a lower percentage of responding DRG neurons does not correlate with a subsequent lower frequency in a burst (Figure 3.13).

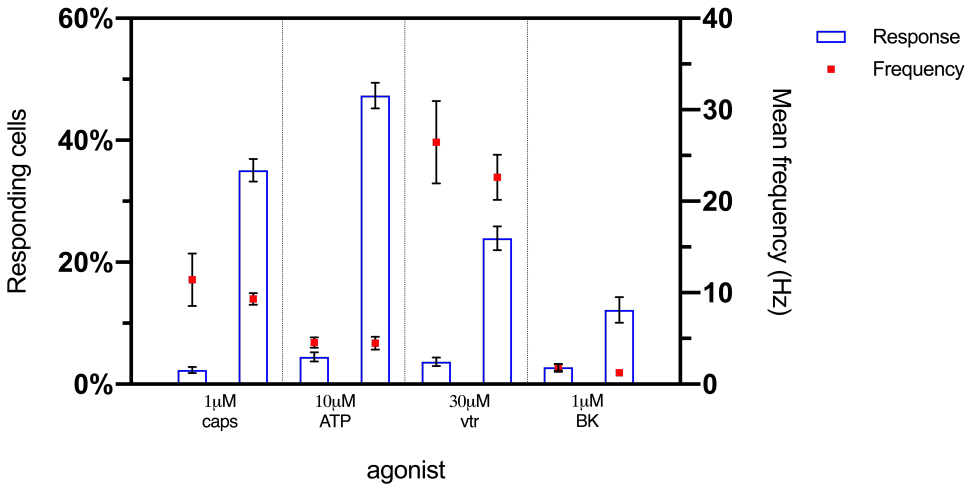

Figure 3.13: Percentages of DRG neurons responding to each agonist, for each condition, after3DIV, in relation to the mean frequency in burst for given agonist and condition (data represented as mean ± S.E.M.).

3.1.2 Electrical stimulation of DRG neurons

Calcium imaging experiments proved that the TRPV1 receptor is still present in purified neurons and demonstrated by the intracellular accumulation of calcium; however, the neurons' entrance does not automatically mean that the neurons can transform their depolarization into an action potential. Therefore, the second hypothesis to explain the lack of excitability in purified neurons implies that the depolarization of the neuronal membrane caused by the opening of the TRPV1 receptor induced by capsaicin occurs as well in purified neurons. However, it is not sufficient to reach the threshold in the membrane voltage necessary to evoke an action potential, thus a response.

Electrical recordings with the classic open MEAs that employ chemical agonists like capsaicin do not allow us to control the neuronal membrane's depolarization or know the ion currents' entity. One way to detect those variables is provided by patch-clamp. However, as already mentioned at the beginning of this chapter, this technique offers low throughput than MEA technology. Furthermore, there is a tendency to choose the "best looking" cell in a culture prepared for a patch-clamp experiment. This tendency leads to biased results, as the "best looking" cell does not always represent the overall cell population.

One of the patch-clamp's critical features is represented by the possibility of stimulating the neurons electrically through the micropipette, either by depolarizing the membrane or by applying a flow of ionic current. This stimulation is not possible with the open MEA system used in the experiments with the different agonists.

There is a possibility of controlling the neurons' stimulation without employing a patch-clamp,

which uses MEA that allows electrical stimulation through special stimulation electrodes. In this way, we are still not able to detect the membrane potential. However, we can control the electrical current applied to dendrites, thus checking any differences in the amount of current necessary to apply to neurons to evoke an action potential. These particular types of MEA have been developed and produced in-house and have been successfully used for different experiments involving primary neurons [49, 51]. As already explained in the Methodology section, these particular MEA have been designed in a way that it is possible to align and attach microfluidics chips made of PDMS, thus producing the so-called MF-MEA. This system allows the compartmentalization of cell cultures in defined macrochannels, the stimulation of the neurites that grow inside the microchannels aligned with the stimulation electrodes, and the recording of the neurites' electrical activity inside the microchannels aligned with the recording electrodes (Figure 3.14).
For this experiment, MF-MEA and DRG neurons were prepared as described in the Methodology section. Non-purified or purified DRG were seeded in the middle channel (Figure 3.14).

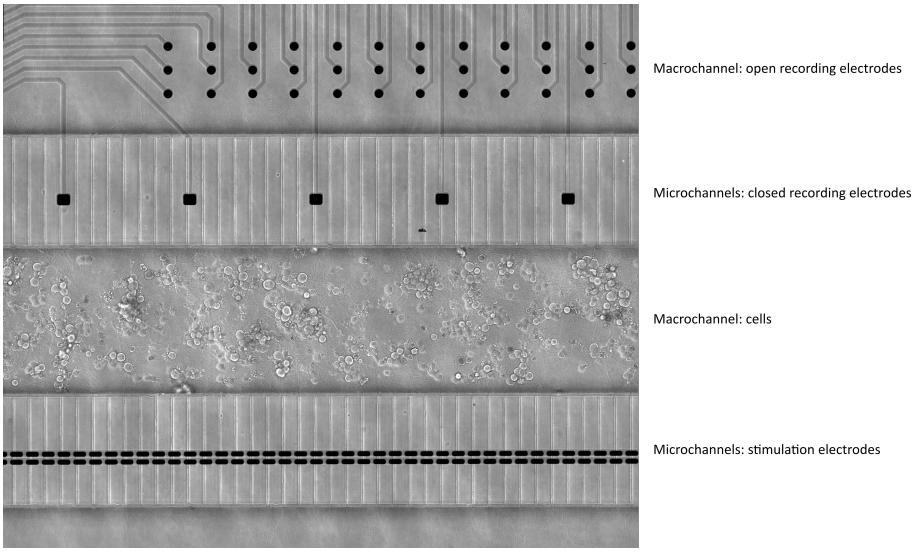

Figure 3.14: Purified DRG seeded in the middle macrochannel in a PDMS-MFC. Neurites grow in all directions and inside the microchannels, making possible the electrical stimulation via the stimulating electrodes (bottom) and the recording via the recording electrodes (top).

For this experiment, we consider the stimulation and the closed recording electrodes. DRG neurons are seeded in the middle macrochannel, and neurites grow in every direction, including inside the microchannels where the two sets of electrodes are located. Neurites are then stimulated through the stimulation electrodes, and the electrical activity is recorded inside the microchannels through the closed recording electrodes.

The protocol used for the electrical stimulation is illustrated here:

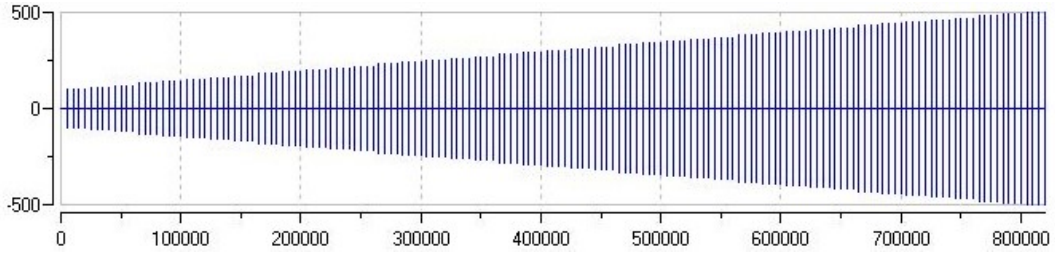

Figure 3.15: Stimulation protocol for microfluidics experiments. The X-axis corresponds to time (ms), while the y-axis represents the intensity of the stimulus in millivolts (mV). Starting from 100mV and up to 500mV, each stimulus is repeated 4 times every 5 seconds.

An example of an experiment's outcome is showed in Figure 3.16, where the 16 recording electrodes are displayed. For each electrode, the X-axis represents the time, and therefore the intensity of the stimulation increases with time; the Y-axis represents millivolts (mV).

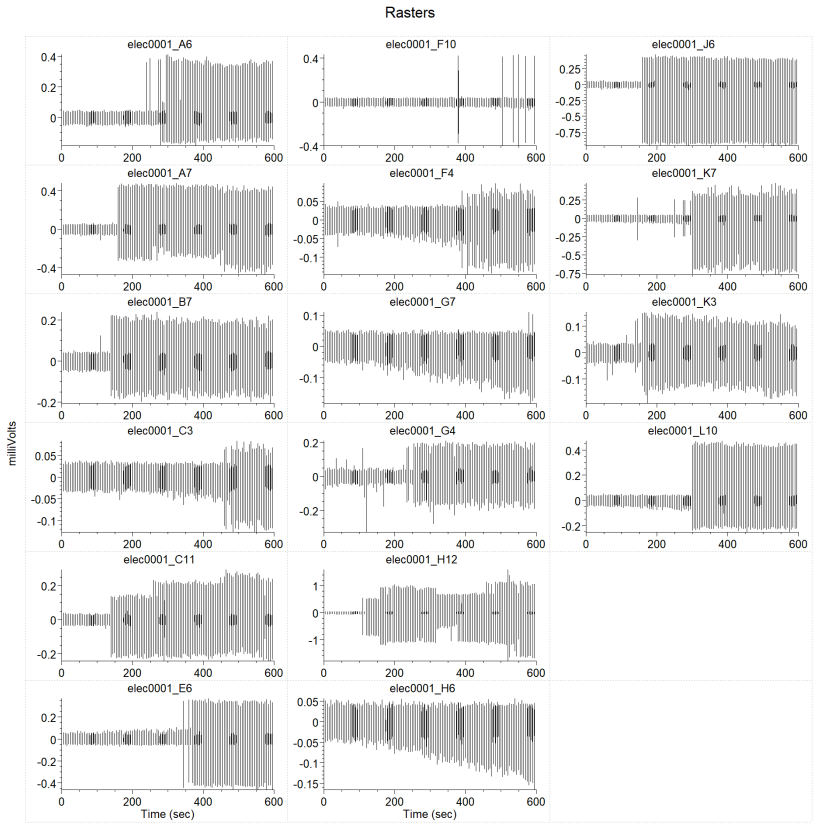

Figure 3.16: Evoked action potentials in MF-MEA. The intensity of the stimulation increases with time (along the X-axis). Notice how there are differences in terms of onset and intensity of the responses among the different electrodes/neurons.

Is it also possible to align all recording electrodes vertically to visualize better the effects of the different stimulation steps among the various electrodes (Figure 3.17).

Figure 3.17: Example of a recording on MF-MEA, with all 16 recording electrodes displayed. For each electrode, the dashes represent the electrical stimuli applied.

By zooming into one electrode, it is possible to appreciate the difference between the stimulation steps that do not evoke an action potential and those that evoke an action potential (Figure 3.18).

Figure 3.18: Example of an electrode responding to electrical stimulation. The intensity of the applied stimulus increases from left to right, and at some point (red arrow), the stimulus is high enough to evoke an action potential.

It is crucial to notice the differences between the two conditions: in the case of non-purified DRG, neurons start responding already around 150mV; on the other side, the pure DRG remains silent until 250mV they begin responding to an electrical stimulus. At higher voltages, the two conditions almost overlap in terms of percentages of responding cells. This demonstrates that even purified DRG can still react to external stimuli and generate action potentials, thus being viable despite glial cells' absence. Most importantly, there is a delay in the excitability of those neurons cultured without glial cells. If we want to evoke a response, it is necessary to apply

higher voltages to purified DRG to obtain the same entity as observed in non-purified DRG (Figure 3.19).

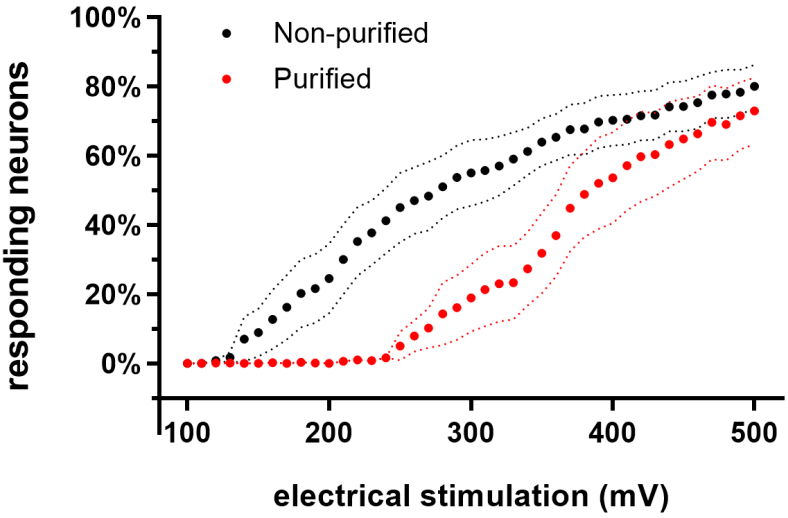

Figure 3.19: Percentage of responding neurons in non-purified and purified DRGs in response to electrical stimulation (n = 28 for non-purified, n= 32 for purified, data expressed as mean ± S.E.M.).

The obtained results would also explain the effects observed previously with agonists experiments on classic MEA: clearly, the ion currents evoked by the application of different agonists are not sufficient to be converted into an action potential in purified DRGs, and the result is, therefore, the absence of recorded responses. This is a further confirmation of what was already shown in the experiments with calcium indicators.

3.2 Exploring the contribution of non-neuronal cells in neuronal excitability

The preliminary results obtained with electrophysiological recordings highlighted the importance of non-neuronal cells' contribution to neuronal excitability. What was still not clear was the extent of this contribution: their physical proximity to neurons may be enough for the neurons' excitability, or it may come from the release of one or more factors in the culture medium.

3.2.1 Culturing DRG neurons with different percentages of glial cells

From the preliminary experiments, we knew that neuronal cells cultured in the absence of their non-neuronal counterpart (100% pure neurons) are not chemically excitable. On the other hand, non-purified neurons, typically composed of 1 neuron every four non-neuronal cells at the time of seeding, are chemically excitable.

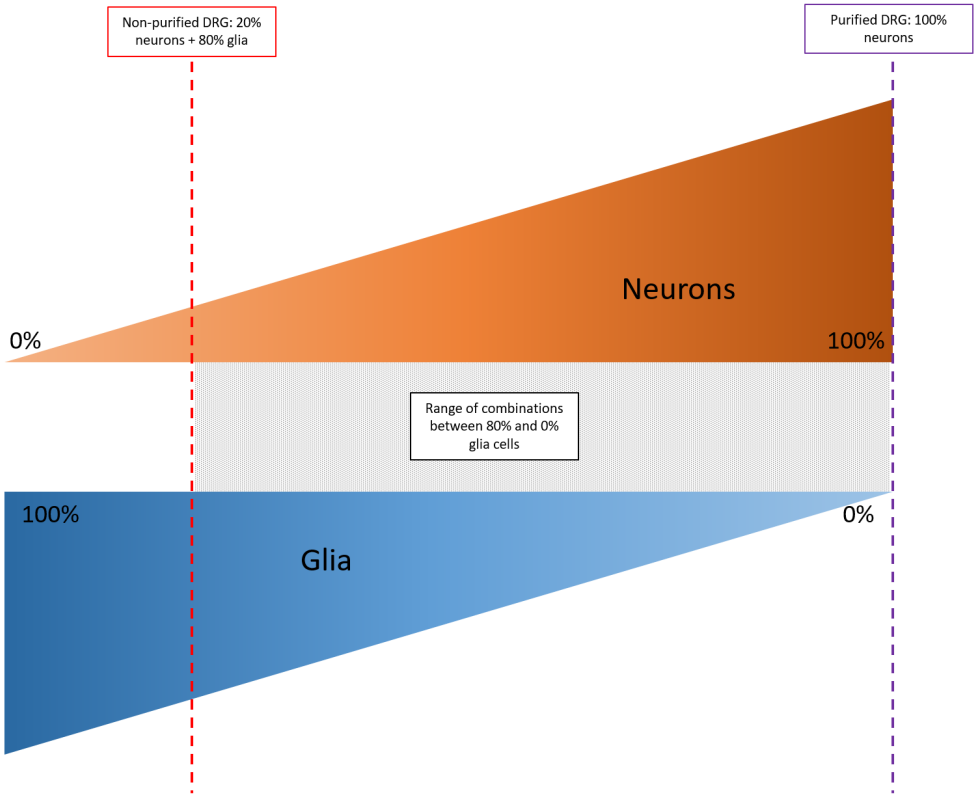

Figure 3.20: Cellular composition of non-purified (red dashed line) and purified (lilac dashed line) DRGs cultures in terms of neurons and glia percentages.

What we do not know is how the neurons behave in terms of excitability in the range between the extreme condition where we do not have any non-neuronal cell (the purified neurons) and the "wild type" condition that comes directly from the dissection, where we have 20% neurons and 80% glial cells (Figure 3.20, grey space). We knew that in non-purified DRGs cultures at 3DIV, approximately 35% of neurons respond to capsaicin. Hence, it is pretty unlikely that by increasing, even more, the non-neuronal portion, there would be a further increase in the excitability. However, we did not know the minimum amount of non-neuronal cells required for neurons to be excitable.

To play around with the concentration of non-neuronal cells, a particular experiment has been set up. After gradient centrifugation, the freshly obtained cell population was split in two: one part was kept as non-purified DRGs culture; on the second part, neuron isolation was performed, and only purified DRGs were obtained. Cells were counted for both populations, and they were mixed in different ratios, keeping the final number of neurons constant but changing the number of non-neuronal cells (Figure 3.21, Table 3.4).

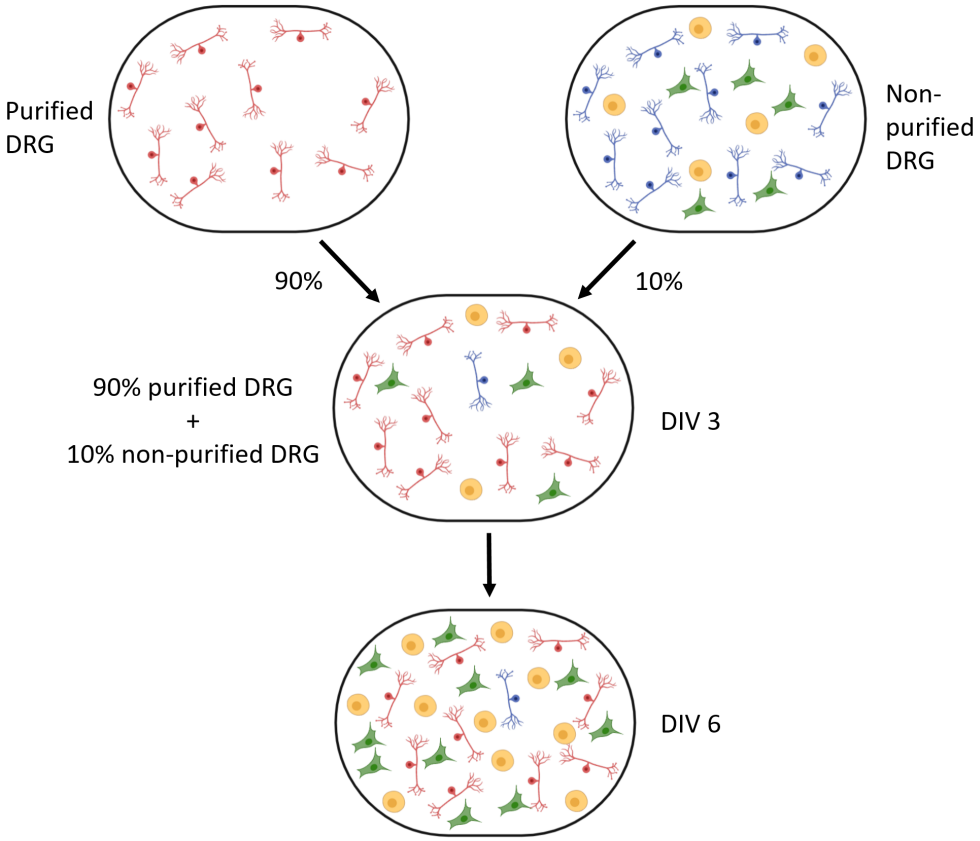

Figure 3.21: Generation of non-purified DRGs cultures with different percentages of glial cells. In this example, the 90% condition is showed and explained (created with BioRender.com).

Condition	Total number of seeded nxeurons	Number of seeded purified DRG	Number of seeded non-purified DRG
Mixed	4,000	0% / 0	100% / 4,000
50%	4,000	50% / 2,000	50% / 2,000
75%	4,000	75% / 3,000	25% / 1,000
90%	4,000	90% / 3,600	10% / 400

Table 3.4: Total number of neurons for the four different conditions.

First of all, the total number of neurons in culture for the four different conditions was checked on the recording day. There was no significant difference between the different groups (one-way ANOVA, F (7, 44) = 0.7353, p = 0.6432), thus demonstrating that the seeding method was consistent (Figure 3.22).

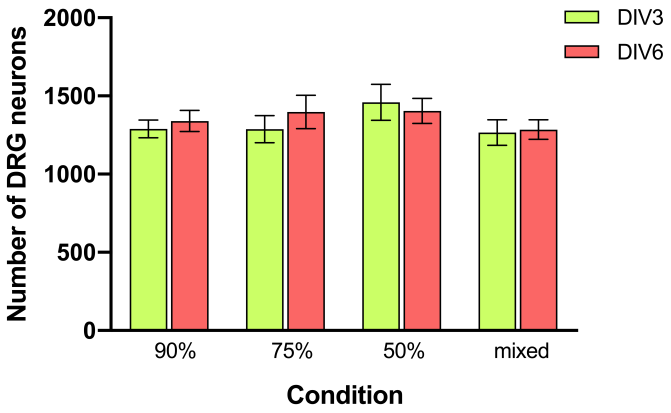

Figure 3.22: Total number of DRG neurons for each condition at the time of recording with 1µM capsaicin (mean ± S.E.M.).

Condition	Time	n	mean ± S.E.M.
90%	3DIV	10	1289 ± 56.61
	6DIV	6	1339 ± 67.58
75%	3DIV	6	1288 ± 86.52
	6DIV	6	1398 ± 107.2
50%	3DIV	6	1459 ± 115.4
	6DIV	6	1404 ± 80.43
mixed	3DIV	6	1265 ± 81.99
	6DIV	6	1285 ± 62.30

Table 3.5: Sample size and number of DRG neurons included in the ROI electrodes area for each condition (data expressed as mean ± S.E.M.; n=number of MEAs).

After validating the seeding protocol by determining the number of seeded neurons, each condition's activity was recorded after 3 and 6 DIV to let the non-neuronal cells proliferate and verify any contribution to neuronal excitability.
The first thing that we can observe is that in the 90% condition (where we have a small number of glial cells at the time of seeding), after 3DIV, the percentage of responding cells is already higher than in the purified neurons without any glial cells in culture (unpaired t-test, $t(1433)=5.851$, $p<0.0001$). This shows that even a tiny amount of glial cells that proliferate with time in culture is sufficient to recover partially the excitability of DRG neurons typically lacking in purified cultures. Also, suppose we let the glial cells proliferate. In that case, we can observe that in the two conditions with the lowest starting number of glial cells (90% and 75%), the percentage of responding neurons significantly increases with time in culture (90%: unpaired t-test, $t(945)=6.793$, $p<0.000.1$; 75%: unpaired t-test, $t(797)=3.381$, $p=0.0008$) (Figure 3.23).

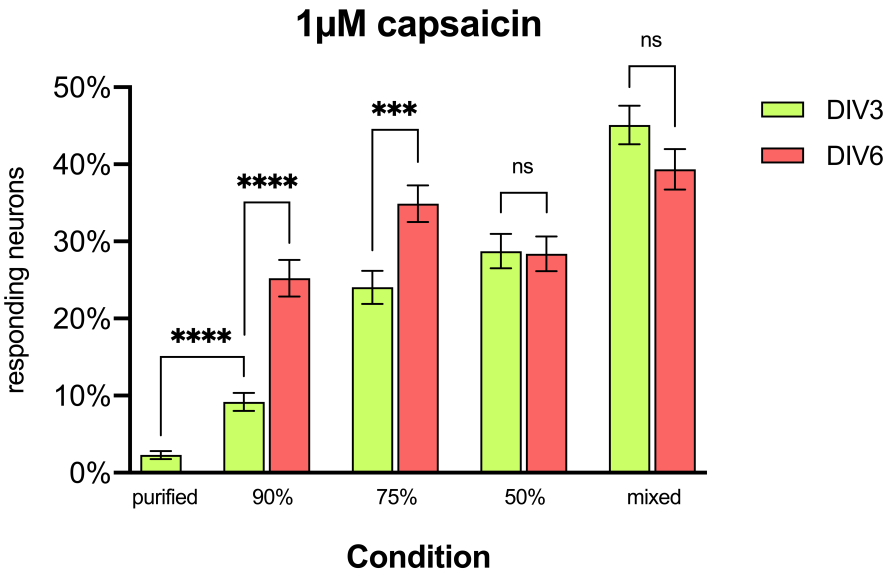

Figure 3.23: Percentage of responding DRG neurons in response to 1µM capsaicin for the different conditions and time-points.

Let us consider only the 90% condition. We can notice a significant difference also between 90% purified and 100% purified DRG neurons after 3DIV (unpaired t-test, $t(1433)= 5851$, $p<0.000.1$), thus demonstrating that even a low amount of glial cells is sufficient for restoring the excitability of DRG neurons.
The proliferation of glial cells with time in culture is confirmed by the ratio glia: neurons; this ratio increases with time in culture due to glial cells' proliferation (Figure 3.24).

The correlation between the presence of glial cells and the excitability of DRG neurons is furtherly confirmed if we plot these two values. We can see that the ratio glia: neurons and the percentage

Condition	Time	n	mean ± S.E.M.
purified	3DIV	825	2.30 ± 0.52
90%	3DIV	610	9.18 ± 1.17
	6DIV	337	25.22 ± 2.37
75%	3DIV	395	24.05 ± 2.15
	6DIV	404	34.90 ± 2.37
50%	3DIV	407	28.75 ± 2.25
	6DIV	405	28.40 ± 2.24
mixed	3DIV	399	45.11 ± 2.49
	6DIV	348	39.37 ± 2.62

Table 3.6: Sample size and percentage of DRG neurons responding to 1µM capsaicin for the different time-points and conditions (data expressed as mean ± S.E.M.; n = number of DRG neurons).

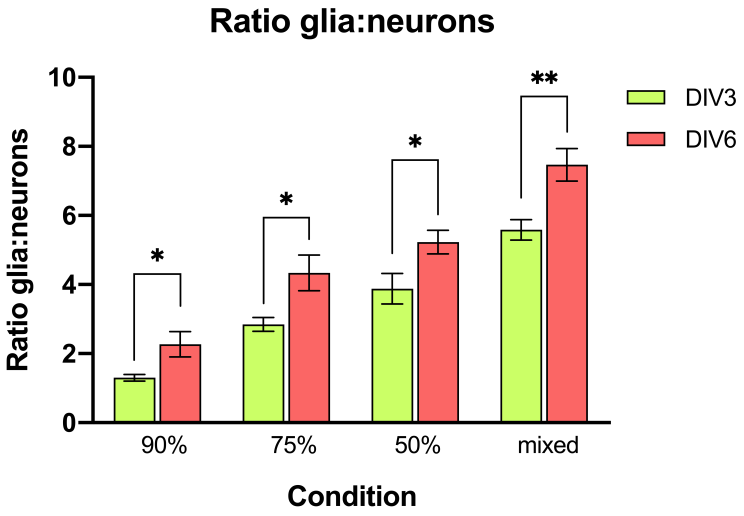

Figure 3.24: Ratio between glial cells and DRG neurons in cultures for different conditions and time in culture.

of responding cells for a given experiment chip were positively correlated with $r(50) = 0.7286$, $p<0.0001$ (Figure 3.25).

This correlation demonstrates that DRG neurons' excitability is strongly dependent on non-neuronal cells' presence and how many of these glial cells are present in the culture.

Condition	Time	n	mean ± S.E.M.
90%	3DIV	10	1.30 ± 0.09
	6DIV	6	2.27 ± 0.37
75%	3DIV	6	2.85 ± 0.20
	6DIV	6	4.34 ± 0.51
50%	3DIV	6	3.88 ± 0.44
	6DIV	6	5.23 ± 0.34
mixed	3DIV	6	5.57 ± 0.30
	6DIV	6	7.47 ± 0.47

Table 3.7: Sample size and mean ratio between glia and DRG neurons for different conditions and time points (data expressed as mean ± S.E.M.; n = number of MEAs).

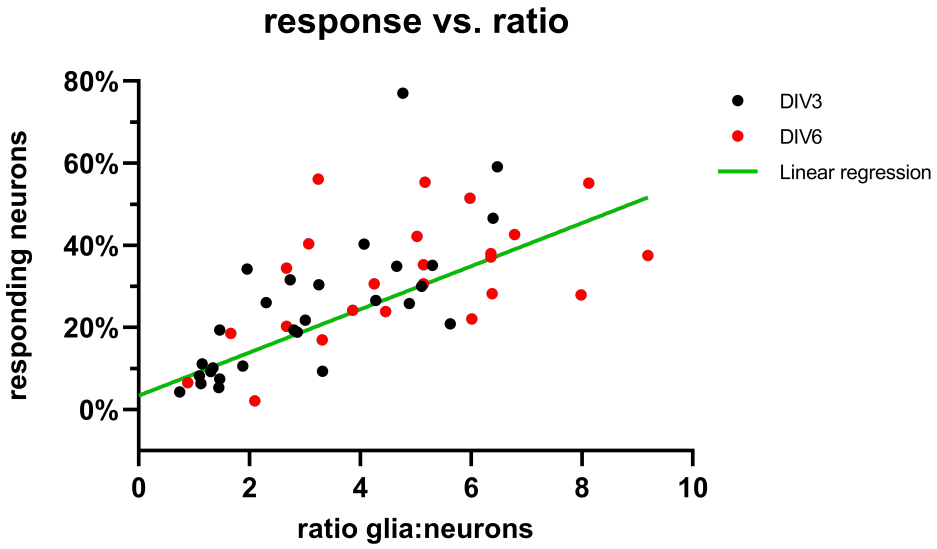

Figure 3.25: Positive correlation between ratio glia:neurons and percentage of responding neurons. Each dot corresponds to one MEA.

3.3 Investigating the non-neuronal population

All experiments performed so far confirmed the hypothesis that non-neuronal cells play a crucial role in neuronal excitability; however, it was still unclear how exactly this interaction between neurons and glia affects neurons' excitability. In particular, whether the contribution comes from a single non-neuronal cell type or instead from the heterogeneous population. Therefore, the next step consisted of investigating this non-neuronal population, which cell types it is composed of, and its relation to neurons.
As already mentioned before, non-neuronal cells consist of a heterogeneous population derived from the primary culture's initial preparation. We can expect Schwann cells for sure, and a small portion of satellite glial cells [63], and some fibroblasts, and probably some blood cells.

3.3.1 Identification of non-neuronal cell subtypes via ICC/IF

One of the most used techniques for identifying different cell subpopulations is represented by ICC ICC. This technique is based on the use of different antibodies directed against antigens, which expression should be limited to specific cell types. One application of ICC is immunofluorescence (ICC/IF). Here, the detection is based on fluorescent molecules linked directly to the antibodies directed against the desired antigens (direct fluorescence) or secondary antibodies that recognize the primary antibodies (indirect fluorescence). This second method is preferred because it significantly increases the fluorescence signal [64].
As Schwann cells cover an essential role in the peripheral nervous system due to their myelination properties, it was decided to look for this cell subtype first. Schwann cells express different markers that change according to their development stage. For example, it is reported that Schwann cells express the astroglial marker GFAP during their non-myelinating phase [65]. One marker ubiquitously expressed, independently on their stage, is S100b [33]. For staining DRG neurons, beta-III-tubulin was chosen [66]. In non-purified DRG cultures at 3DIV, Schwann cells have been identified thanks to the expression of the marker GFAP (Figure 3.27, B, 3.28, F), reported in the literature as a marker for glial cells in particular non-myelinating Schwann cells [65]. In contrast to what was reported in the literature, S100b provided unspecific staining of Schwann cells (Figure 3.27, A, 3.28, E) [33, 67]. Previous studies already questioned whether S100b is a suitable marker for staining Schwann cells [68], and the results obtained with this ICC confirmed these concerns. It can be noticed how a small neuronal portion also expresses S100b (Figure 3.27, 3.28, white stars), thus demonstrating how its expression is not selective for Schwann cells only.

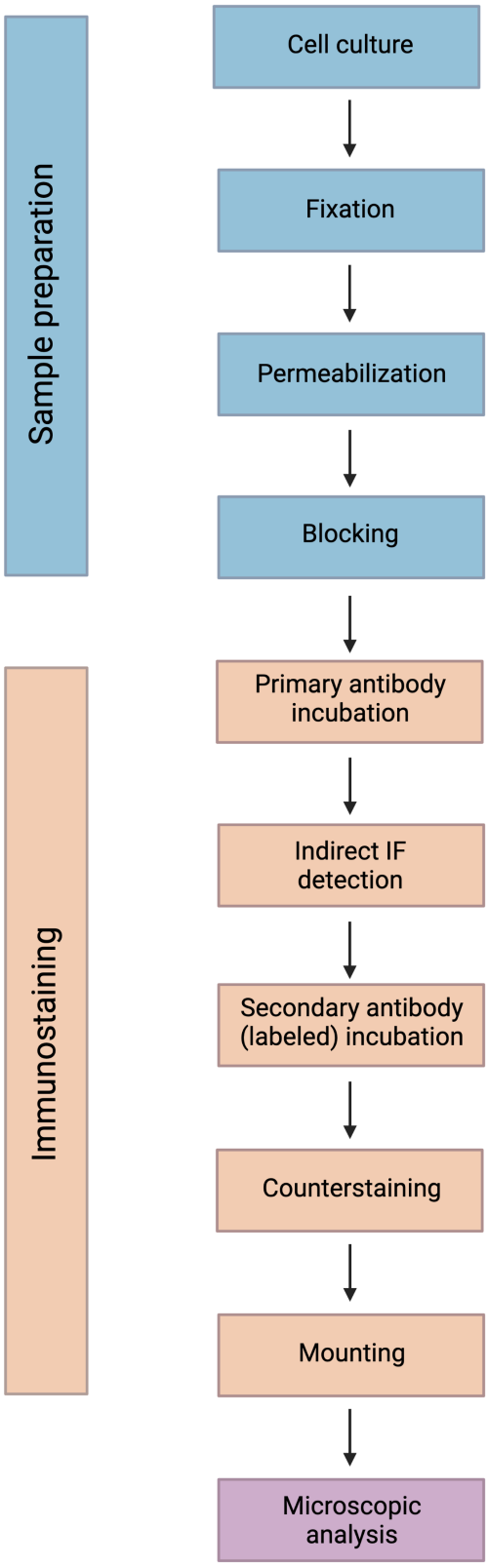

Figure 3.26: General workflow for ICC/immunofluorescence (ICC/IF) (created with BioRender.com).

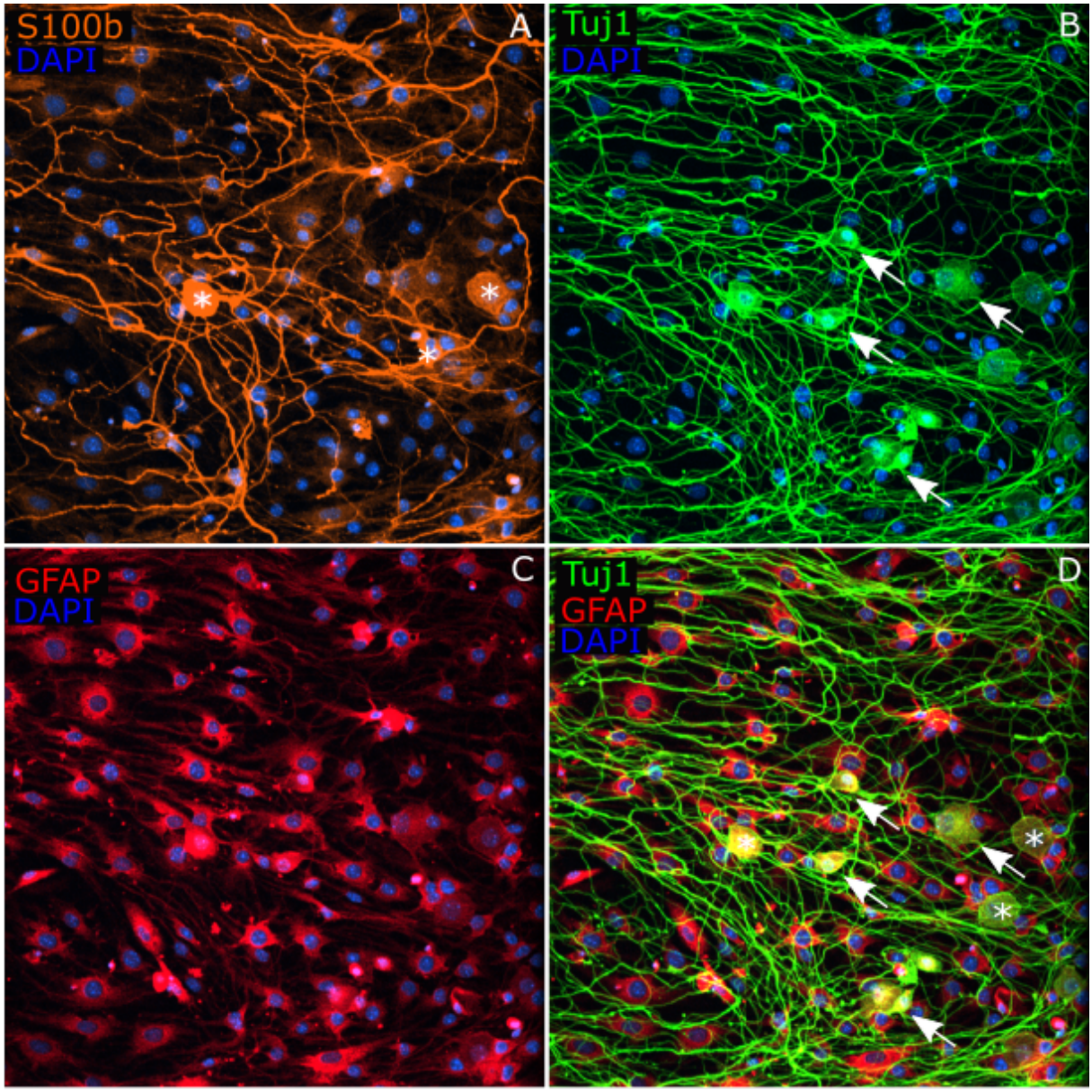

Figure 3.27: Non-purified DRG neurons 3DIV stained for S100b (orange, A), GFAP (red, B), Tuj1 (green, (C), and merged (D). White arrows indicate DRG neurons soma; white stars indicate DRG neurons soma stained for S100b. Area focused on the center of the culture plate, to show both neurons and glial cells

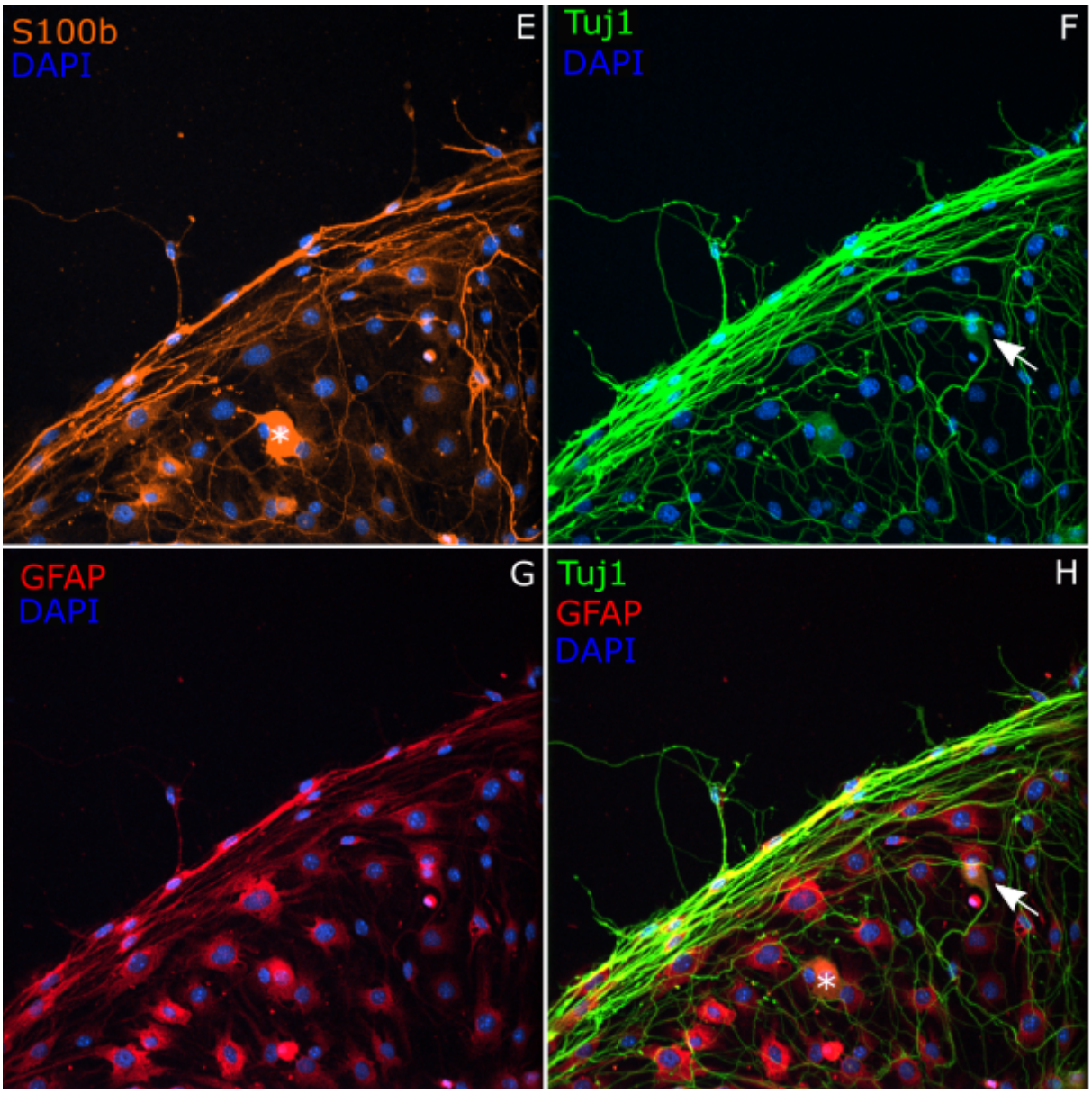

Figure 3.28: Non-purified DRG neurons 3DIV stained for S100b (orange, E), GFAP (red, F), Tuj1 (green, G), and merged H). White arrows indicate DRG neurons soma; white stars indicate DRG neurons soma stained for S100b. Area focused on the borders of the cell culture, to highlight the presence of glial cells

By analyzing in detail the composition of the different cell types, it can be noticed how DRG neurons represent a small fraction of the overall population compared to glial cells' contribution (Figure 3.29, red bars).

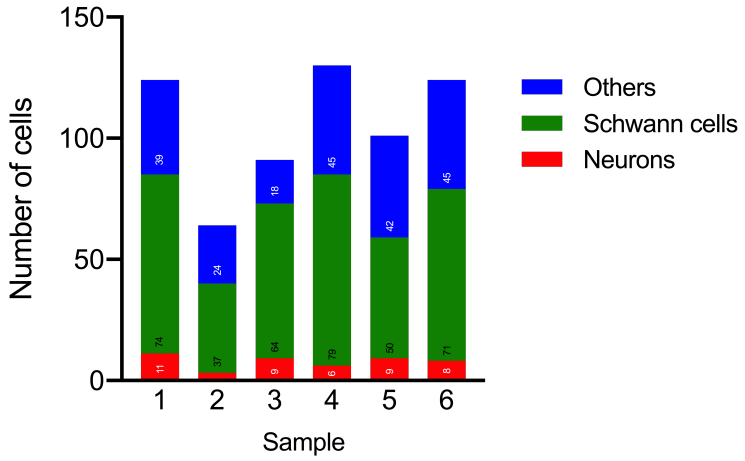

Figure 3.29: Number of Schwann cells, DRG neurons, and other glial cells for six different non-purified DRGs samples after 3DIV.

By looking into the detailed composition of the non-neuronal fraction, it can be noticed that for all samples, Schwann cells represent up to 75% of the glial cells in the whole glial cells population (Figure 3.30, red bars).

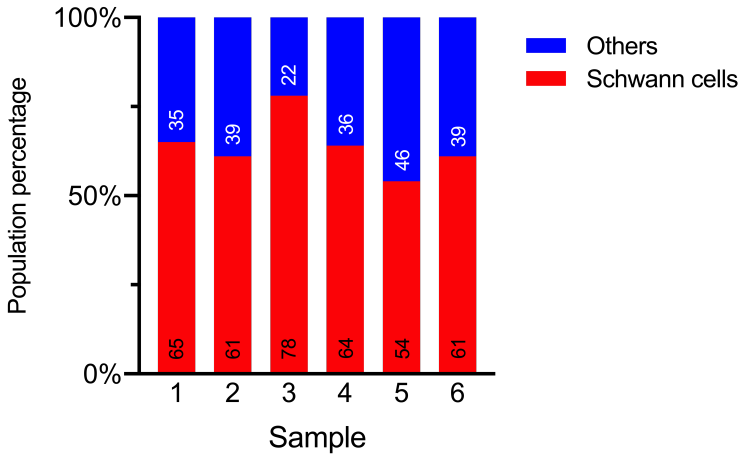

Figure 3.30: Representation of the percentages of Schwann cells over the total glial population.

This demonstrated that Schwann cells constitute the significant subpopulation in the fraction of the glial cells in non-purified DRGs.

3.3.2 Generation of non-neuronal cells monocoltures via MACS

Despite the encouraging results obtained with ICC, to investigate the non-neuronal cells, it was still necessary to sort this heterogeneous population into the different cell types that constitute it.

One of the most used techniques for sorting a heterogeneous cell population into single-cell subpopulations is FACS. This technique exploits the fact that different cell types express unique membrane receptors that can be recognized by specific antibodies conjugated to a fluorophore. Cells are then analyzed using lasers and detectors and separated according to their fluorescence characteristics and light scattering [69]. However, the lack of well-established and specific surface markers for glial cells makes this technique unsuitable for this particular cell population.

An alternative to FACS but similar is represented by MACS, the same technology used routinely to isolate pure DRG neurons. Here, primary non-purified DRG neurons freshly isolated are incubated with one or more antibodies against one specific type of non-neuronal cell. The cell suspension is then applied to a magnetic column, and the labeled cells are captured thanks to the magnetic interactions between the column itself and the magnetic beads attached to the cells [63].

For this purpose, two different sets of antibodies have been used. The first one consisted in four commercially available antibodies that recognized four different types of non-neuronal cells:

Antibody	Cell recognized
Anti-O4	Oligodendrocytes/Schwann cells
Anti-ACSA-2	Astrocytes
Anti-CD31	Mature endothelial cells
Feeder removal	Fibroblasts

Table 3.8: List of the four Miltenyi commercial antibodies and their respective targets to isolate single types of non-neuronal cells.

The first setup consisted of incubating freshly isolated non-purified DRGs with three of the four antibodies; thus, it was expected to obtain a co-culture constituted by neurons and one non-neuronal cell type recognized by the missing antibody. For example, incubation with all antibodies except the anti-O4 should have led to a culture constituted by DRGs and Schwann cells only.

However, as we can notice from the culture picture, there was no apparent difference between the different cultures (Figure 3.31). Even though the statistical analysis evidenced a significant difference (one-way ANOVA, $F\ (4, 2292) = 4.360$, $p = 0.0016$), this difference does not emerge clearly from any of the antibodies used (Figure 3.32).

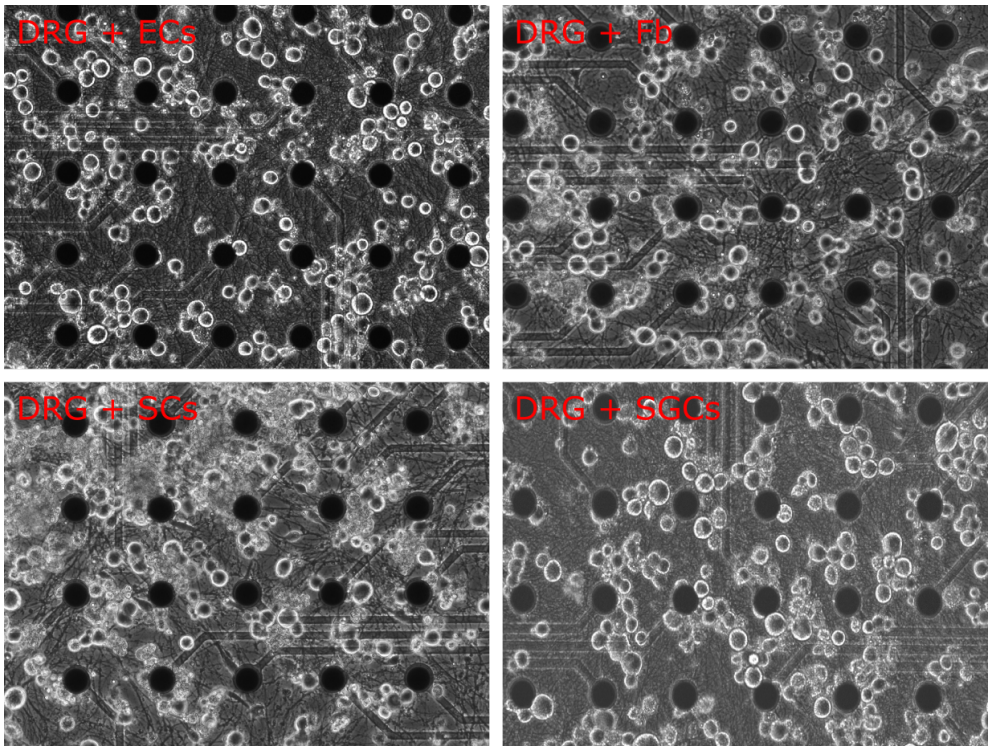

Figure 3.31: Co-cultures of DRG neurons with one type of non-neuronal cell. ECs: endothelial cells; Fb: fibroblasts; SCs: Schwann cells; SGCs: satellite glial cells.

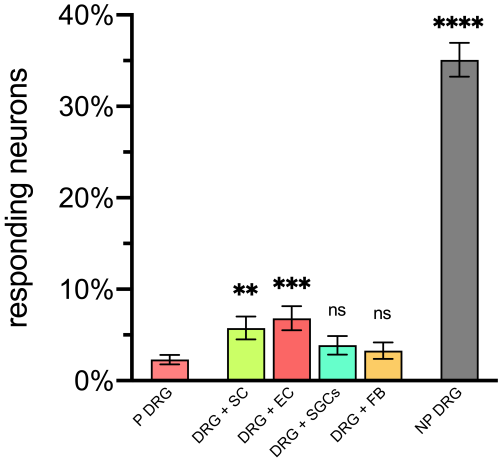

Figure 3.32: Percentage of responding DRG co-cultured in different conditions to 1µM capsaicin after 3DIV (data expressed as mean ± S.E.M.). SC: Schwann cells; EC: endothelial cells; SGCs: satellite glial cells; FB: fibroblasts.

Co-Culture	n	mean ± S.E.M.
Purified DRG	825	2.30 ± 0.52
DRG+SC	347	5.76 ± 1.25
DRG+EC	366	6.83 ± 1.32
DRG+SGCs	263	3.87 ± 1.01
DRG+FB	397	3.27 ± 0.89
Non-purified	664	35.09 ± 1.85

Table 3.9: Sample size and percentage of DRG neurons responding to 1µM capsaicin for the different co-cultures (data expressed as mean ± S.E.M.; n = number of DRG neurons).

Since the approach that implied commercial antibodies' use did not provide any significant result, a second setup was designed. This design was based on the use of the antibodies contained in the commercial Neuron Isolation Kit; as the kit was working well in depleting non-neuronal cells, it meant that the kit's antibodies were effective in recognizing non-neuronal cells.
As the exact composition of the kit is protected by a trade secret, we request the manufacturing company (Miltenyi Biotec GmbH) if they could provide us with the single antibodies, but without revealing their names or targets, and with the disclosure that we will not do any further analysis for determining their structure. Three "custom antibodies" were obtained in a known concentration and titrated in different ways.
The Neuron Isolation Kit's actual concentrations were not provided due to the trade secret and therefore needed to be defined. For each antibody, four different concentrations were tested, starting from 0.1µg/100µl down to 0.0001µg/100µl, with a 10X dilution for each step.
High concentrations of each antibody lead to the complete depletion of non-neuronal cells, thus obtaining a pure DRGs culture. On the other hand, the first concentration low enough for not depleting completely non-neuronal cells did not have any visible effect. The obtained culture resembles a non-purified DRGs culture (Figures 3.33, 3.34, and 3.35). This highlighted two significant issues: the first problem was that there was a cross-reactivity between the antibodies, explained by the fact that each of the antibodies used singularly in sufficiently high concentrations leads to the same results as that obtained with the mixing of the three antibodies in the Neuron Isolation Kit, that was, the complete depletion of all non-neuronal cells. The second issue was linked to the previous one and corresponded to the titration of each antibody: testing few concentrations of the single antibodies was already time-consuming, and even though two concentrations were defined as the minimum and the maximum needed for depleting completely or not depleting at all non-neuronal cells, the further titration between those two concentrations to determine the exact one that would deplete only one type of non-neuronal cell would have also required a significant amount of time, and therefore not feasible in the short-term.

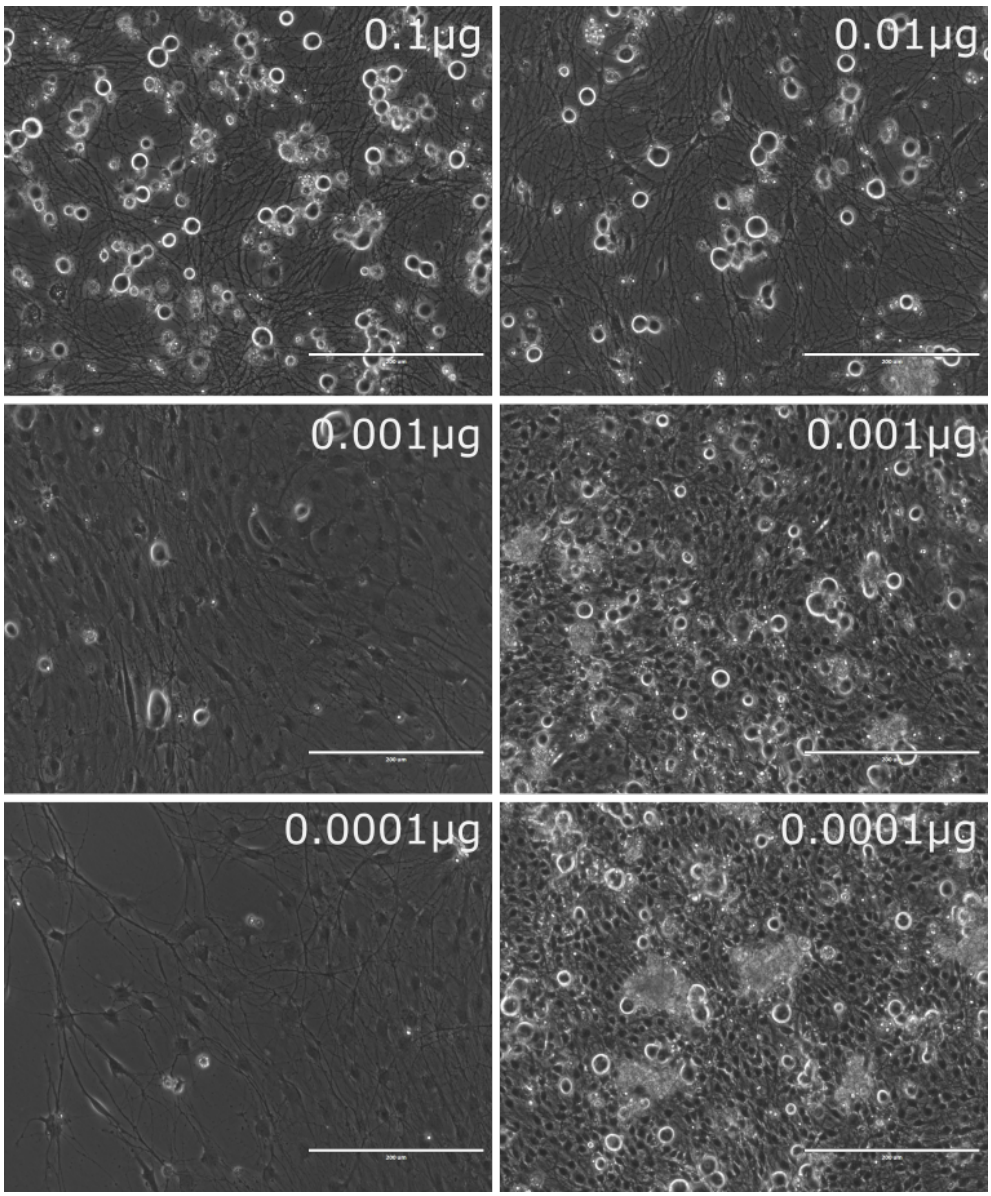

Figure 3.33: Titration results for Custom Antibody nr. 1. 286 DRG/mm^2 6DIV.

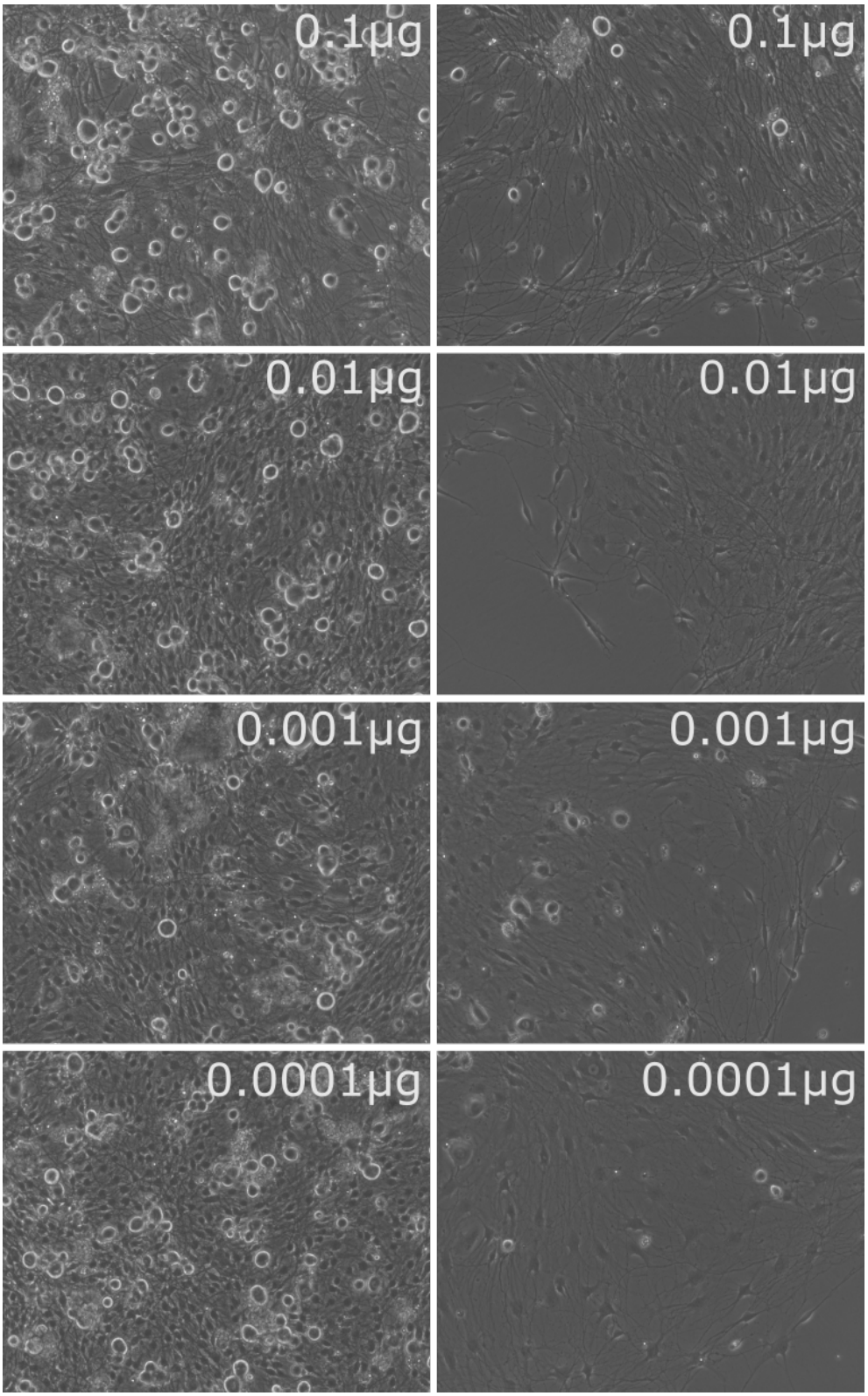

Figure 3.34: Titration results for Custom Antibody nr. 2. 286 DRG/mm^2 5DIV.

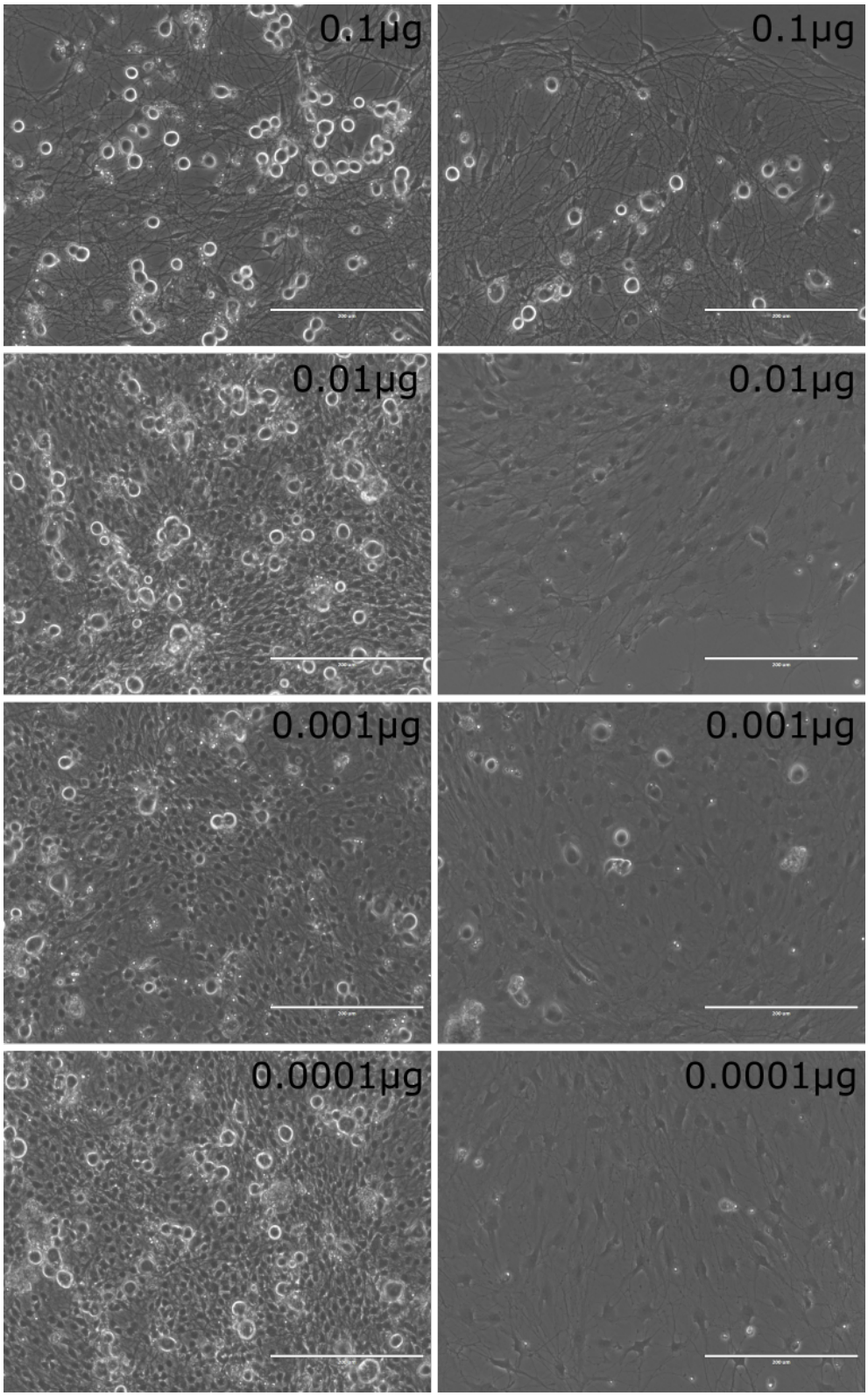

Figure 3.35: Titration results for Custom Antibody nr. 3. 286 DRG/mm^2 6DIV.

Despite the suboptimal results obtained from the titration of the antibodies, two different experiments were designed. In the first one, primary dissociated cells were incubated with one of the three enzymes, as in the titration experiments; thus, non-purified cultures were depleted of only one type of non-neuronal cells (Figure 3.36).

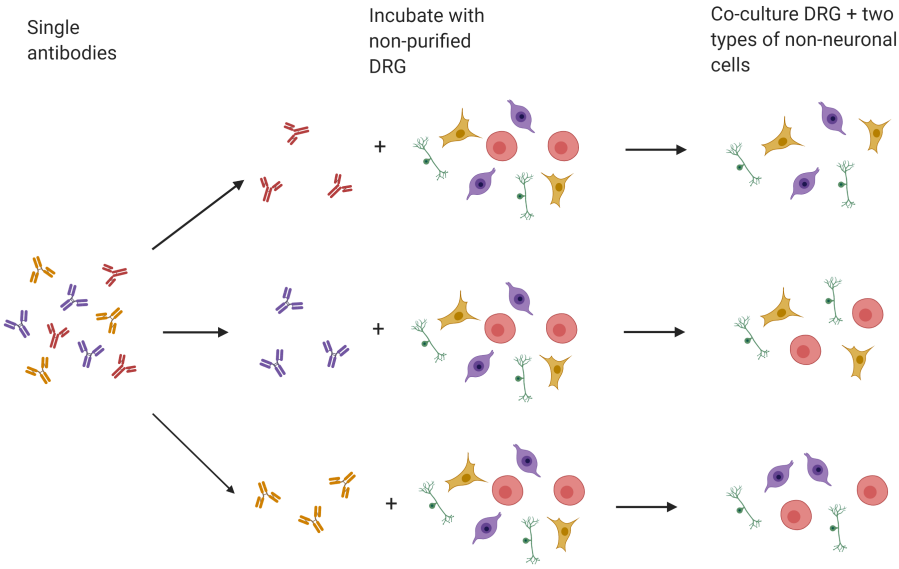

Figure 3.36: Schematic representation of the first experimental set-up (created with BioRender.com).

The number of antibodies used was 0.3µg for antibodies 1 and 2 and 1µg for antibody 3; cells were visualized after 1, 3, and 9 DIV to verify any differences in the non-neuronal population among the three different conditions. No apparent difference could be appreciated between the three different conditions (Figure 3.37).
Furthermore, for the first antibody, the concentration of non-neuronal cells in culture seemed lower than the other two antibodies (Figures 3.38, 3.39, and 3.40).

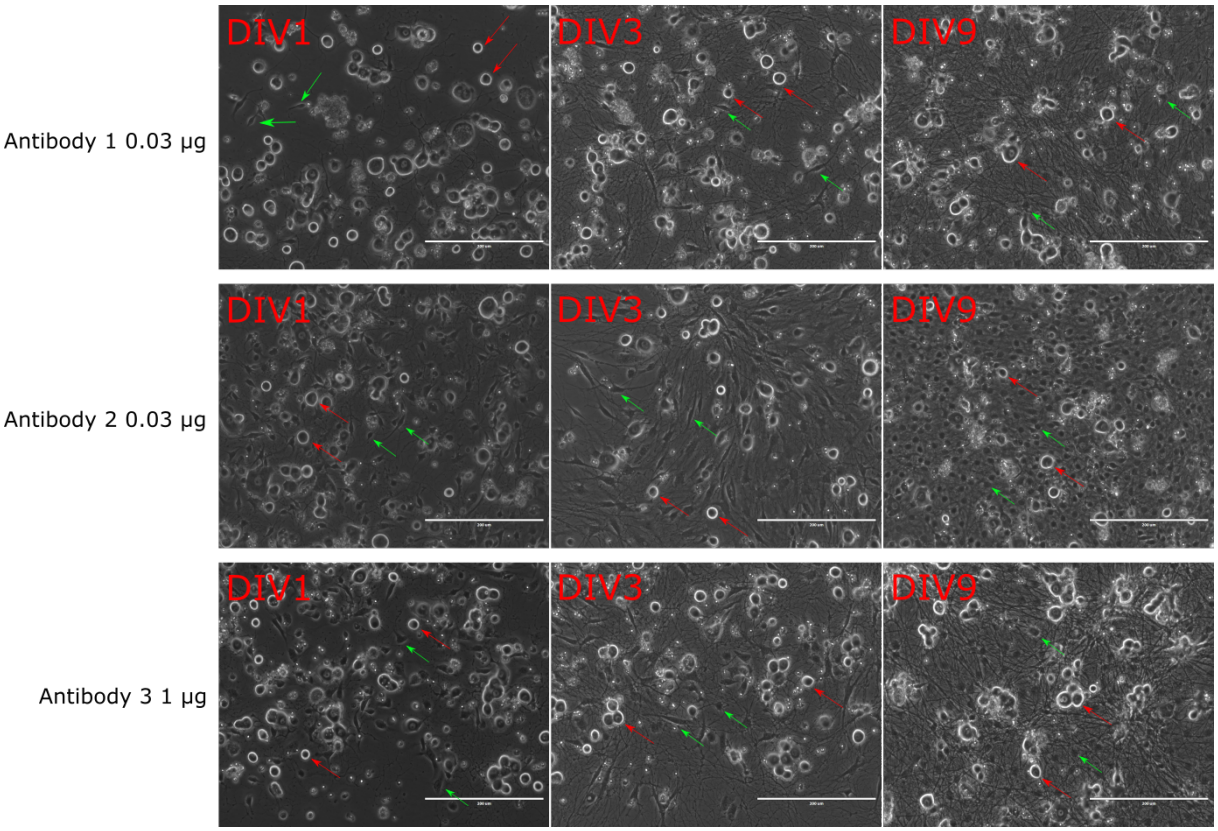

Figure 3.37: Summary of the three antibodies at different time points. Red arrows indicate DRG neurons; green arrows indicate glial cells.

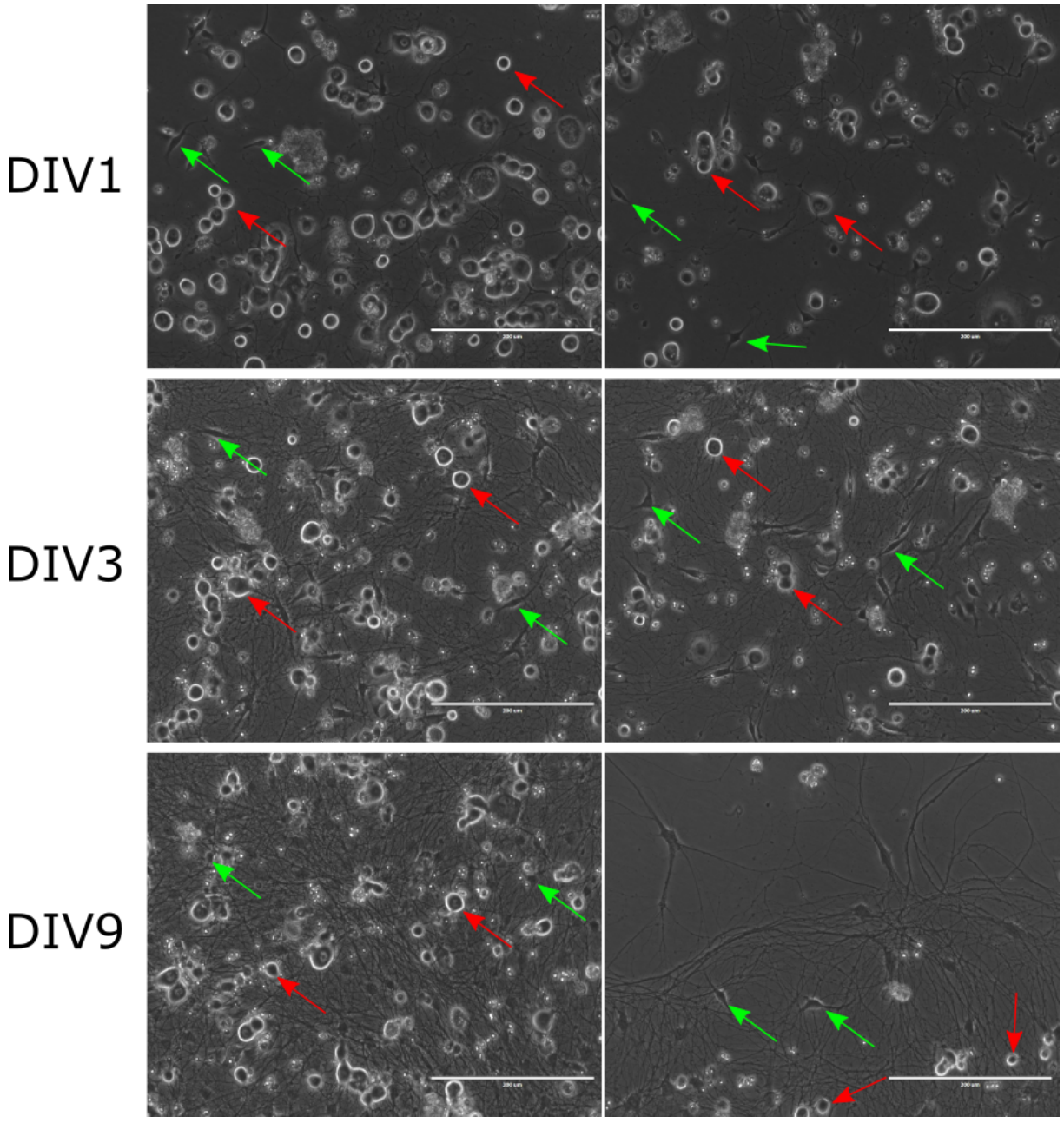

Figure 3.38: DRG incubated with 0.03µg of antibody 1. Green arrows: glial cells; red arrows: DRG neurons.

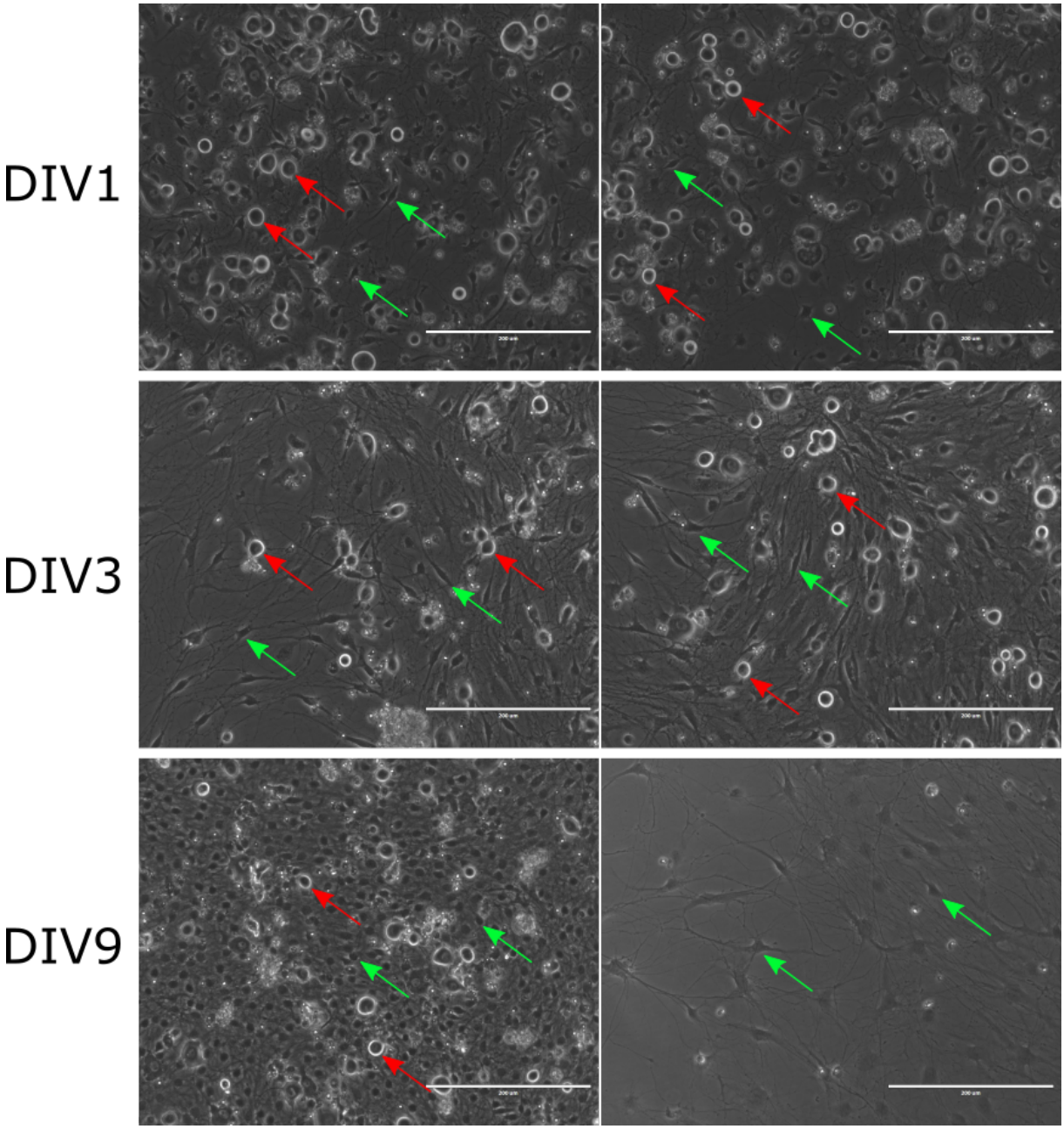

Figure 3.39: DRG incubated with 0.03 µg of antibody 2. Green arrows: glial cells; red arrows: DRG neurons.

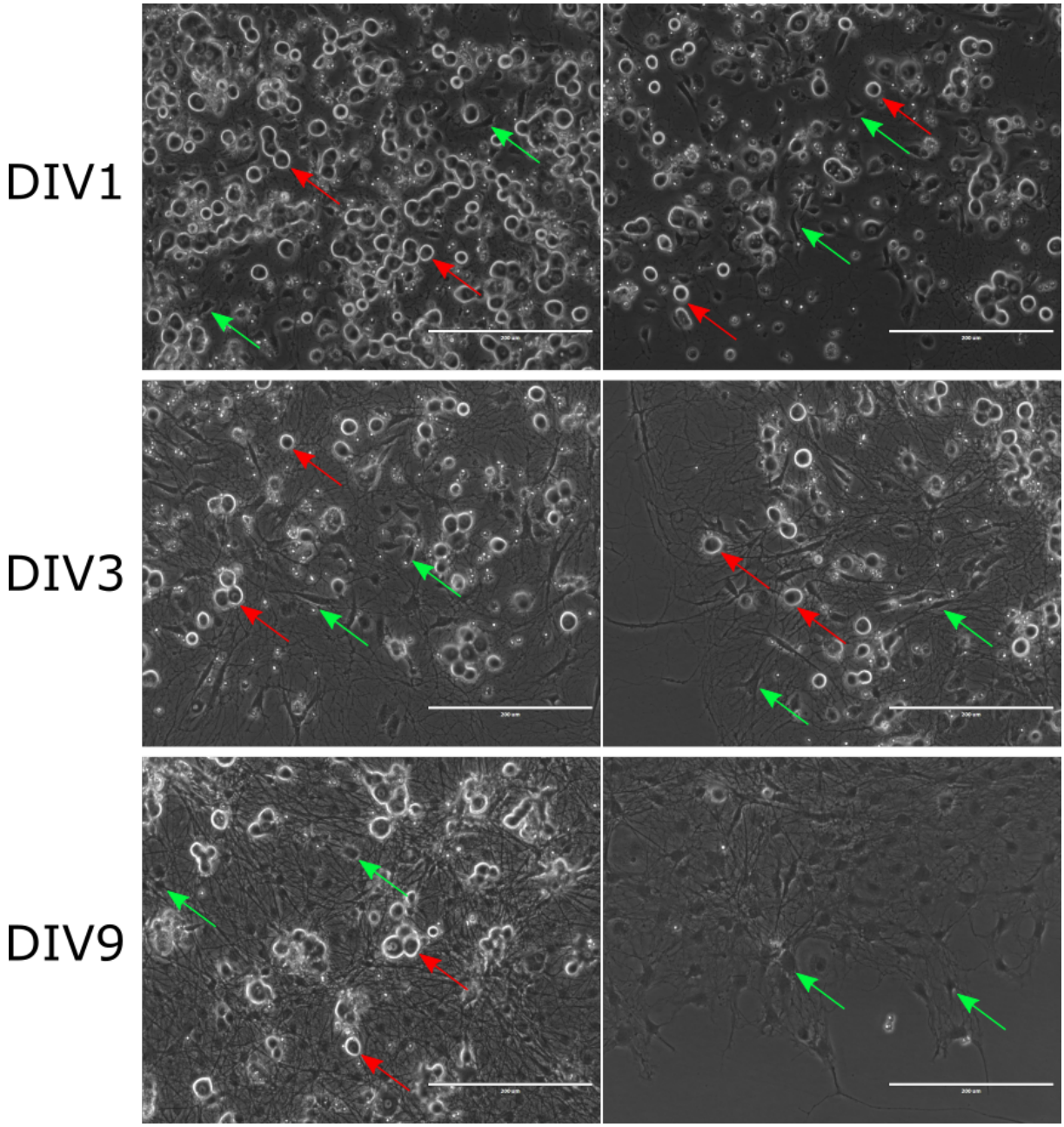

Figure 3.40: DRG incubated with 1µg of antibody 3. Green arrows: glial cells; red arrows: DRG neurons.

In the second experiment, cells were incubated with two out of three antibodies, generating a co-culture of DRG neurons plus one type of non-neuronal cells (Figure 3.41).

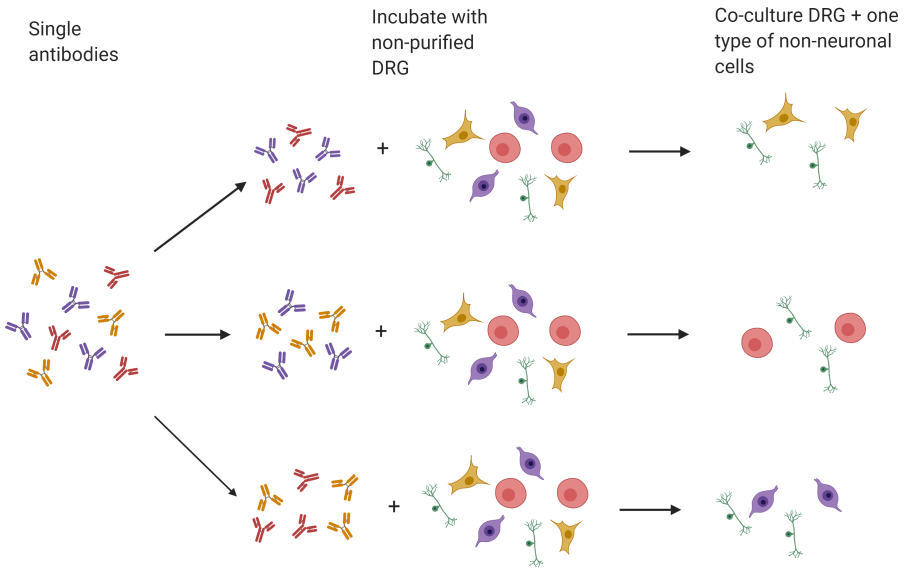

Figure 3.41: Schematic representation of the second experimental set-up (created with BioRender.com).

The concentration of antibodies used was the same used in the first experimental setup.
Once again, there was no apparent difference between the three different combinations of antibodies in non-neuronal cell morphology and concentration (Figure 3.42). From the two experimental setups, we expected to obtain co-cultures of DRGs and all glial cells except one subtype (Figure 3.41) or co-cultures of DRGs and one type of glial cells (Figure 3.36) to seed these co-cultures on MEA and observe any differences in neuronal excitability. Ideally, neuronal excitability should have been restored when DRG neurons were cultured in the presence of one specific type of non-neuronal cell (experiment one). Simultaneously, the excitability should have dropped when non-purified DRGs were depleted of the same kind of non-neuronal cell (experiment two). However, as the preliminary experiments showed no clear distinction between the different antibodies, experiments on MEA were not performed. The approach of isolating single non-neuronal cell types via MACS technology was not further pursued.

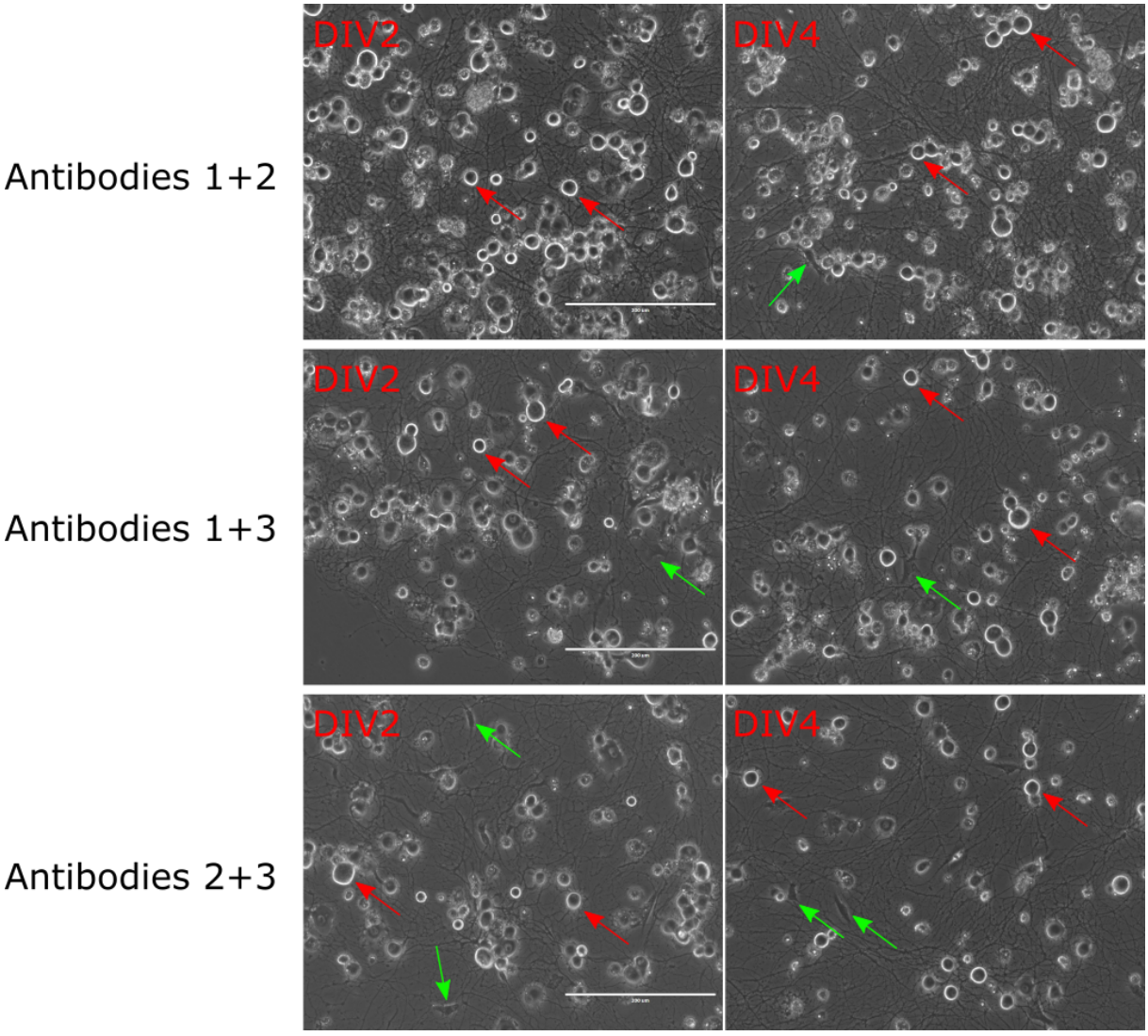

Figure 3.42: DRGs incubated with different combinations of antibodies. Green arrows: glial cells; red arrows: DRG neurons.

3.3.3 Generation of non-neuronal cells monocoltures via limiting dilution

Basing on the unsuccessful outcome from the first experimental setup involving MACS technology, a second approach was designed. This second approach was based on the application of the pure technical principle of limiting dilutions. Starting from a cell suspension with a defined concentration, the suspension is then seeded subsequentially; between one seeding and the following one, the concentration is diluted by a known factor. By keeping diluting the cells, the final concentration plated would be of only 0.5 cell/well. As it is impossible to plate only half a cell per well, we have to consider this as the average number of cells plated per well; therefore, some wells will have no cells, while some will have one cell/well. All the wells with only one cell/well will then generate a single clone colony [70] (Figure 3.43).

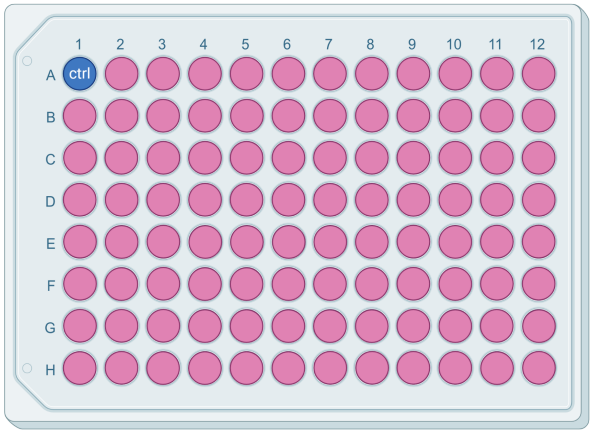

Figure 3.43: Preparation of a single colonies 96-well plate. The top-left control well is needed for setting the focus while checking the cells proliferation with a microscope. Cells were seeded in modified Neurobasal-A medium for non-neuronal cells (created with BioRender.com).

The medium was changed regularly, and cells were left to proliferate. After 14 days, each well was checked under a light microscope and categorized accordingly to the following scheme:

- White: wells with no colony; not considered.
- Red: wells with two or more colonies; not considered.
- Yellow: wells with at least one clear colony and a probable second colony; considered with reserves.
- Green: wells with only one colony; considered.

The cloning protocol worked well; 25 out of 95 wells (26%) had a colony generated by a single cell, thus a single clone colony (Figure 3.44). However, after two weeks, the colonies stopped

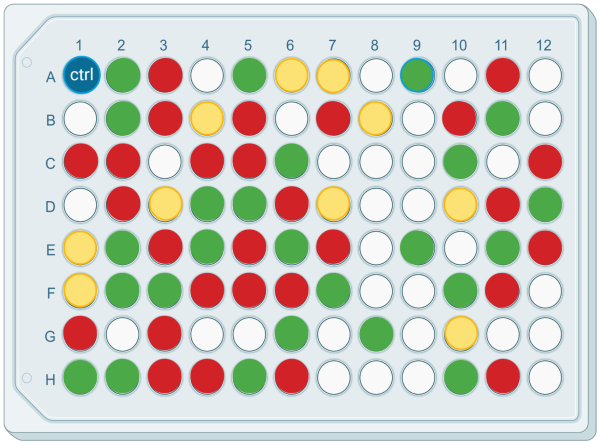

Figure 3.44: After 14 DIV, single clone colonies are visible under the microscope, and each well is categorized according to the previously described criteria (created with BioRender.com).

proliferating, even though the medium used was enriched with 10% FBS to promote glial proliferation. After further two weeks (a total of four weeks since the seeding date), no other change was noticed in the colonies, and therefore the experiment was not carried on anymore.
Even though there was initial success in generating single clone colonies, the inhibition in the proliferation of the single colonies, despite the presence of serum in the culture medium, lead to the decision not to perform further experiments with single clone colonies.

3.3.4 Expansion of non-neuronal population via low-density seeding

All the experiments performed to obtain cultures of single non-neuronal cells did not provide the desired results. One possible alternative way to expand the non-neuronal component for further identifying its cellular components is seeding non-purified DRGs in low density and letting them proliferate [71].
This protocol induced glial cells' proliferation over DRG neurons, basing on neurons and glial cells' characteristics. When DRG neurons are seeded in low-density, their survival is inhibited thanks to the low-density. At the same time, glial cells can proliferate. The absence of serum in the culture media was essential to recreate the same conditions encountered in non-purified DRG neurons. In this way, any results should reflect what happens in those non-purified DRGs cultures. Even though serum promotes high proliferation of glial cells, results obtained in the absence of serum in cell proliferation, distribution, and viability were satisfactory and sufficient for the following experiments.
For this experiment, non-purified DRG neurons were seeded in low-density, and the glial cells were let proliferating for at least one week (Figure 3.45).

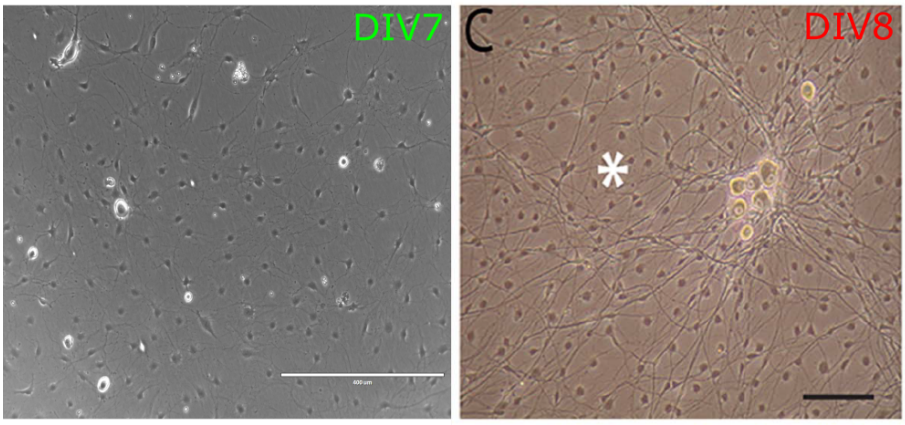

Figure 3.45: Non-purified DRGs seeded in low-density (left) generates cultures of glial cells that resemble those reported in literature (right, modified from [71]).

To verify the subtypes of glial cells present in the low-density cultures, ICC was performed. The antibodies used were the same used in three days non-purified DRGs cultures. Despite a still massive presence of neurites, the somata number is significantly lower than any other cell type. This shows that DRG neurons represent a minor fraction of the overall cell population (Figure 3.46, white arrows), constituted mainly by non-neuronal cells (Figure 3.46, A). Compared to cells cultures after 3DIV, the number of soma expressing s100b is significantly reduced.
Furthermore, the expression of S100b appears to be slightly higher than after 3DIV. Surprisingly, GFAP appears no longer in glial cells after 8DIV than 3DIV cultures (Figure 3.46, C). Together with the increased expression of S100b, this is consistent with previous studies that demonstrated that S100b inhibits the expression of GFAP in glial cells [65, 72, 73].

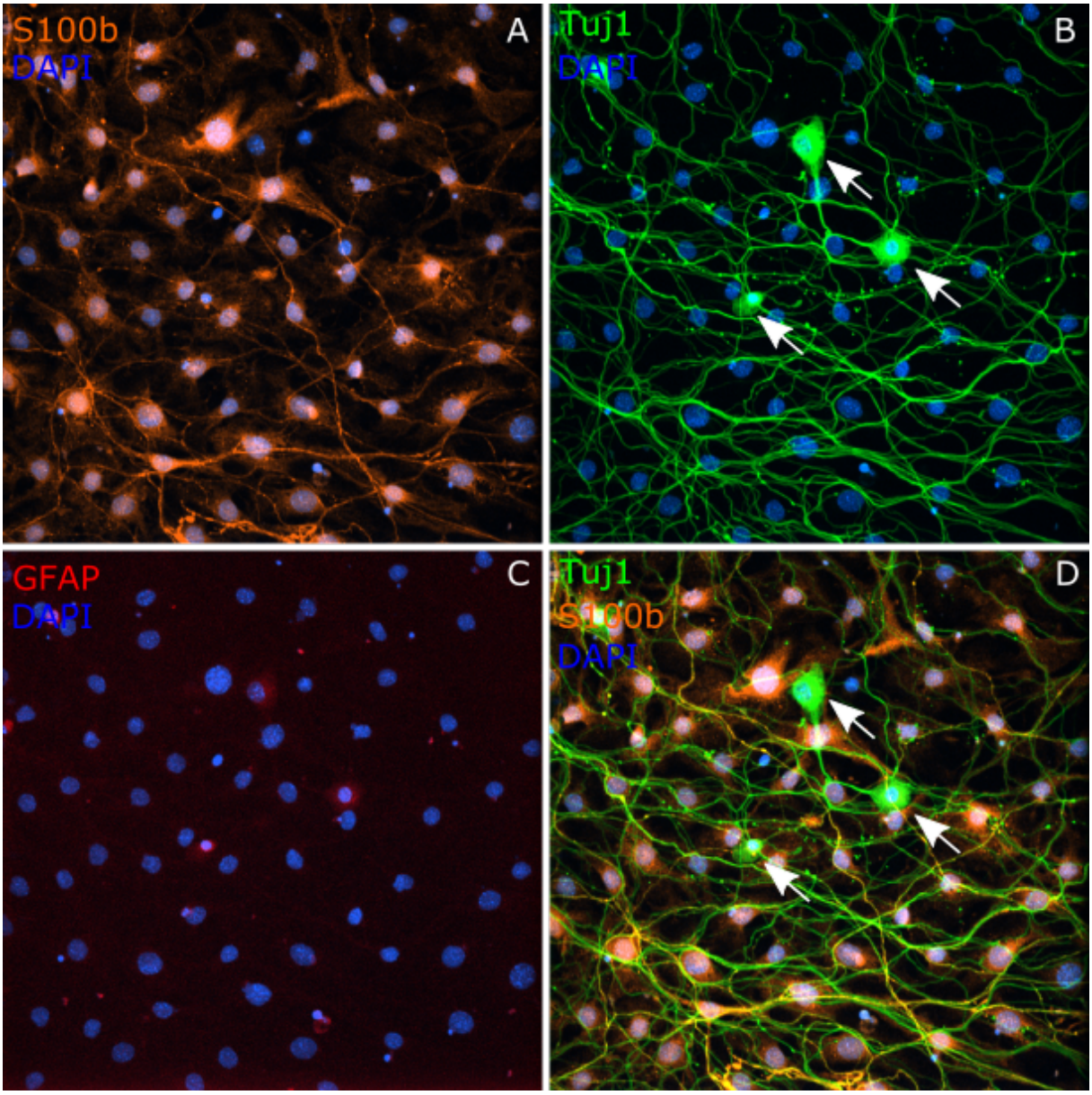

Figure 3.46: Low-density DRG (37 DRG/mm2) 8DIV stained for S100b (Schwann cells, red, A), beta-III-tubulin (green, soma and neurites, B), GFAP (astroglia, orange, not stained, C), and merged (D), 20X single field. White arrows indicate DRG soma.

3.3.5 Co-culturing purified DRG neurons with immortalized mouse Schwann cells (IMS32)

To overcome the issue encountered in the single clone experiments, and considering the results previously obtained with ICC, it was decided to purchase an immortalized cell line of mouse Schwann cells [74, 75]. In this way, it would have been possible to obtain enough Schwann cells and co-cultured them with purified DRGs.
Cells were handled according to the manufacturer's indication (previously described in the Methodology section). After several subculturing passages, the cells looked nice and well-growing on the pre-coated flasks provided by the manufacturer (Figure 3.47).

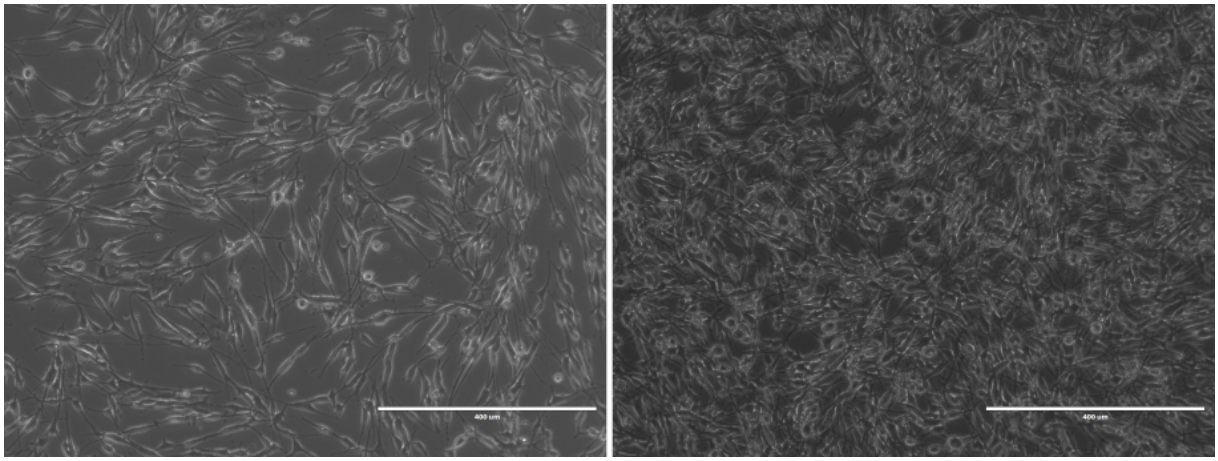

Figure 3.47: P4 immortalized mouse Schwann cells (IMS32) growth on PriCoat™ T25 flask, cultured with modified Prigrow III medium, 200 cells/mm2, 1DIV.

As DRG neurons required different coating and medium, various tests were carried on the IMS32 cell line to understand whether they would keep their viability with non-ideal culturing conditions. We can notice how the polyethyleneimine-laminin coating provides worse results than when pre-coated flasks were used (Figure 3.48). In terms of culture medium, modified Prigrow seems to give better results in cell proliferation compared to modified Neurobasal-A medium for DRG; however, it can be noticed how cells tend to clump and not distribute homogeneously (Figure 3.49).
Despite the results obtained during the testing of the different coatings and culture mediums, IMS32 cells were co-cultured with purified DRG on MEA to record the electrical activity after 3DIV.
The day following the plating, the co-cultures grown with modified Prigrow III medium seemed viable and well-distributed among the electrodes (Figure 3.50a). The cultures that were grown in the presence of modified Neurobasal-A medium for DRGs also showed a good distribution of the cells (Figure 3.50b).

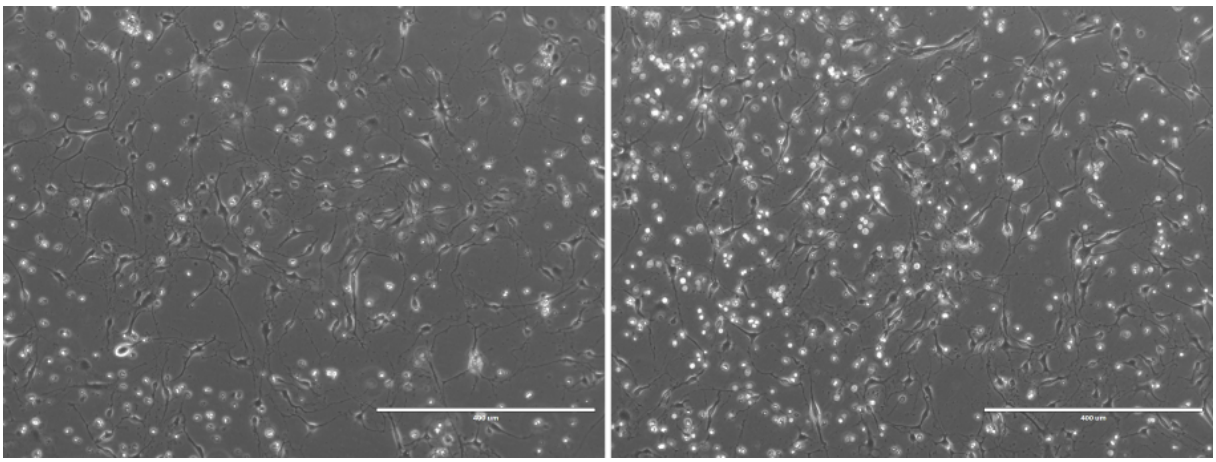

Figure 3.48: IMS32 P8 3DIV, 240 cells/mm2, grown on polyethyleneimine-laminin coated well-plate with modified Neurobasal-A medium for DRG.

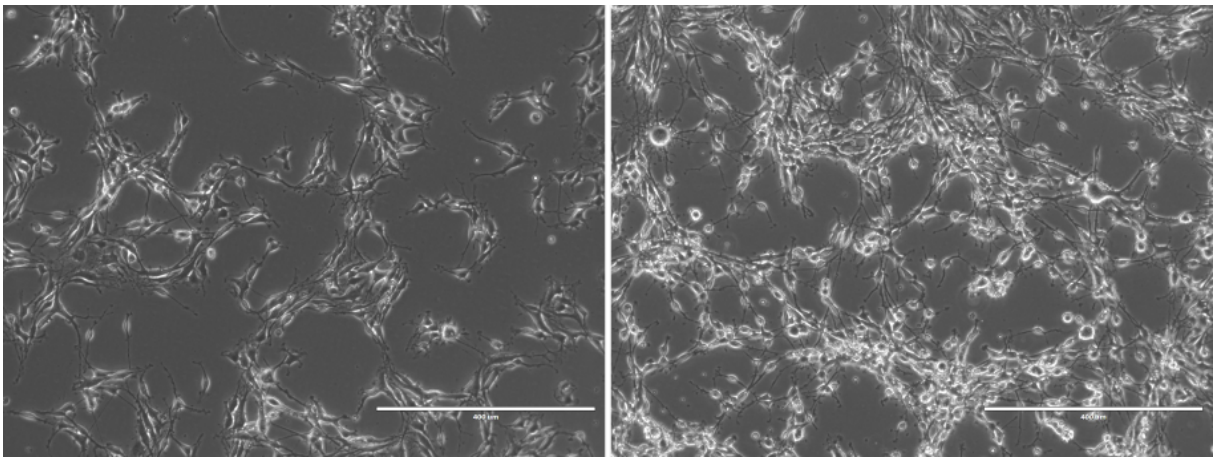

Figure 3.49: IMS32 P8 3DIV, 240 cells/mm2, grown on polyethyleneimine-laminin coated well-plate with modified Prigrow III medium.

However, after 3DIV, co-cultures that were grown with modified Neurobasal-A medium for DRGs clumped, and the IMS32 cells were not recognizable anymore, as they lost their characteristic elongated-shape (Figure 3.51a). Co-cultures grown with modified PriGrow III medium seemed to have kept the characteristic shape in the IMS32 population. However, clamping was present here as well, and among the area of the electrodes, it was not possible to determine whether the IMS32 cells were still present or not (Figure 3.51b).
As only one MEA among those cultured with modified Neurobasal-A medium showed a slightly better distribution of the cells, it was decided to record only those co-cultured with PriGrow III media.

Figure 3.50: DRG-IMS32 co-cultures 1DIV

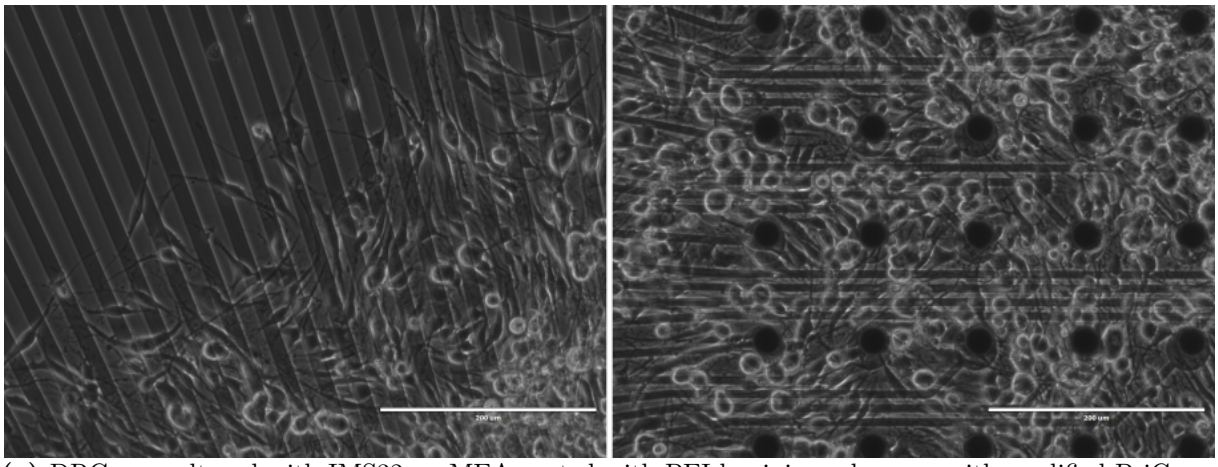

(a) DRGs co-cultured with IMS32 on MEA coated with PEI-laminin and grown with modified PriGrow III medium, 1DIV, focusing on the external seeding area (left) and the electrodes (right), 20X. Concentrations seeded: 570 DRG/mm2, 2285 IMS32/mm2 (ratio 1:4 DRG: IMS32).

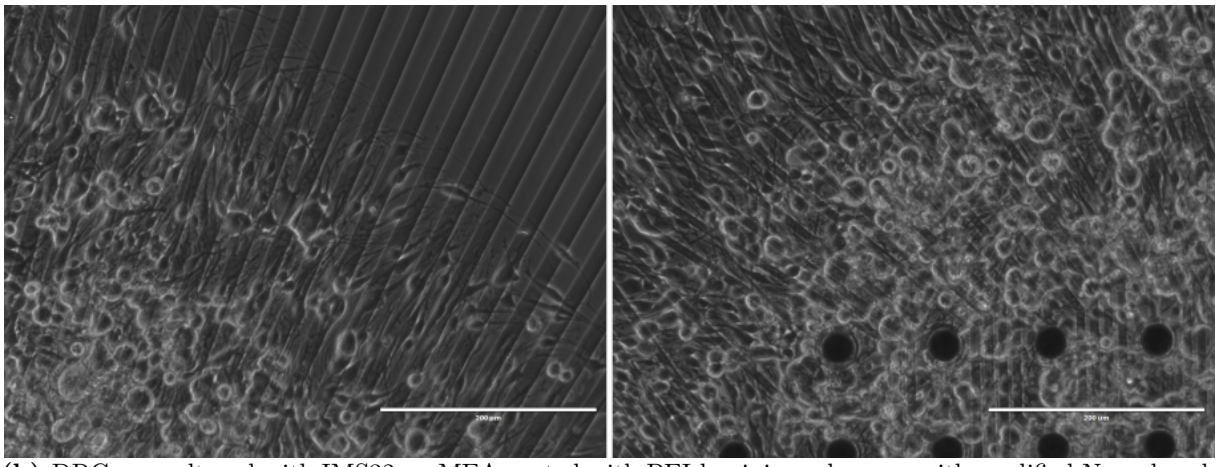

(b) DRGs co-cultured with IMS32 on MEA coated with PEI-laminin and grown with modified Neurobasal-A medium for DRGs, 1DIV, focusing on the external seeding area (left) and the electrodes (right), 20X. Concentrations seeded: 570 DRG/mm2, 2285 IMS32/mm2 (ratio 1:4 DRG: IMS32).

Figure 3.51: DRG-IMS32 co-cultures 3DIV

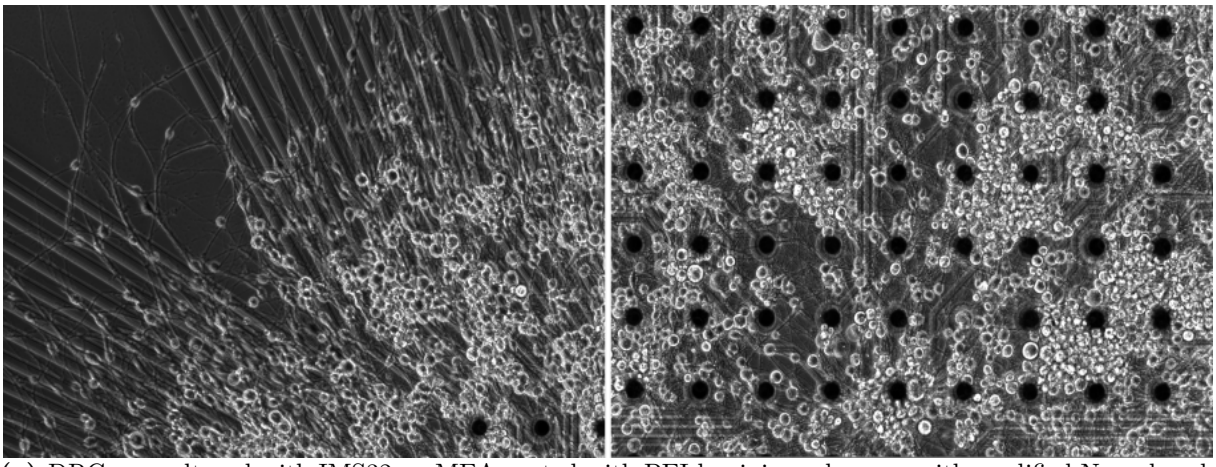

(a) DRGs co-cultured with IMS32 on MEA coated with PEI-laminin and grown with modified Neurobasal-A medium for DRGs, 3DIV, focusing on the external seeding area (left) and the electrodes (right), 20X. Concentrations seeded: 570 DRG/mm2, 2285 IMS32/mm2 (ratio 1:4 DRG:IMS32).

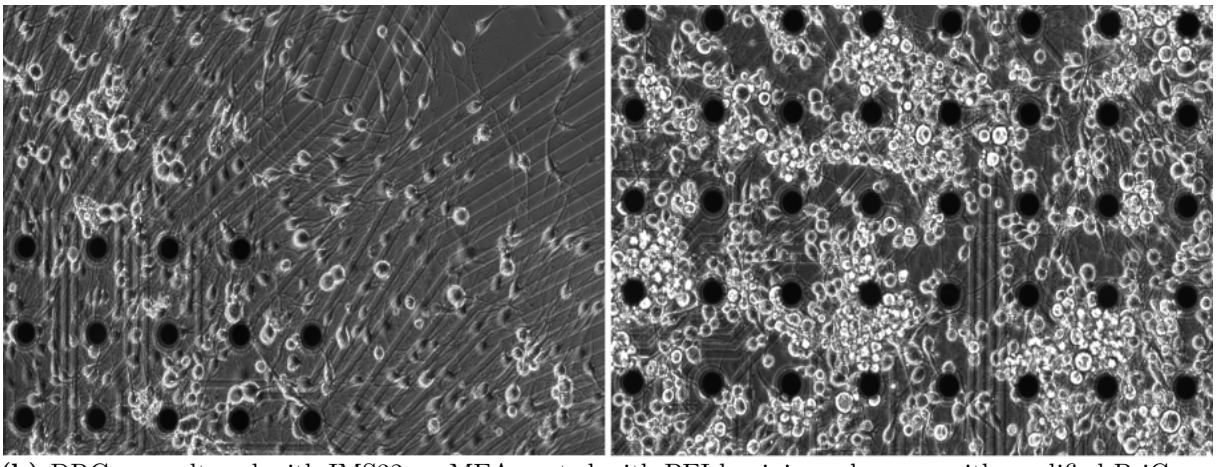

(b) DRGs co-cultured with IMS32 on MEA coated with PEI-laminin and grown with modified PriGrow III medium, 3DIV, focusing on the external seeding area (left) and the electrodes (right), 20X. Concentrations seeded: 570 DRG/mm2, 2285 IMS32/mm2 (ratio 1:4 DRG:IMS32).

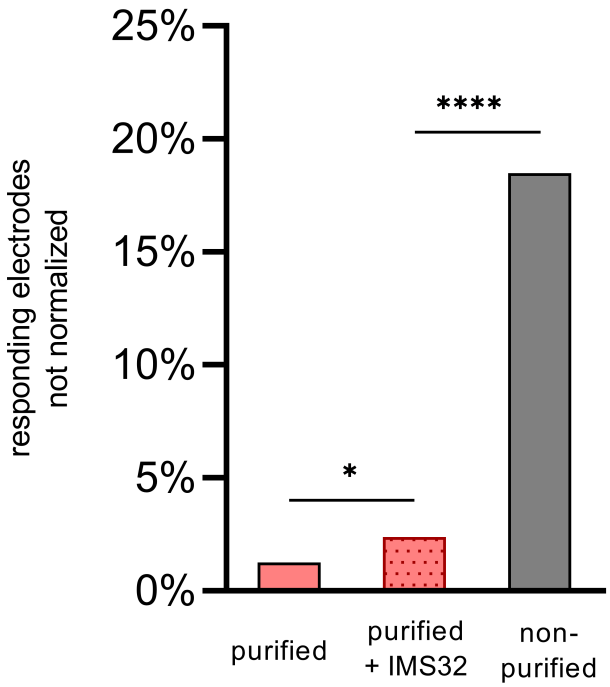

Figure 3.52: Percentage of responding electrodes in response to 1µM capsaicin after 3DIV (data are not normalized and expressed as mean ± S.E.M.).

Sample	n	mean ± S.E.M
Purified DRGs	1512	1.26 ± 0.29
DRGs + IMS32	1764	2.38 ± 0.36
Non-purified DRGs	1260	18.49 ± 1.094

Table 3.10: Sample size and percentage of electrodes responding to 1µM capsaicin (data are not normalized and expressed as mean ± S.E.M.; n = number of electrodes).

Even though the recordings displayed a significant difference between purified DRGs and purified DRGs co-cultured with IMS32 (unpaired t-test, $t(3274)=2.375$, $p=0.0176$), there was not a recovery of the excitability comparable to that observed in non-purified DRGs (unpaired t-test, $t(3022)=15.80$, $p<0.0001$) (Figure 3.52). As it was impossible to distinguish between DRGs and IMS32 cells in the pictures, the data displayed above were not normalized and reported only the total number of responding electrodes.

3.3.6 Single-cell sequencing

All the experiments performed to identify and isolate non-neuronal cells did not provide stable and precise results. It was acknowledged that Schwann cells are present in the non-neuronal fraction, but it was impossible to isolate and purify them. All studies and experiments conducted with MEA that confirmed a difference in neuronal excitability between purified and non-purified DRGs led to the hypothesis that this lack of excitability in purified DRGs could be addressed differently at the level of ion channels. These differences could occur, for example, at the transcriptional level: mechanisms of RNA interference or DNA methylation could lead to the production of lower transcripts levels; post-translational modifications (PTMs), such as phosphorylation, could deactivate proteins or even result in proteolysis. While the detection of protein levels is feasible for a small, defined amount of targets, it would be challenging, almost impossible to perform on a whole proteome, where all targets need to be analyzed. Furthermore, the possible presence of unknown PTMs makes everything even more challenging, almost impossible.
One way to determine differences at the transcriptional level is provided by RNA sequencing. This group of techniques yields information regarding the transcripts present in a cell, or bulk, at the specific time the experiment is performed. If we temporarily do not consider the PTMs, the transcript level correlates to the translation's protein level.
The easiest way to perform RNA sequencing is bulk sequencing, where an entire cell population is analyzed. Previous studies already demonstrated a difference in the expression of nociception-related genes in purified and non-purified DRGs through transcriptomics [63]. Even though this method is fast and cheap, it requires many cells material to provide sufficiently precise results. Furthermore, in the case of a mixed cell population (as in the non-purified DRGs), it is impossible to separate the transcripts from different cell types, and the results could be misleading.
The alternative to bulk sequencing is brought by single-cell sequencing. Despite being more challenging and expensive than bulk sequencing, it requires lower amounts of cells. Nevertheless, most importantly, it provides the analysis of the transcripts at the level of single cells, thus making it possible for the study of cell cultures constituted by different cell types (Figure 3.53) [76, 77].

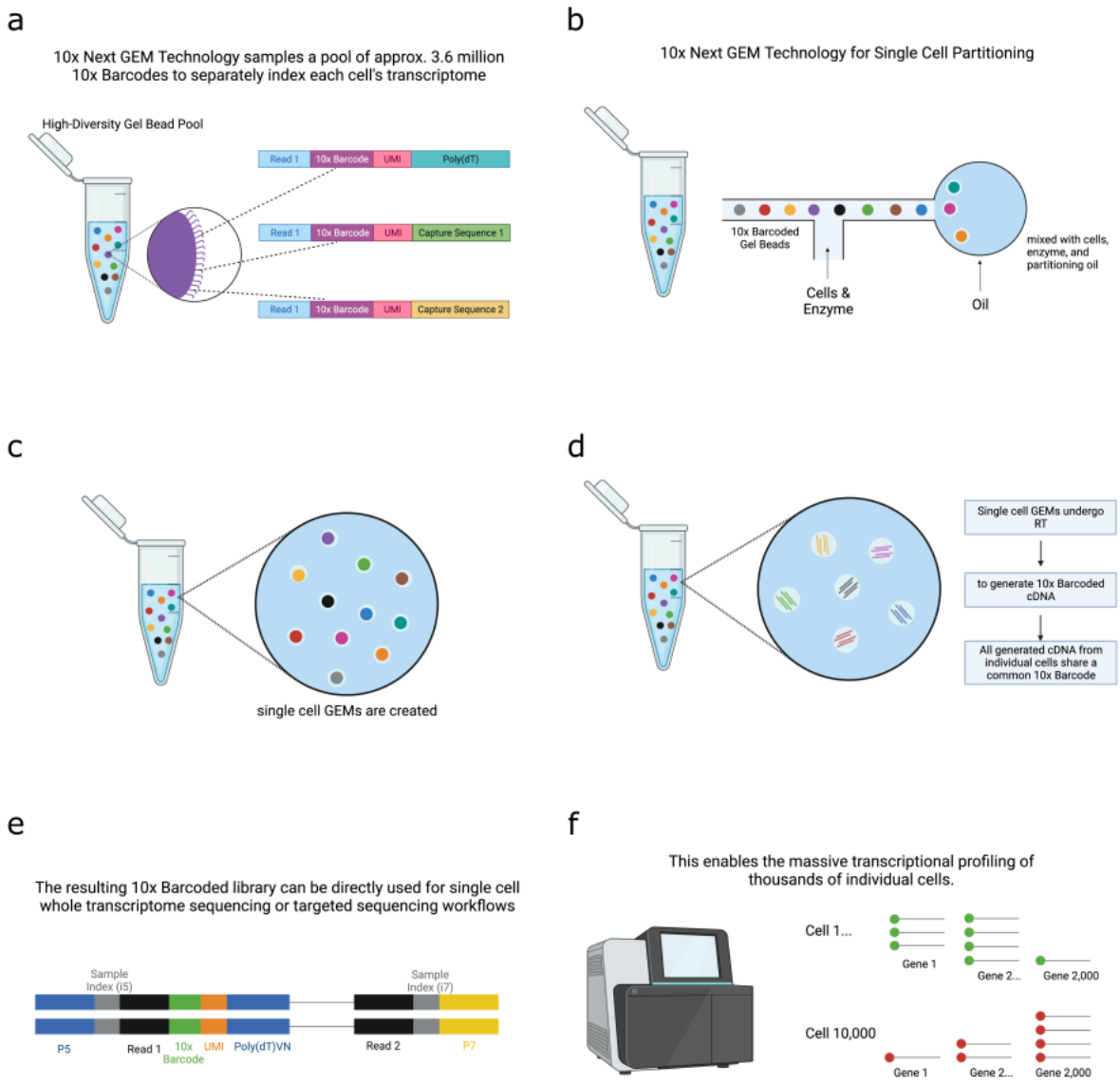

Figure 3.53: Single-cell sequencing protocol, according to [76] (created with BioRender.com). The cell culture is detached from the culture plate and resuspended to obtain a single-cell suspension. Cells are then incubated with a gel beads pool (a, b), where each bead carries a specific barcode, and each cell is assigned with one particular "barcode" (c). Each cell-bead construct undergoes reverse transcription, and a cDNA library is thus generated for every single cell (d). The library is then used for sequencing at the level of single-cell (e, f).

The experimental setup started from two conditions: purified and non-purified DRGs seeded on a well-plate (570 DRG/mm2) and cultured as usual. After three days, cells were detached with trypsin, and four different conditions were prepared:

- Sample 1: non-purified DRGs detached and analyzed;
- Sample 2: purified DRGs detached and analyzed;
- Sample 3: non-purified DRGs detached, purified, and analyzed;
- Sample 4: purified DRGs detached, re-purified, and analyzed.

The loading cassette for the sequencing can analyze a maximum of 10,000 cells; for the first condition, where non-purified DRGs were analyzed, the neuronal fraction is only a tiny part of the total number of loaded cells; the rest is constituted by non-neuronal cells. For the remaining three conditions, the number of loaded cells corresponded to the number of loaded DRG neurons (Figure 3.54).

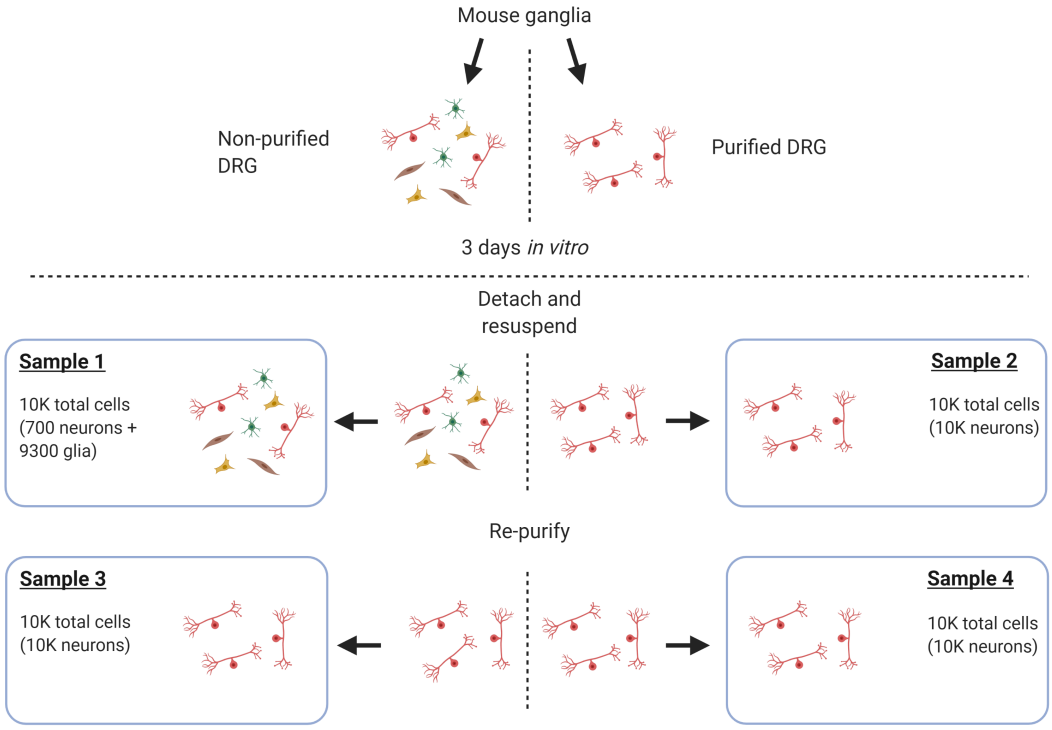

Figure 3.54: Schematic representation of single-cell sequencing experimental set-up (created with BioRender.com).

The first important thing that can be noticed among the different conditions is their cellular composition. For non-purified DRGs, the significant cell fraction is constituted by glial cells, represented mainly by satellite glial cells and Schwann cells; this supports the fact that these

two subpopulations are the most represented in DRGs cultures [37, 38].
Secondly, after DRG neurons' isolation, the glial population fraction is dramatically reduced to fee numbers of glial cells. This furtherly demonstrated that the Neuron Isolation Kit is efficient in the depletion of glial cells. Moreover, independently of the starting source, the three conditions with purified DRGs lead to obtaining the same types of subpopulations (Figure 3.55).

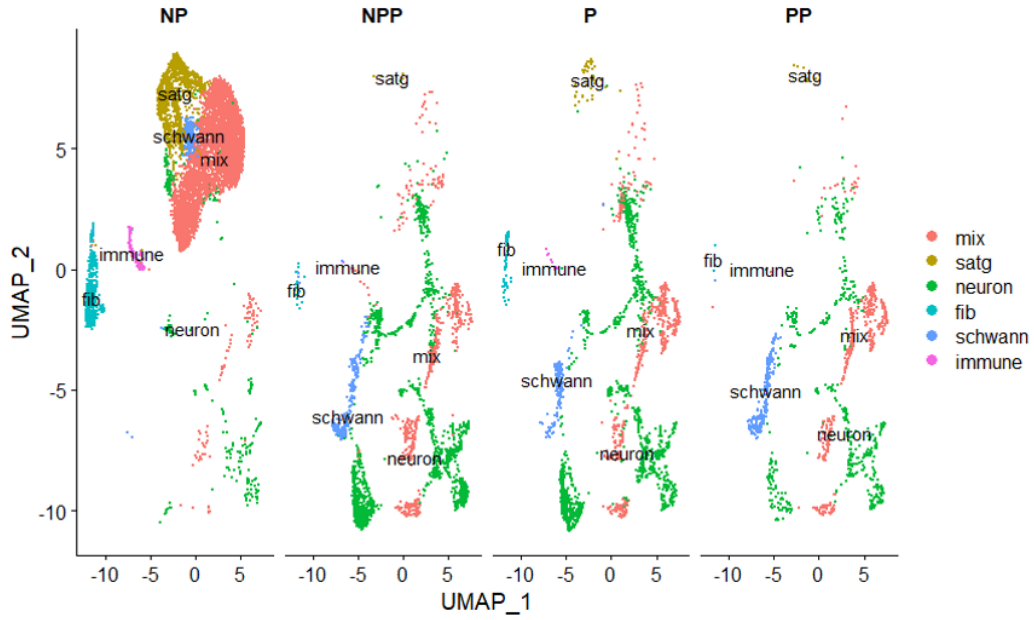

Figure 3.55: Results of single-cell sequencing on 4 different conditions. NP: non-purified DRGs; NPP: non-purified DRGs detached and purified before sequencing; P: purified DRG; PP; purified DRGs detached and repurified before sequencing.

As the goal was to verify any differences in gene expression between non-purified and purified DRG neurons, the data analysis was not performed for the sample corresponding to non-purified DRGs, to increase the number of neurons available for the analysis. As indicated in KCL results, eleven regeneration markers in purified DRG neurons were reported as downregulated than their non-purified counterparts. These results are consistent with the literature, where the same genes are reported to be upregulated in DRG neurons following sciatic nerve ligation [78, 79, 80].

The results obtained with single-cell sequencing proved a difference between non-purified and purified DRGs in gene transcriptions, leading to differences in protein expression and neuronal excitability. Given that these differences were not limited to a single gene but rather to several genes involved in different pathways that could affect neuronal excitability, more studies are required to understand which of these genes and entities are involved in neuronal modulation excitability.

Gene	Name	Type	Function (possible other function)
Gal	Galanin	Neuropeptide	Nociception, homeostasis
Lgals1	Galectin 1	Beta-galactoside-binding protein	Cell-cell interactions, cell-matrix interactions(autocrine negative growth factor regulating cell proliferation)
BDNF	Brain-Derived Neurotrophic factor	Growth factor	Promotes neuronal survival, axonal growth (regulation in stress response)
Nsg1	Neuronal Vesicle Trafficking Associated 1	Clathrin light chain binding	Receptor recycling mechanisms in neurons, regulation of synaptic transmission, apoptosis
Timp1	TIMP Metallopeptidase Inhibitor 1	Inhibitor of metalloproteinases	Cell proliferation, inhibition of extracellular matrix degradation (anti-apoptotic)
Serpinb1a	Serpin Family B Member 1	Protease inhibitor	Maintaining homeostasis, regulation of inflammation
Gadd45g	Growth Arrest And DNA Damage Inducible Gamma	Cell cycle regulator	Regulation of environmental stresses following DNA damage
Vim	Vimentin	Type III intermediate filament protein	Constitutes cytoskeleton, maintaining cell shape and cytoplasm integrity
Kif22	Kinesin Family Member 22	Kinesin-like protein	Organelles transport, chromosome moving during cell division (role in metaphase)
Arxes1	Adipocyte-related X-chromosome expressed sequence 1	Peptidase	Adipogenesis, fat cell differentiation
Krt19	Keratin, type I cytoskeletal 19	Keratin family	Organization of myofibers, structural integrity

Table 3.11: Regeneration markers downregulated in purified DRG neurons and upregulated after sciatic nerve ligation [81, 82].

3.3.7 Chemical contribution of glial cells on neuronal excitability

The nature of the non-neuronal cells that compose the glial fraction of non-purified DRG cultures has been explored. Even though several experiments proved that glial cells are essential in determining neuronal excitability, their contribution was still unclear. It was speculated that glial cells might release a compound (or a cocktail of compounds) in the proximity of DRG neurons, affecting their survival and ability to generate action potentials. On the other hand, it may also be the only presence of glial cells responsible for DRG neurons' excitability. To assess these hypotheses, two different experiments were designed.

Treatment of purified DRG neurons with conditioned medium

This first experiment's scope was to verify whether the glial cells directly release any chemical factors in the medium that are responsible for the excitability of sensory neurons in non-purified cultures. Different setups have been used, each developed and modified according to the previous one's results.

1st experimental setup The first and most straightforward setup consisted of seeding purified and non-purified DRGs on MEA and leaving them in the PDMS inserts. On days 1 and 2 in vitro, medium from purified DRGs was removed and replaced with medium coming from non-purified DRGs (Figure 3.56).

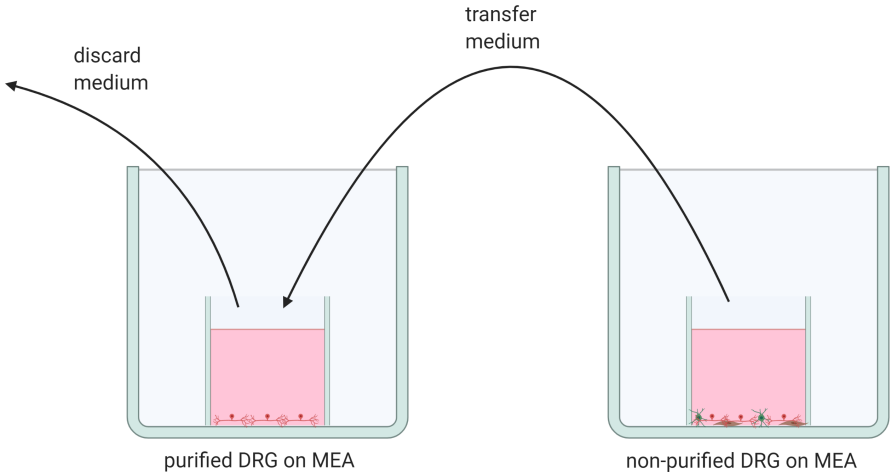

Figure 3.56: Schematic representation of the first experimental set-up in conditioned medium experiments (created with BioRender.com).

Unfortunately, there was no significant difference between purified DRGs and purified DRGs treated with control medium (unpaired t-test, $t(1171)=0.07427$, $p>0.05$) or purified DRGs treated with conditioned medium (unpaired t-test, $t(1232)=3.118$, $p>0.05$) (Figure 3.57).

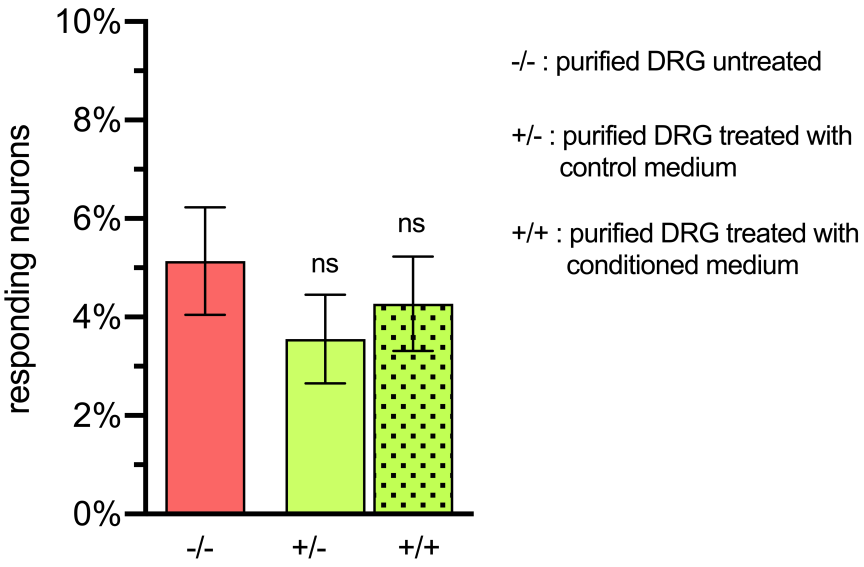

Figure 3.57: Percentage of responding DRGs to 1µM capsaicin after 3DIV (data are expressed as mean ± S.E.M.; statistical analysis was performed comparing purified DRGs with all other conditions).

Condition	n	mean ± S.E.M.
-/-	409	5.13 ± 1.09
-/+	764	3.55 ± 0.90
+/+	825	4.27 ± 0.95

Table 3.12: Sample size and percentage of DRG neurons responding to 1µM capsaicin for the different conditions (data expressed as mean ± S.E.M.; n = number of neurons).

2nd experimental setup The second setup consisted of the first seeding of non-purified DRGs in low-density (20-25 DRG/mm2) on a multiwell plate. In this way, the glia cells were able to proliferate. The neurons' survival was hindered both by the neuronal cells' low-density and the parallel proliferation of glial cells at the neurons' expense. After one week, the medium was collected and concentrated via ultracentrifugation with Amicon® Ultra Centrifugal filters (15mL, 3KDa cut-off); as a counterbalance, fresh Neurobasal-A medium for DRGs was used (Figure 3.58). After the centrifugation, both concentrated mediums were collected and stored at 4°C before proceeding with the preparation of purified DRG neurons. Purified neurons were then treated either with conditioned concentrated medium or with control concentrated medium once a day until the activity recording.

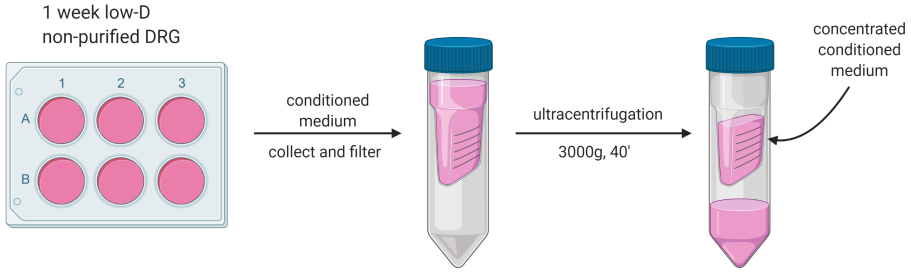

Figure 3.58: Schematic representation of the second experimental setup in conditioned medium experiments (created with BioRender.com).

The medium was changed once on day one and days 2 in vitro. After 3DIV inserts were removed, the residual medium was washed, and cells were recorded with the protocol previously described.

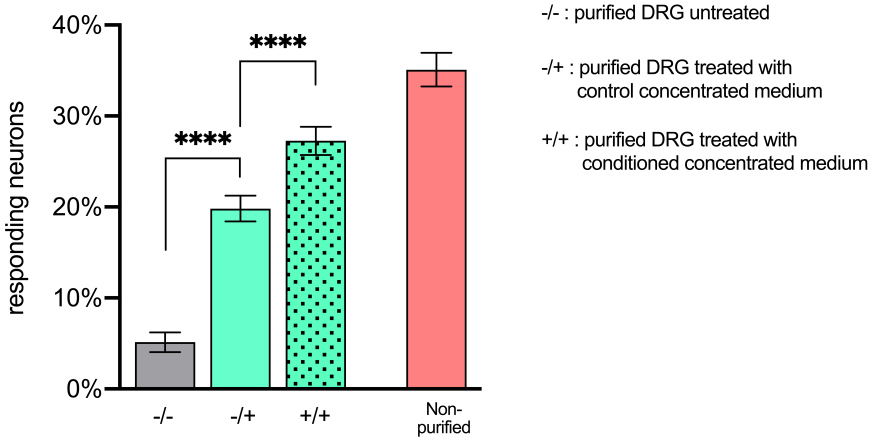

Figure 3.59: Percentage of responding DRGs to 1µM capsaicin after 3DIV (data expressed as mean ± S.E.M.).

Compared to the first setup, here we can notice a significant increase in the excitability of purified DRGs treated with conditioned concentrated medium compared to purified DRGs (unpaired

Condition	n	mean ± S.E.M.
-/-	409	5.13 ± 1.09
-/+	787	19.82 ± 1.42
+/+	825	27.27 ± 1.55
Non-purified DRG	664	35.09 ± 1.85

Table 3.13: Sample size and percentage of DRG neurons responding to 1µM capsaicin for the different conditions (data expressed as mean ± S.E.M.; n = number of neurons).

t-test, $t(1232)=9.484$, $p<0.0001$). However, a significant increase was also noticed in the DRGs treated with the control medium (unpaired t-test, $t(1194)=6.914$, $p<0.000$.) (Figure 3.59). Keeping in mind that the ultracentrifugation concentrates not only any factor released by the glial cells in culture but also factors already present in the culture medium (for example, NGF), with a molecular weight higher than the 3KDa provided in the centrifugation filters, it could be that the increase in the excitability was caused by an increase in these factors already present in the medium, rather than factors released by glial cells.

3rd experimental setup Given the results obtained with the second setup, where also purified DRG treated with control concentrated medium increased their excitability, the protocol was slightly modified in the third setup. Here, low-density DRG were initially cultured with the standard Neurobasal-A medium for DRG neurons to promote the cells' initial survival. After two days, the medium was changed with Neurobasal-A medium containing only penicillin-streptomycin as an additional factor to avoid contamination. In this way, any factor present in the medium must come from the glial cells. After one week, the medium was collected again and concentrated via ultracentrifugation with Amicon® Ultra Centrifugal filters (15mL, 3KDa cut-off); as a counterbalance, fresh Neurobasal-A medium with Penicillin-Streptomycin only as an added factor was used. After the centrifugation, both concentrated mediums were collected, and the missing factors (NGF, SM1, GlutaMAX, and N2) were added in the same concentrations they are typically used (Figure 3.60). Purified neurons were again prepared, seeded, and treated either with conditioned concentrated medium or with control concentrated medium once a day until the activity recording.

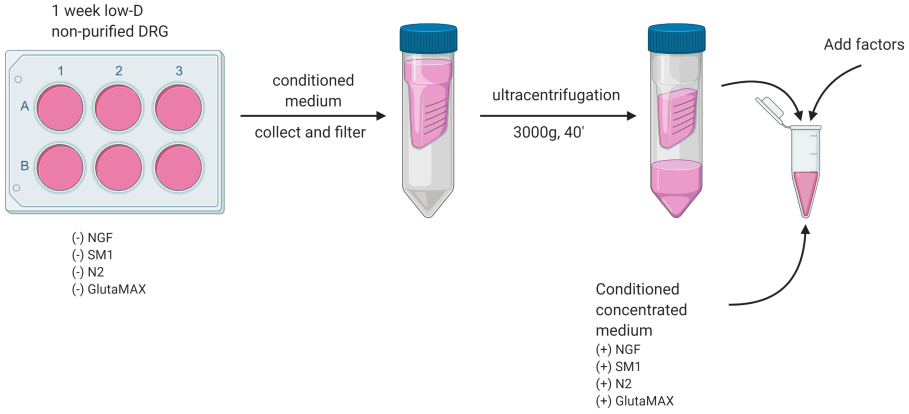

Figure 3.60: Schematic representation of the third experimental set-up in conditioned medium experiments (created with BioRender.com).

Unfortunately, no significant difference was noticed between purified DRG and purified DRG treated either with control (unpaired t-test, $t(988)=0.48$, $p=0.6313$) or with conditioned concentrated medium (unpaired t-test, $t(1187)=1.156$, $p=0.2480$). Therefore, the second setup's positive results were most likely caused by the concentration of the added factors already present in the culture medium (Figure 3.61).

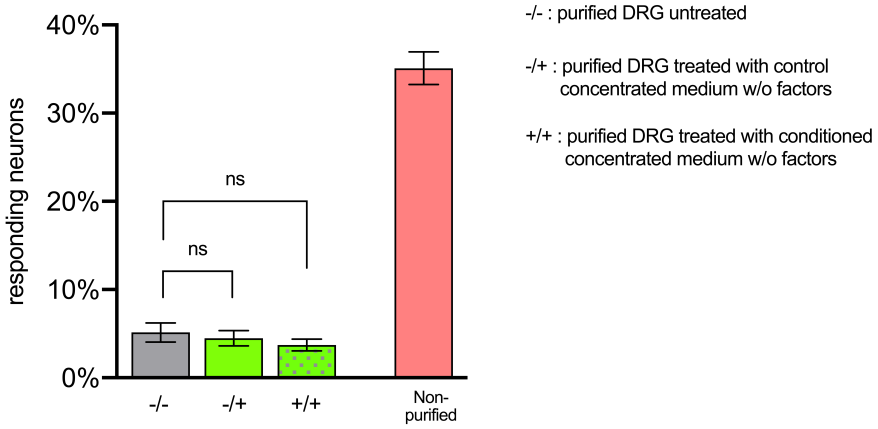

Figure 3.61: Percentage of responding DRGs to 1µM capsaicin after 3DIV (mean ± S.E.M.).

Condition	n	mean ± S.E.M.
-/-	409	5.13 ± 1.09
-/+	581	4.47 ± 0.85
+/+	780	3.72 ± 0.68
Non-purified DRG	664	35.09 ± 1.85

Table 3.14: Sample size and percentage of DRG neurons responding to 1µM capsaicin for the different conditions (data expressed as mean ± S.E.M.; n = number of neurons).

4th experimental setup The fourth and last setup was a combination of some features from the previous three. Non-purified DRGs were again seeded in low-density on a multiwell plate. After one week, purified DRGs were prepared and seeded on MEA; both concentrated mediums were collected and stored at 4°C before proceeding with the preparation of purified DRG neurons. Purified neurons were then treated with conditioned medium once a day until the activity recording (Figure 3.62). Compared to the first setup, the difference compared to the first setup is that the concentration of glial cells that provided the conditioned medium was higher this time. Therefore, "more factors" should have been released in the medium.

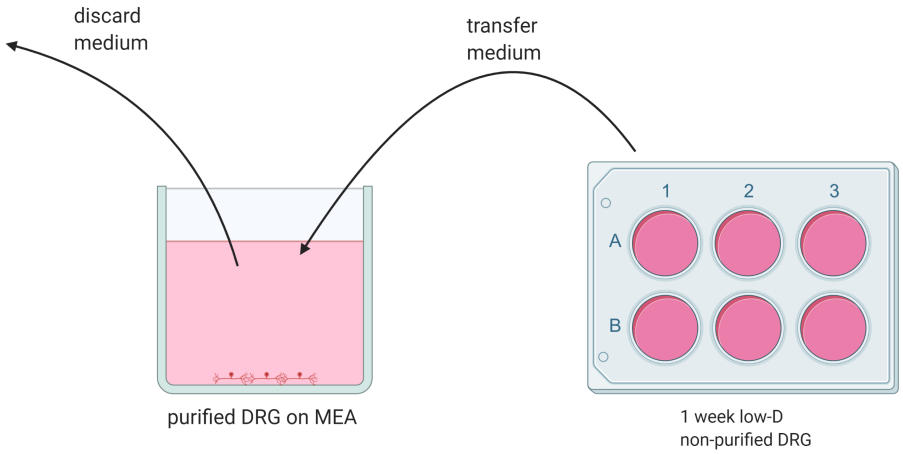

Figure 3.62: Schematic representation of the fourth experimental set-up in conditioned medium experiments (created with BioRender.com).

Even though a significant difference was noticed between purified DRGs and purified DRGs treated with conditioned medium derived from high-density glia cultures (unpaired t-test, $t(1780)=3.147$, $p=0.0017$), we can notice from the barplot that the percentage of responding neurons treated with the conditioned medium is even lower compared to untreated purified DRGs (Figure 3.63).

Condition	n	mean ± S.E.M.
-/-	409	5.13 ± 1.09
+/+	1373	2.18 ± 0.39
Non-purified DRG	664	35.09 ± 1.85

Table 3.15: Sample size and percentage of DRG neurons responding to capsaicin for the different conditions (data expressed as mean ± S.E.M.; n = number of neurons).

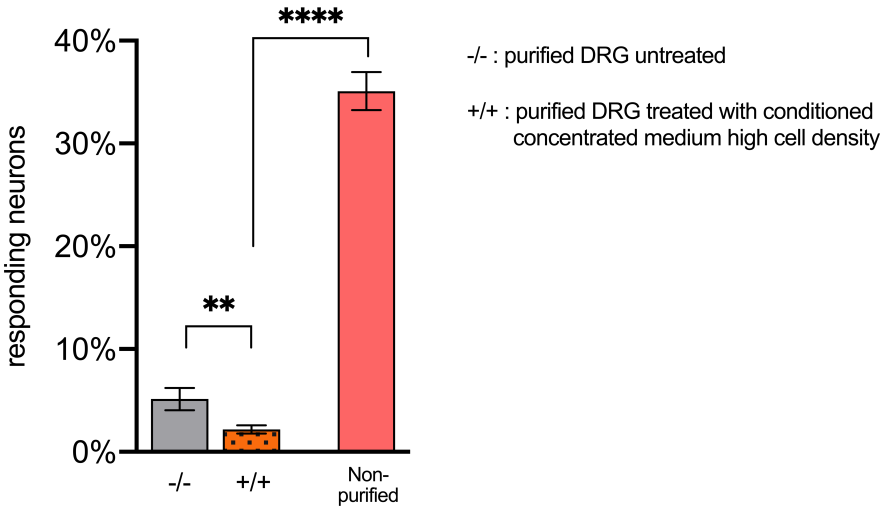

Figure 3.63: Percentage of responding DRGs to 1µM capsaicin after 3DIV (mean ± S.E.M.).

Co-culturing purified DRG neurons and glial cells grown separately on two different layers

Experiments with conditioned medium did not provide further information regarding the contribution of glial cells in neuronal excitability. Although an increase in the excitability of purified sensory neurons was noticed in some experimental setups, it was likely caused by an increase in the factors ordinarily present in the culture medium that are essential for neuronal survival, such as NGF. However, at the same time, they arose new questions and hypothesis: it could be that glial cells are releasing some factor(s) the culture media, but it could be that the released concentration is so low that the neurons immediately capture the factors, and therefore not even ultracentrifugation can concentrate them.
Another hypothesis is that the factors are released only in the presence of the neurons. Therefore, when we culture glial cells alone, their conditioned medium is not sufficient to recover the neuronal excitability once the medium is transferred to purified DRG neurons cultures, independently of whether the medium has been concentrated or not. These hypotheses lead to the question: is it necessary for the glial cells to be in close contact with DRG neurons (as it usually occurs in non-purified DRGs cultures), or is it sufficient for them to be in proximity of the neurons?
To physically separate neurons and glial cells but keeping them in the same culture device, special devices were used. These cell culture inserts (Merck Millipore, Darmstadt, Germany) consists of a semi-permeable membrane that allows cells culturing (Figure 3.64). These inserts' physical features will enable them to be placed in cell culture dishes, where another cell culture is seeded. This allows co-culturing of different cell types, with an exchange of cell media and any compound released still possible, thanks to the semi-permeable membrane.

Figure 3.64: Millicell® standing cell culture inserts, suitable for 6-well (back) and 24-well (front) plate. Each filter has three tiny feet that prevent the membrane from touching the bottom of the well, thus allowing not only culturing cells on the well but also ensuring an adequate cell culture medium distribution.

Membrane type	Pore size
PCF Isopore (polycarbonate)	1 µm
HA MF-Millipore™ (mixed cellulose esters	0.45 µm
CM Biopore® (PTFE)	0.4 µm

Table 3.16: Characteristics of the three Millicell® inserts tested.

By testing all three different membrane types, it turned out that the mixed cellulose esters membrane is not suitable, as it does not allow live imaging of the cell cultures. Between PCF and CM, the difference in cell visualization was minimal, with the CM performing slightly better; therefore, the CM Biopore® inserts were chosen for the experimental setup (Figure 3.65).

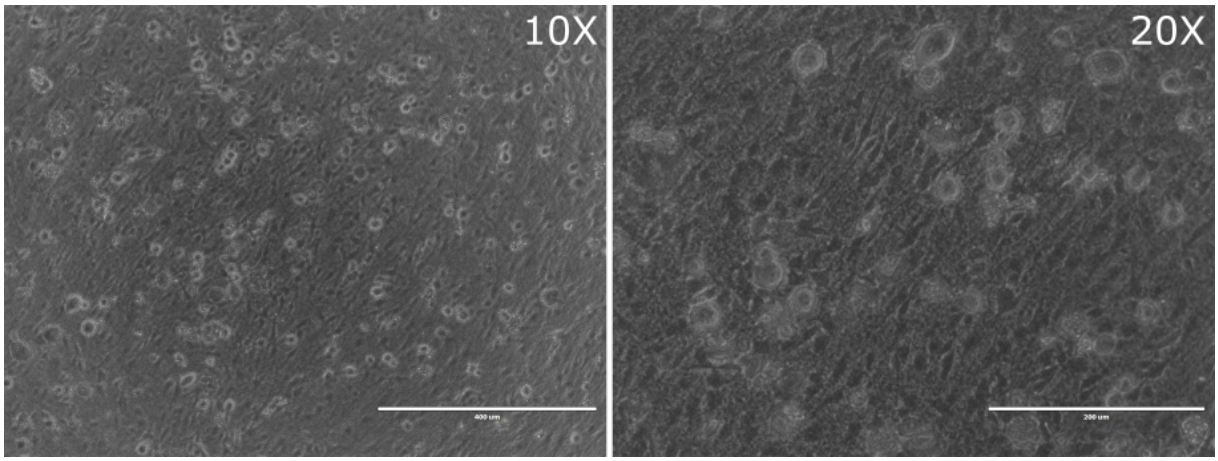

Figure 3.65: DRGs seeded on Millicell® insert with CM Biopore® membrane (70 DRG/mm^2, 2DIV).

DRGs were seeded on Millicell® inserts in low-density to promote glia proliferation over neuronal survival. Seeding was done on the membrane's outer side to reduce the distance with purified DRGs seeded on MEA (Figure 68). After one week, purified DRGs were prepared and seeded on MEA. Each MEA was then combined either with one Millicell® inserts previously seeded or with an insert without cells as control. MEAs were cultured for three days when the neuronal activity was recorded with the usual protocol previously described (Figure 3.66).

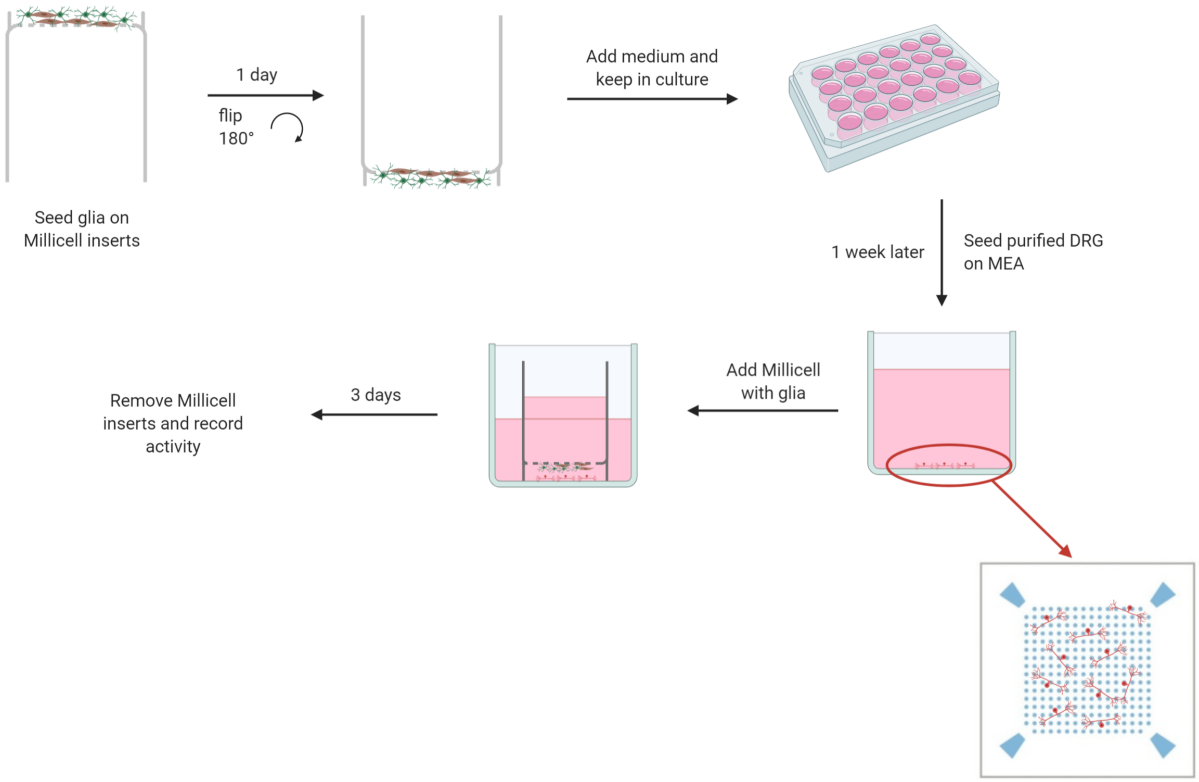

Figure 3.66: Setup of co-cultures of glial cells and purified DRG neurons on Millicell® inserts and MEA (created with BioRender.com).

There was a significant difference between purified DRGs and purified DRGs with cells on the filter (unpaired t-test, $t(2222) = 11.77$, $p<0.0001$). Furthermore, no significant difference was observed between the purified DRGs untreated and purified DRGs treated with control filters (unpaired t-test, $t(1515)=1.514$, $p=0.1302$) (Figure 3.68).

Although the neuronal excitability was not recovered to the same levels as that typically observed in non-purified DRGs, there was nevertheless a significant improvement in it in the purified population, thus proving that it is not the tight contact between neurons and glia responsible for neuronal excitability, but the presence of glial cells in the same environment is sufficient, probably thanks to the release of chemical factors from glial cells that are essential for the neurons in order to be chemically excitable.

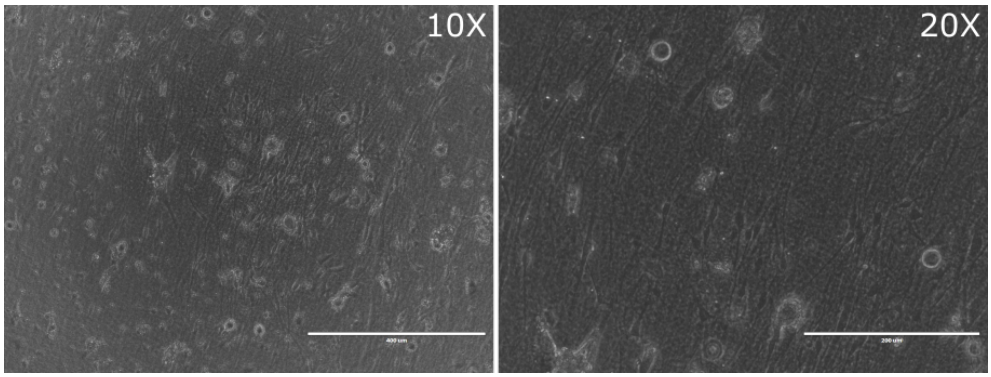

Figure 3.67: DRGs seeded on Millicell® insert with CM Biopore® membrane (70 DRG/mm2, 8DIV). Left: 10X; right: 20X. Notice a reduction in the number of DRG neurons (round cells) compared to the same condition after 2DIV, thanks to the low-density seeding that promotes glia proliferation and neuronal death.

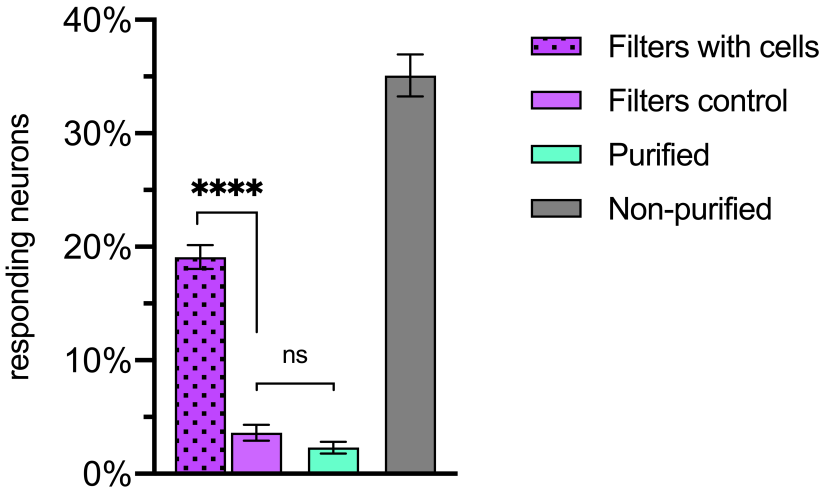

Figure 3.68: Percentage of responding DRGs to 1µM capsaicin after 3DIV (mean ± S.E.M.).

Condition	n	mean ± S.E.M.
Filter control	692	3.61 ± 0.71
Filter with cells	1399	19.09 ± 1.05
Purified DRGs	825	2.30 ± 0.52
Non-purified DRGs	664	35.09 ± 1.85

Table 3.17: Sample size and percentage of DRG neurons responding to 1µM capsaicin for the different conditions (data expressed as mean ± S.E.M.; n = number of neurons).

4 | Discussion

In this section, the results obtained are furtherly discussed to identify the limits of the different techniques used and the possible outcomes.
Despite the availability of different electrophysiological techniques, for this project, it was decided to use a system based on microelectrode array technology, which allowed a higher throughput compared to other methods, such as patch-clamp [28, 83]. The possibility of a higher throughput was essential considering the nature of the cells used for this project. Sensory neurons in DRG can detect a wide range of stimuli, and those responsible for nociception are just a fraction of them [28]. As separating neurons basing on their nature would not have been possible, it was necessary to record as many cells as possible to increase the fraction of cells able to respond to stimuli associated with pain mechanisms. Using a microelectrode array system, it was possible to record purified and non-purified DRG neurons' electrical activity with little statistical noise. The first experiments highlighted the most crucial difference between the two conditions: purified DRGs are not excitable chemically, independently on the type of agonists used (and consequently, the signal transduction pathway involved). This fact is independent of the burst's mean frequency, which appears to be constant between purified and non-purified DRG for a given agonist. This lack of excitability can't be addressed to a downregulation of the corresponding agonist receptor; this was demonstrated by calcium imaging experiments. We could see a clear and significant difference between the almost absent pure electrophysiological response in purified neurons and their counterpart relative to calcium imaging. There was clear calcium inward inside the cell soma for both capsaicin and veratridine, demonstrating that the neurons expressed the correspondent receptors. Together with the lack of difference in the mean burst frequency, it showed that purified DRG cultures are still viable, despite the absence of glial cells.
However, there was still the possibility that even though the receptors were expressed and fully functional, the depolarization of purified DRGs following calcium inward was not sufficient for reaching the threshold necessary for the generation of an action potential. To verify this hypothesis, non-purified and purified DRGs were seeded in MFC-MEA devices, where it was possible to stimulate neurons electrically [14, 49, 51] The results obtained confirmed the theory of the threshold: purified DRGs are still excitable and capable of generating action potentials; however, they require a higher stimulation compared to non-purified DRGs. Purified DRG neurons required approximately 150 mV more than non-purified DRGs to generate an action potential. With an increase in the stimulation, both conditions reach a point where they need roughly the same stimulus for activating the same percentage of neurons.

The preliminary results obtained both with open MEA and MFC-MEA confirmed that glial cells play an essential role in neuronal excitability; however, this contribution's nature was still unclear and needed to be furtherly investigated.
The first approach for investigating the relationship between DRG neurons and glial cells consisted of seeding purified and non-purified DRGs in different combinations to modify the starting percentage of glial cells in culture. This allowed us to explore other conditions between the extreme pure DRGs culture and the "natural" occurring non-purified DRGs culture. The essential information extrapolated from this experiment can be addressed to the "90%" condition, where 90% of the DRGs seeded were purified, and only 10% were non-purified, thus having a few glial cells, enough for the culture to not be classified as "pure" DRGs (100%). This condition can be noticed in how DRG neurons' electrical activity after three DIV is already significantly higher than their purified counterpart. Furthermore, if the culture was let proliferating until six DIV, the neuronal activity also increased. The fact that the 90% culture after six DIV did not reach the same excitability as non-purified DRGs can be explained by looking at the ratio between glia and neurons. After three DIV, the excitability of non-purified DRG neurons corresponded to a ratio of approximately six glial cells for each DRG neuron.
On the other hand, the 90% condition after six days in culture showed only two glial cells for each DRG neuron. These glial cells were enough for observing an increase in neuronal excitability but probably not enough for observing an activity comparable to that observed in non-purified DRGs, as the number of glial cells was three times lower. This relationship between the number of glial cells in culture and neuronal excitability was confirmed by linear regression, which showed an increase in the number of glial cells in culture correlated positively with the percentage of responding neurons for that particular culture.
These experiments where DRG neurons were cultured with different amounts of glial cells confirmed that non-neuronal cells' presence positively affects neuronal excitability [84, 85, 13, 54]. The extent of this effect depends on the share of non-neuronal cells. It was necessary to start exploring this non-neuronal population better to understand the size of its contribution to neuronal excitability. Of the several techniques available for cell sorting, it was decided to perform MACS, mainly because the same approach was already routinely used to isolate pure DRG neurons, and therefore already established [12].
The first approach used antibodies directed against non-neuronal cells typically encountered during primary neuronal preparations; these antibodies were already available commercially. Therefore, they were already tested for their application on primary cells derived from the CNS. However, when tested on primary cells derived from DRGs preparations (thus, cells from the PNS), the results weren't satisfying. All antibodies lead to almost complete removal of non-neuronal cells from the cultures, as observed routinely when neuron isolation is performed. Despite this issue, DRG neurons' electrical activity co-cultured with only one type of non-neuronal cells was recorded. As no significant difference was noticed among the four different co-cultures, compared

to purified DRG neurons cultured alone, we can say that the approach using commercially available antibodies directed against non-neuronal cells didn't provide the expected results.
Given the results obtained with this first experiment, another experiment was designed; this approach was based on the fact that the antibodies in the non-neuronal antibodies cocktail in the neuron isolation kit provide effective removal of non-neuronal cells starting from non-purified DRG. Therefore, three single antibodies were obtained directly from the manufacturer, which corresponded to the kit's antibodies. The idea was to seed DRG neurons with either one type of non-neuronal cell or two out of three types of non-neuronal cells on MEA and evaluate any difference in neuronal excitability between the different conditions. The expectation was to restore neuronal excitability when DRG neurons were cultured with the single type of non-neuronal cell responsible for the excitability. Simultaneously, there should have been a decrease in the excitability when DRG neurons were depleted of the same non-neuronal cell type responsible for the restoration of the excitability.
As the concentration of each antibody employed in the neuron isolation kit was disclosed by trade secret and not provided, it was necessary to titrate each antibody to define the optimal working concentration. During this process, some issues were encountered: too high concentrations of each antibody lead to the complete depletion of non-neuronal cells, as obtained with the neuron isolation kit; too low antibody concentrations didn't deplete any non-neuronal cells, and the resulting cultures resembled those of non-purified DRGs. Therefore, every antibody provided was capable of cross-reactivity against other non-neuronal cells when applied in high concentrations, thus losing the aimed specificity.
Between the highest and the lowest concentration for each antibody, there is a range of possible optimal concentrations that would contribute to achieving the goal of depleting only one type of non-neuronal cells.
Despite the issues encountered during the titration phase, it was decided to try the two designed experimental set-ups and seed co-cultures of DRG neurons and non-neuronal cells. The concentrations chosen for each antibody were based on the partial results obtained during the titration phase.
For the first experimental set-up, non-purified DRGs were incubated with only one antibody. We can notice in the case of antibody 1 that the number of glial cells in culture is lower compared to antibodies 2 and 3. For all three antibodies, with time in culture, glial cells can proliferate. The condition with antibody 2 leads to the highest number of non-neuronal cells in culture, which resembles those obtained when non-purified DRGs are seeded in low-density to promote glial cells proliferation.
However, for the three antibodies, it was not possible to identify different types of non-neuronal cells for each condition.
For the second experimental set-up, non-purified DRGs were incubated with a combination of two antibodies at the same concentrations used for the first experimental set-up.

In this case, the combination of any of the two antibodies leads to obtaining pure DRGs cultures, once again raising the issue of each antibody's ability to cross-react with other antigens. For these reasons, it was decided not to proceed furtherly with the isolation of non-neuronal cells via MACS technology.

Proven that the results obtained via MACS technology were not sufficient for obtaining single colonies of glial cells, it was necessary to use a different approach. This second approach was based on applying a classical cell culture technique known as limiting dilution [70]. The goal was to end up with several wells containing one single cell colony derived from one clone. Even though the method worked from a technical point of view, and approximately 25% of the wells had one single cell clone, the colonies that originated from each clone stopped proliferating after two weeks in culture. This occurred despite the regular medium change, and even if the medium was enriched with 10% FBS to promote cell proliferation further. For this reason, it was decided not to continue with limiting dilution experiments, and different approaches were considered for obtaining single non-neuronal cell cultures.

So far, the methods used to obtain cell cultures of one type of non-neuronal cell somehow involved the depletion of all cell types but one, either via MACS technology or limiting dilution. Given that these experiments did not provide the expected results, it was decided to change the approach. Rather than trying to remove other non-neuronal cell types, it was decided to promote their proliferation over the neuronal population. This approach would not allow the obtaining of single-cell type colonies, but it still brought some advantages. First of all, it allowed the expansion of the non-neuronal cells fraction derived from the preparation of non-purified DRGs. In this way, it should have facilitated identifying different types of non-neuronal cells, for example, via ICC. Secondly, obtaining a cell culture of exclusively or almost glial cells could have helped any further experiments requiring high numbers of glial cells.

Following a previously published protocol, non-purified DRGs were seeded on multiwell plates in a known, low-density concentration [71]. In this way, the number of neurons in culture was too low for their excellent survival, and most neuronal cells died naturally in culture. On the other hand, glial cells (which are, contrary to neuronal cells, able to divide) proliferated in culture, and within one week of culturing, reached the confluency. Usually, glial cells' cultures are grown in the presence of serum to facilitate their growth and proliferation. In this case, it was decided not to add serum in the cell culture media for two reasons. First of all, it was noticed that glial cells that grew in the presence of serum change their morphology, acquiring a more spindled shape over the typical "three edges" shape observed in cultures of non-purified DRGs. Second, even though it was confirmed that serum accelerates the growth of glial cells, it was possible to keep the glial cells growing even without serum. Only, it would take approximately three more days for the cells to reach confluency. Even though, in this way, the time required for obtaining a glial cells culture suitable for the following experiments was longer, culturing glial cells without serum would have recreated the same conditions typically used when non-purified DRGs were

cultured. Therefore, any source of variability attributed to the different culturing conditions between non-purified DRGs cultured without serum and glial cells cultured with serum would have been eliminated. This elimination of variability was crucial for the following experiments, where co-cultures of expanded glial cells and purified DRG neurons were set-up.

Different approaches and techniques were available to identify the different cell types in the culture of glial cells. One of the most used methods for identifying (and eventually separating) cells in a mixed population is FACS [69]. The name may resemble MACS, used for isolating pure neurons from a culture of neurons and glial cells. FACS is also a technique used for sorting cells (as stated in its name); while MACS is based on magnetic interactions between beads bound to specific cells and a magnetic column, FACS is based on the membrane properties of the cells. As described already in the "Results" section, this technique allows the identification and separation of different cell types basing on the expression of different markers recognized by an antibody ligated to a specific fluorophore. This also enables a quantification of the different cell subpopulations in a culture of mixed cell types. If these markers are expressed on the cell membrane, it is also possible to label living cells and reuse them after the separation for cell culturing. This technique was not considered for two main reasons. First of all, glial cells in the peripheral nervous system haven't been wholly characterized so far. Therefore their markers haven't been identified in a way that guarantees specificity for separating cell types. In few cases, specific markers have been identified. That is the case of satellite glial cells that have been shown to express glutamine synthetase, absent in neurons and Schwann cells [86, 87]. However, this is an intracellular marker, meaning that it is necessary to permeabilize the cell membrane to have the fluorescent antibodies recognizing its target. This means that the cells expressing the marker will be dead at the time of the cell sorting, turning the impossibility of using them for different cell cultures afterward.

ICC provides an alternative to FACS in terms of the identification of cell types. This technique's advantage is that it does not require specific instruments to be performed, except for an excellent confocal microscope for imaging the samples. But other than that, it is a technique routinely used in many research groups, relatively straightforward and standardized in its protocol, and easy to learn and manage [88].

The markers used for identifying the different cell populations were based on the availability of antibodies already used in the laboratory and literature research. For the identification of neurons, beta-III-tubulin was chosen as a marker, while nuclei were stained for DAPI [66]. To identify glial cells, it was decided to start with Schwann cells, mainly because a first visual analysis of the low-density, expanded glial cells culture suggested that Schwann cells were the most represented non-neuronal cell population [71]. For their identification, it was decided to use S100b as a marker, mainly because it is the only marker that Schwann cells always express, independently on their developmental stage and whether they are in their myelinating or non-myelinating state [33].

Other than S100b, it was also decided to try identifying Schwann cells with GFAP, as reported in the literature, as a marker for non-myelinating Schwann cells [72, 73, 89, 90]. Furthermore, GFAP was routinely used in the laboratory in other projects to identify astrocytes in projects involving the CNS, with satisfactory results.
The results obtained with ICC on non-purified DRGs cultures 3DIV showed good staining for the nuclei and DRG neurons, where somas and neurites were stained. On the other hand, staining for S100b did not provide satisfying results, and Schwann cells were not marked compared to neurons. Furthermore, several neurons appeared to be expressing S100b as well, meaning that this marker is not very specific for Schwann cells. Surprisingly, staining with GFAP provided better results, and Schwann cells could be detected among the cultures. When ICC was performed on glial cell cultures generated from low-density seeding, the results obtained were unexpected: staining with GFAP was negative, meaning no cells were expressing the marker. On the other hand, staining for S100b slightly improved compared to previous experiments, and the co-staining of neurons previously reported in non-purified DRGs cultures was absent in low-density glial cell cultures. This could indicate that Schwann cells require some time in culture before they start expressing S100b. The absence of GFAP in low-density cultures could suggest that this marker is expressed by Schwann cells only in the early stage of their culture, and their expression is inhibited after a specific time in culture [89]. This is supported by published work that proves that the expression of GFAP in Schwann cells cultured in vitro is inhibited by S100b, which also explains why the signal from S100b improved with the signal from GFAP disappearing completely in low-density cultures after 8DIV [73].
By quantifying DRG neurons and glial cells in 3DIV ICC pictures, it was assessed that the Schwann cells represented the majority of the glial cells in the non-neuronal cell fraction, which lead to focusing on this particular cell type in the following experiments.
Seeding non-purified DRG neurons provided an excellent proliferation of glial cells despite the absence of serum in the culture media, also demonstrated with ICC experiments. However, the issue related to isolating single cell types of non-neuronal cells was still not solved, and it was necessary to overcome this hurdle.
Given that the previously applied techniques for separating or obtaining single clones of glial cells did not provide the desired outcome, it was decided to change the approach. It was demonstrated that Schwann cells represented the majority of non-neuronal cells in non-purified DRGs cultures. For this reason, it was decided to purchase commercially available murine Schwann cells directly from a manufacturer and expand them in the laboratory [74, 75]. The chosen cell line was an immortalized murine Schwann cell line, and therefore it was first necessary to expand the cell population, perform several subculturing passages, and freeze them properly for cryopreservation for subsequent experiments. The procedure did not raise any particular issue; the cells were adequately expanded and froze, and they always had the phenotype reported both in literature and from the manufacturer. However, when the first tests with different coatings were performed,

the results changed. Cells were surviving and proliferating in a satisfactory way only when pre-coated flasks provided by the manufacturer were used for seeding the cells and when the culture media suggested by the manufacturer was used. However, DRG neurons were usually grown on PEI-laminin-coated glass MEA and grown with modified Neurobasal-A medium suitable for neuronal cultures. Therefore, it was necessary to adjust the culturing conditions for the immortalized Schwann cells towards the same conditions used for neurons that would have been used lately, when immortalized Schwann cells would have been co-cultured with purified DRG neurons. The first tests did not provide the expected results. Coating with PEI-laminin leads to faster and vast cell death, together with culturing in the presence of modified Neurobasal-A medium. A combination of the two different conditions with PEI-laminin coating and Prigrow medium for immortalized Schwann cells improved the cultures' quality compared to when only neuronal conditions were used. However, cells tended to clump with time in culture. Despite the discouraging results obtained with preliminary tests, it was decided to try co-culturing purified DRGs with immortalized Schwann cells on MEA and eventually record the electrical activity three DIV customarily done. For this experimental set-up, it was decided to try two different conditions. All MEA were coated with PEI-laminin, as this was the best coating suitable for neuronal survival. However, the culture medium was from two different types: either modified Neurobasal-A medium or modified Prigrow medium for immortalized cells. In both conditions, the co-cultures showed a fair cell distribution after one day in vitro, with the electrodes covered with neurons and, therefore, suitable for recording the electrical activity. However, after three days in culture, co-culture grew with Neurobasal-A medium clumped. Consequently, it was impossible to distinguish between neuronal and Schwann cells anymore, as all cells showed the same morphology.

On the other hand, co-cultures grown in the Prigrow medium's presence seemed to have kept a distinction between neurons and Schwann cells in terms of morphology. However, clumping was present there, especially towards the central areas with electrodes on the MEA. Despite these issues, it was decided to record the co-cultures electrical activity grown in the Prigrow medium's presence. As it was not possible to distinguish between neuron and Schwann cells in most cases, it was not possible to normalize the data recorded.

Although the statistical analysis showed a significant difference between purified DRGs and purified DRGs co-cultured with immortalized Schwann cells, the percentage of responding electrodes in the co-cultures was still way lower compared to non-purified DRGs cultures. This meant that the co-culture was not sufficient for restoring the excitability of purified DRG neurons.

The unsuccess of the co-cultures with immortalized Schwann cells could be addressed for different reasons. First of all, immortalized cells, even if derived from an organism (in this case, murine), still are immortalized, and therefore not 100% equal to their primary counterpart. Not only may they show a different morphology, but they may also behave differently from a biological point of view. This was explained by the fact that primary murine glial cells could survive and proliferate

just fine when cultured with Neurobasal-A medium, while immortalized Schwann cells did not. The coating of the culture flasks, or MEA lately, highlighted the differences between the two cell types.

The experiments performed to identify and obtain single clones of the glial cells population did not provide the desired or expected results. It was assessed that most glial cells in the non-neuronal fraction in non-purified DRGs cultures are constituted by Schwann cells. Still, it was impossible to obtain a pure colony of them, neither through direct isolation from primary cultures nor by commercially available immortalized Schwann cells. For these reasons, it was decided to move towards a different field in which glial cells may affect neuronal excitability. The reduced excitability in purified DRGs may be caused by differences in the ion channels responsible for generating and maintaining the membrane potential responsible for neuronal cells' electrical properties. The most straightforward difference consists in a modification of the number of ion channels expressed by purified DRGs. This modification of the expression can occur at different levels: 1) a difference in the transcription, 2) a difference in the translation, and 3) a difference at the level of post-translational modifications that do not directly alter the expression in terms of transcription or translation but rather activate or deactivate the channels. Post-translational modifications are challenging to detect, especially if the target is unknown and the whole-cell proteome analysis is necessary.

For this reason, a good solution is provided by RNA sequencing. This technique does not provide information regarding the state of a specific target. Instead, it gives information about the transcripts' level, which should reflect and explain the cells' protein level. Given that bulk sequencing was not suitable for purified DRGs cultures' intrinsic characteristics, it was decided to opt for single-cell RNA sequencing. This technique has an additional advantage over bulk sequencing: it can provide information regarding the nature of each cell analyzed, therefore giving information about the types of cells present in the culture and their numbers [76].

Single-cell sequencing demonstrated once again that the isolation of DRGs via MACS is working, marking a significant reduction of glial cells in purified DRGs cultures compared to non-purified ones. Second, there was no difference in the cell compositions between the three different purified conditions analyzed. This meant that: 1) a second purification on already purified DRG neurons does not affect the outcome in terms of cell composition, and 2) the purification of non-purified DRG neurons after detaching leads to obtaining a pure DRGs culture similar to that found in seeded purified DRGs.

Looking at the expression of specific markers, it was found that several genes were downregulated in purified DRG neurons. These results were consistent with other results reported in the literature. The same genes resulted in being upregulated in rodent models of the sciatic nerve, where an increase in neuronal excitability was observed [78]. As many genes resulted in a change in their expression levels, it is essential to consider them as a whole thing in any future studies.

All experiments performed so far confirmed that glial cells are essential for neuronal excitability [10, 12, 13, 85, 86, 91, 92, 93]. Their absence in culture leads to the development of states that are the exact opposite of pain, where sensory neurons show a hyperexcitability state. What was still lacking was information regarding the nature of this contribution. Glial cells may contribute to neuronal excitability by releasing some factor(s) essential for neuronal survival and guaranteeing their functionality [74]. To assess this contribution, two approaches were used: one based on the conditioned medium and the second one based on the physical separation between neurons and glia through a semi-permeable membrane.

Different experimental set-ups were designed for the experiments involving the use of conditioned media. The most straightforward implied a simple transfer of culture media from non-purified DRGs to purified DRGs. The lack of significant difference between the different conditions can be addressed because the factors are released by glial cells in such low concentrations that are immediately captured by the nearby neurons, and therefore absent in the culture medium.

To overcome this issue, a second approach was used. This new set-up implied the use of glial cell cultures generated by seeding low-density DRG neurons, as previously described. In this way, the number of glial cells in the culture was higher than in non-purified DRGs cultures. Consequently, the concentration of released factors would have been higher if dependent on the number of cells in the culture able to release such factors. To further increase the factors' concentration, ultracentrifugation was performed, with a cut-off of 3KDa (the smallest available commercially) to retain any possible factor released by glial cells. This approach resulted in a significant difference between purified DRGs untreated and purified DRGs treated with conditioned ultracentrifugated medium. However, a significant difference was also observed within purified DRGs treated with a control ultracentrifugated medium. This could have been addressed because ultracentrifugation also concentrated any factors higher than 3KDa that were already present in the culture media. In this way, it was impossible to assess whether the contribution to neuronal excitability was caused by factors released directly by glial cells or by factors already present in the culture media that happened to be concentrated and already proven to have a role in neuronal survival, like NGF.

To overcome the issues brought by the concentration of external factors, a new approach was designed. In this third set-up, the complete Neurobasal-A medium was used for growing glial cells only during the first two days of culturing to support their growth during the earliest phase after seeding. Afterward, cells were considered able to survive on themselves, and the complete medium was replaced with Neurobasal-A medium enriched exclusively with penicillin-streptomycin to prevent any bacterial contamination. In this way, any factor present in the culture medium at the time of the ultracentrifugation would come solely from the glial cells. Unfortunately, the results obtained with this approach were not expected. There was no significant difference in the excitability between purified DRGs and purified DRGs treated either with the control or the conditioned ultracentrifugated medium. This meant that the results obtained with the previous

set-up had to be addressed exclusively to the presence of concentrated factors not released by glial cells.
Despite the discouraging results obtained with the first three set-ups, a fourth and last experiment was designed. In this case, a simple medium transfer was used again. However, differently from the first set-up, the conditioned medium used was derived from high-density glial cell cultures to increase the concentration of any factor released by forenamed glial cells. Although a significant difference between purified DRGs treated with control or conditioned medium was accounted for, both conditions' excitability was still lower than for non-purified DRGs, meaning that the treatment was not sufficient for a recovery of the excitability.
Despite the lack of a clear positive outcome, experiments with the conditioned medium helped develop a new hypothesis for explaining glial cells' contribution to neuronal excitability. Apart from the already mentioned hypothesis where the neurons immediately capture the factors released by glial cells in proximity, a second hypothesis was developed: glial cells release factors necessary for neuronal survival and functionality only in the presence of neuronal cells themselves. Therefore, culturing glial cells alone leads to the production of a medium lacking such factors. However, it was unclear whether glial cells in the same culture plate are sufficient for recovering neuronal excitability or necessary close contact between the two cell populations, as generally encountered in non-purified DRGs. To answer this question, it was necessary to develop a culture system where purified DRGs and glial cells were cultured in the same system and physically separated, though still allowing the exchange of medium between the two populations. Although several co-culture systems based on multiwell plates were available commercially, none was explicitly designed to record the electrical activity from excitable cells. Therefore, it was necessary to find a co-culturing system that would allow the use of MEA for seeding DRGs, to be able to record their electrical activity. To achieve this, special cell inserts were purchased and used for seeding glial cells. These inserts allowed the physical separation between neurons and glia. However, their seeding surface was composed of a semi-permeable membrane that allowed the flow of culture media, thus enabling exchanges between the two different cell populations.
After testing different membranes, it turned out that the CM Biopore® membrane was the best in terms of cell visualization under the microscope. As glial cells' growth was crucial for the experiment, it was decided to use this membrane. In this case, DRGs were seeded on the membrane in low-density to promote glial proliferation and grew for one week. After this time, the membrane inserts with glial cells were co-cultured on top of MEA seeded with purified DRGs, and the activity was recorded after three days. A significant difference between purified DRGs cultured alone and purified DRG co-cultured with glial cells was observed, meaning that the presence of glial cells in culture was sufficient for recovering the excitability of purified DRGs. Even though the recovery was not large enough to reach non-purified DRG neurons' excitability, it was improved compared to the experiments with a conditioned medium.
These last experiments with co-culturing glial cells and DRG neurons separated by a membrane

provided significant insight into exploiting glial cells' contribution to neuronal excitability. It is not required that glial cells are in close contact with DRG neurons (for example, through gap junctions in the case of satellite glial cells or by wrapping axons in Schwann cells) [36, 47, 94, 95]. Instead, their presence in the environment makes neuronal cells excitable and capable of responding to stimuli. This outcome is crucial for designing new experiments to understand glial cells' contribution to painful states' development, including those associated with neuropathic pain.

5 | Conclusion

This project provided further confirmation of the role of glial cells in neuronal excitability in the PNS. The use of MEA for recording the electrical activity of sensory neurons provided a satisfying throughput, considering the alternative techniques available at the time. The importance of the presence of glial cells for restoring and maintaining the excitability in sensory neurons was determined by the mere presence of such glial cells in culture, independently of whether they were in strict contact with neuronal cells or not. This suggested that glial cells release specific factors in the culture media that affect the survival and sensory neurons' activity. Future studies should aim to identify these factors, including their cellular targets, with the scope of developing novel therapies and drugs to treat neuropathic pain.

The first step to take should be the identification of all glial cell subtypes in non-purified DRG cultures. Even though this task appears challenging for the lack of suitable cell markers, recent studies on SGCs suggested their possible role in developing painful states, thanks to the release of specific markers associated with painful conditions [42]. Therefore, the identification of such cell types should be achieved. SGCs could be identified through FACS, thanks to the expression of glutamine synthetase [86]. However, this is an intracellular marker, and therefore useful only for the identification and quantification of SGC, but not for their live isolation for subsequent application. Different studies have highlighted how SGCs may contribute to pain states by identifying pain mediators' release of ATP and its receptor [11, 42]. Furthermore, recent studies have shown how the activation of SGCs leads to the development of stronger gap-junctions between DRG and SGCs, suggesting a possible role of gap-junctions in the development of painful states [11]. With these premises, following the identification of SGCs in non-purified DRG cultures, it could be interesting to try to act on the gap-junctions, for example, by blocking them and verify whether this affects neuronal excitability.

However, Schwann cells should not be put aside, as they also express the ATP receptor P2X [29]. Different protocols that describe the isolation of pure Schwann cells cultures from rat sciatic nerve have been published, and they should be translatable for the application in mice as well [96] [97]. In this way, it would be possible to generate co-cultures of pure sensory neurons and Schwann cells and eventually reproduce some experiments involving conditioned medium, semi-permeable membrane, or even other forms of co-culturing. A new approach for studying co-cultures of sensory neurons and glia would involve the use of MF-MEA again. In this case, purified DRG would be seeded in the middle channel, and Schwann cells (or glial cells in general) would be seeded in the left channel (Figure 5.1).

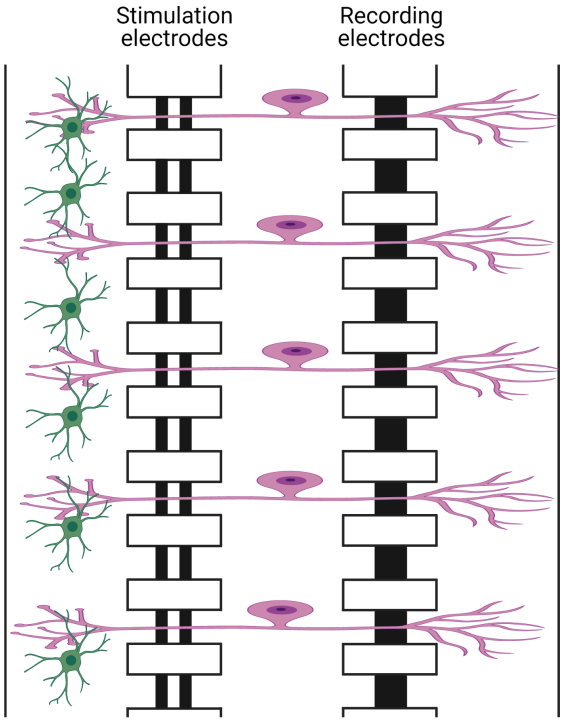

Figure 5.1: Example of a co-culture of purified DRG and glial cells in a MF-MEA system (created with BioRender.com).

In this way, it is possible to stimulate DRG through the stimulation electrodes and record their activity through the recording electrodes, as usual, to study whether the interaction between DRG neurites and glial cells affects neuronal excitability in a matter of action potential onset. This experimental set-up should also be recreated using the glial cells generated through low-density seeding. Experiments with semi-permeable membranes highlighted that glial cells' mere presence in proximity is enough for restoring partially neuronal excitability.

Despite the presence of NGF in the culture media, purified DRGs showed a drastic reduction in excitability compared to non-purified DRGs. This finding was in contrast with what was reported in the literature, where the presence of NGF affects neuronal excitability and the development of painful states in a way that immunotherapies against NGF have been proposed for treating chronic pain conditions [20, 21, 23, 24]. For these reasons, it would be worth furtherly investigate the possible role of NGF in maintaining neuronal excitability. In particular, whether NGF is also released by cells in culture. There are several ways to verify whether a specific compound is released by cells in culture and whether its absence affects the cells somehow (in the case of DRG, by altering their excitability). Blocking either NGF or its receptor would not provide the desired results and information, as it won't distinguish between exogenous and endogenous NGF but block all molecules indifferently. For this reason, it is necessary to act

more at a cellular level, either altering the transcription or the translation. Genetic knockout is the best method possible that guarantees a complete silencing of the selected gene/target when performed successfully. However, the complete silencing of NGF may have adverse effects on the animals' nervous system's development. Another way to perform genetic knockout is by using CRISPR/Cas9. Here, silencing is performed post-natally, thus eliminating the risk of affecting the animal's development. In case transgenic mice are not feasible, an alternative is provided by RNA interference. This technology uses specific nucleic acids, called short interference RNA (siRNA), which binds to the target protein's mRNA before its translation, promoting its degradation, thus ending in a non-expression of the target protein. Even though this technology does not require transgenic animals, it is necessary to have the siRNA entering the target cell without being degraded during the process. Furthermore, compared to gene silencing, the success rate of RNA interference is lower.

Another way to identify endogenous proteins in the culture media involves using amino acid isotopes in culture. This technique is called Stable Isotope Labelling in Culture (SILAC). In this technique, cells are grown in the presence of "heavy" amino acids, meaning that one of their atoms is an isotope. In this way, the peptide expressed by the cells will have a higher molecular weight than their "wild type" counterparts, thanks to these isotopes' presence. The cells are then harvested, the proteins extracted, and LC/MS is performed. In this way, it is possible to differentiate between NGF produced by the cells, which will have a "heavy" chain, from NGF directly in the culture media, with its canonical molecular weight. This difference is provided by a shift in the molecular weight in the mass spectrum produced (Figure 5.2, bottom).

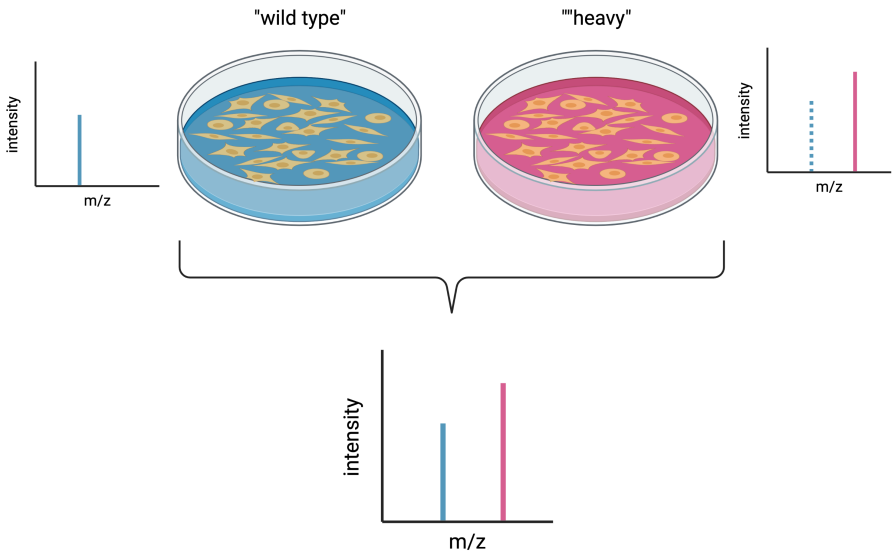

Figure 5.2: SILAC workflow. In this example, the proteomes analysed are derived from two different cell cultures, one "wild type", and one grown in presence of isotopes. For studying the release of endogenous NGF versus the presence of exogenous one, the culture analysed would be only one [98] (created with BioRender.com).

This technique has the advantage of not affecting the cells' growth and survival, as NGF will still be present in the culture. Furthermore, with LC/MS, it is also possible to quantify both the NGF produced by the cells and that provided externally in the culture media. However, it cannot forecast whether the presence of isotopes in the culture would affect the survival of the cultures themselves.

Despite its importance proven by literature, NGF may not be the only factor essential for neuronal survival and excitability. Conditioned medium experiments did not provide the expected results because any factor released by glial cells is released in such low quantity that it is not possible to detect its activity with such conventional methods. Therefore, it may be interesting to analyze the composition of conditioned medium with more sophisticated technologies that allow the detection of even the lowest amount of any compound. One technology that allows such detection is Simoa®. This technology principle is similar to ELISA, where an antigen in a solution is detected through antibody-antigen reaction [99]. The difference is that, in the case of Simoa®, the sensitivity is up to 1.000X times higher than ELISA, resulting in lower quantities of antigen required for their detection [100]. This feature makes this technology suitable for detecting DRGs cultures, where the amount of culture medium available for the analysis is low and, consequently, biomarkers levels. Another advantage of Simoa® is its ability to detect tens of biomarkers with one sample, thanks to its sensitivity. Furthermore, it uses standardized chip plates, suitable for

detecting most biomarkers, without requiring any prior validation. Alternative techniques, like peptide mapping via LC/MS, would require specific experimental conditions for each biomarker to be investigated, together with an in-depth analysis of the mass spectra to identify the peptides. The results obtained with RNA sequencing highlighted 11 downregulated genes in purified DRGs, consistent with studies that report an upregulation in sciatic nerve injury pain models [78]. It would be interesting to validate these targets with these premises to understand their contribution to neuronal excitability. For this purpose, the same techniques described for studying the role of NGF may be applied. These include the generation of knockout animals, RNA interference, and the post-natal genetic knockout through CRISPR /Cas9. In case the target is represented by a membrane protein (for example, an ion channel), a different approach is provided by merely using a channel blocker. Some of these may be already available as medicaments used to treat specific neurological conditions, while others may be identified among new molecular entities currently in development.

Last but not least, an aspect to consider is the use of animals in research. Because of this field's characteristics, neuroscience research still requires animals for most of its applications. Recently, there have been signs of progress in developing alternative methods involving iPSCs in neuroscience, and the first models for sensory iPSCs are under development at this time [101] [102]. However, one of the major drawbacks of these sensory iPSCs is the time required for their maturation: at least five weeks are necessary for obtaining the first functional sensory iPSCs. After this time, it is still essential to fully characterize them to assess that the derived cells possess sensory neurons' characteristics. This makes these cells unsuitable for pharmaceutical research, where time is one of the significant components in the drug discovery and development process. Nevertheless, studies in this field are rising year after year, and the first iPSCs-derived glial cells from the PNS have been developed as well [98]. Given the increasing requirements for further reducing the use of animals in research, it is expected to further growth of pain studies involving iPSCs-derived sensory neurons and glial cells.

Bibliography

[1] Luana Colloca et al. "Neuropathic pain". In: *Nature Reviews Disease Primers* 3.1 (Feb. 2017). DOI: 10.1038/nrdp.2017.2.

[2] Eugenio Cavalli et al. "The neuropathic pain: An overview of the current treatment and future therapeutic approaches". In: *International Journal of Immunopathology and Pharmacology* 33 (Jan. 2019). DOI: 10.1177/2058738419838383.

[3] Jonathan De Courcy et al. "A burden of illness study for neuropathic pain in Europe". In: *ClinicoEconomics and Outcomes Research* (Apr. 2016), p. 113. DOI: 10.2147/ceor.s81396.

[4] O van Hecke, N Torrance, and B.H. Smith. "Chronic pain epidemiology and its clinical relevance". In: *British Journal of Anaesthesia* 111.1 (July 2013), pp. 13–18. DOI: 10.1093/bja/aet123.

[5] João M. Bráz et al. "Forebrain GABAergic Neuron Precursors Integrate into Adult Spinal Cord and Reduce Injury-Induced Neuropathic Pain". In: *Neuron* 74.4 (May 2012), pp. 663–675. DOI: 10.1016/j.neuron.2012.02.033.

[6] Gang Chen et al. "Intrathecal bone marrow stromal cells inhibit neuropathic pain via TGF-β secretion". In: *Journal of Clinical Investigation* 125.8 (July 2015), pp. 3226–3240. DOI: 10.1172/jci80883.

[7] Edward C Emery, Ana Paula Luiz, and John N Wood. "Nav1.7 and other voltage-gated sodium channels as drug targets for pain relief". In: *Expert Opinion on Therapeutic Targets* 20.8 (Apr. 2016), pp. 975–983. DOI: 10.1517/14728222.2016.1162295.

[8] Andrew S C Rice et al. "EMA401, an orally administered highly selective angiotensin II type 2 receptor antagonist, as a novel treatment for postherpetic neuralgia: a randomised, double-blind, placebo-controlled phase 2 clinical trial". In: *The Lancet* 383.9929 (May 2014), pp. 1637–1647. DOI: 10.1016/s0140-6736(13)62337-5.

[9] M.J Elliott et al. "Randomised double-blind comparison of chimeric monoclonal antibody to tumour necrosis factor α (cA2) versus placebo in rheumatoid arthritis". In: *The Lancet* 344.8930 (Oct. 1994), pp. 1105–1110. DOI: 10.1016/s0140-6736(94)90628-9.

[10] Pavel Dublin and Menachem Hanani. "Satellite glial cells in sensory ganglia: Their possible contribution to inflammatory pain". In: *Brain, Behavior, and Immunity* 21.5 (July 2007), pp. 592–598. DOI: 10.1016/j.bbi.2006.11.011.

[11] Menachem Hanani and David C. Spray. "Emerging importance of satellite glia in nervous system function and dysfunction". In: *Nature Reviews Neuroscience* 21.9 (July 2020), pp. 485–498. DOI: 10.1038/s41583-020-0333-z.

[12] Linda R. Watkins and Steven F. Maier. "GLIA: A novel drug discovery target for clinical pain". In: *Nature Reviews Drug Discovery* 2.12 (Dec. 2003), pp. 973–985. DOI: 10.1038/nrd1251.

[13] Joachim Scholz and Clifford J Woolf. "The neuropathic pain triad: neurons, immune cells and glia". In: *Nature Neuroscience* 10.11 (Dec. 2007), pp. 1361–1368. DOI: 10.1038/nn1992.

[14] E. R. Kandel et al. *Principles of neural science*. McGraw-Hill, 2013.

[15] Ana Isabel Nascimento, Fernando Milhazes Mar, and Mónica Mendes Sousa. "The intriguing nature of dorsal root ganglion neurons: Linking structure with polarity and function". In: *Progress in Neurobiology* 168 (Sept. 2018), pp. 86–103. DOI: 10.1016/j.pneurobio.2018.05.002.

[16] S. B. McMahon et al. *Wall and Melzack's textbook of pain*. Elsevier, 2013.

[17] A. Siegel and H. N. Sapru. *Essential Neuroscience, 2nd ed.* Lippincott Williams & Wilkins, 2011.

[18] Larry R. Squire. *Fundamental Neuroscience*. Elsevier LTD, Oxford, Nov. 1, 2012. ISBN: 0123858704.

[19] Susan M Carlton and Richard E Coggeshall. "Peripheral capsaicin receptors increase in the inflamed rat hindpaw: a possible mechanism for peripheral sensitization". In: *Neuroscience Letters* 310.1 (Sept. 2001), pp. 53–56. DOI: 10.1016/s0304-3940(01)02093-6.

[20] Philip A. Barker et al. "Nerve Growth Factor Signaling and Its Contribution to Pain". In: *Journal of Pain Research* Volume 13 (May 2020), pp. 1223–1241. DOI: 10.2147/jpr.s247472.

[21] A. Chalazonitis, E. R. Peterson, and S. M. Crain. "Nerve growth factor regulates the action potential duration of mature sensory neurons." In: *Proceedings of the National Academy of Sciences* 84.1 (Jan. 1987), pp. 289–293. DOI: 10.1073/pnas.84.1.289.

[22] Franziska Denk, David L. Bennett, and Stephen B. McMahon. "Nerve Growth Factor and Pain Mechanisms". In: *Annual Review of Neuroscience* 40.1 (July 2017), pp. 307–325. DOI: 10.1146/annurev-neuro-072116-031121.

[23] Judy J Watson, Shelley J Allen, and David Dawbarn. "Targeting Nerve Growth Factor in Pain". In: *BioDrugs* 22.6 (2008), pp. 349–359. DOI: 10.2165/0063030-200822060-00002.

[24] Franz Hefti. “Pharmacology of nerve growth factor and discovery of tanezumab, an anti-nerve growth factor antibody and pain therapeutic”. In: *Pharmacological Research* 154 (Apr. 2020), p. 104240. DOI: 10.1016/j.phrs.2019.04.024.

[25] Peter W. Beck and Hermann O. Handwerker. “Bradykinin and serotonin effects on various types of cutaneous nerve fibres”. In: *Pflügers Archiv European Journal of Physiology* 347.3 (1974), pp. 209–222. DOI: 10.1007/bf00592598.

[26] Ratan Kumar Banik et al. “B2 Receptor–Mediated Enhanced Bradykinin Sensitivity of Rat Cutaneous C-Fiber Nociceptors During Persistent Inflammation”. In: *Journal of Neurophysiology* 86.6 (Dec. 2001), pp. 2727–2735. DOI: 10.1152/jn.2001.86.6.2727.

[27] Sara G. Hamilton et al. “ATP in human skin elicits a dose-related pain response which is potentiated under conditions of hyperalgesia”. In: *Brain* 123.6 (June 2000), pp. 1238–1246. DOI: 10.1093/brain/123.6.1238.

[28] Bryan J. Black et al. “Adult mouse sensory neurons on microelectrode arrays exhibit increased spontaneous and stimulus-evoked activity in the presence of interleukin-6”. In: *Journal of Neurophysiology* 120.3 (Sept. 2018), pp. 1374–1385. DOI: 10.1152/jn.00158.2018.

[29] Mark D. Baker. “Electrophysiology of mammalian Schwann cells”. In: *Progress in Biophysics and Molecular Biology* 78.2-3 (Feb. 2002), pp. 83–103. DOI: 10.1016/s0079-6107(02)00007-x.

[30] Kristjan R. Jessen and Rhona Mirsky. “The origin and development of glial cells in peripheral nerves”. In: *Nature Reviews Neuroscience* 6.9 (Sept. 2005), pp. 671–682. DOI: 10.1038/nrn1746.

[31] Peter G. Noakes and Max R. Bennett. “Growth of axons into developing muscles of the chick forelimb is preceded by cells that stain with Schwann cell antibodies”. In: *The Journal of Comparative Neurology* 259.3 (May 1987), pp. 330–347. DOI: 10.1002/cne.902590303.

[32] Bruce R. Ransom. *Neuroglia*. Oxford University Press, Dec. 28, 2012. 864 pp. ISBN: 0199794596.

[33] Zhangyin Liu et al. “Specific Marker Expression and Cell State of Schwann Cells during Culture In Vitro”. In: *PLOS ONE* 10.4 (Apr. 2015). Ed. by Maria Cristina Vinci, e0123278. DOI: 10.1371/journal.pone.0123278.

[34] John W. Griffin and Wesley J. Thompson. “Biology and pathology of nonmyelinating Schwann cells”. In: *Glia* 56.14 (Nov. 2008), pp. 1518–1531. DOI: 10.1002/glia.20778.

[35] Menachem Hanani. “Satellite glial cells in sensory ganglia: from form to function”. In: *Brain Research Reviews* 48.3 (June 2005), pp. 457–476. DOI: 10.1016/j.brainresrev.2004.09.001.

[36] Li-Yen M. Huang, Yanping Gu, and Yong Chen. "Communication between neuronal somata and satellite glial cells in sensory ganglia". In: *Glia* 61.10 (Aug. 2013), pp. 1571–1581. DOI: 10.1002/glia.22541.

[37] Oshri Avraham et al. "Satellite glial cells promote regenerative growth in sensory neurons". In: *Nature Communications* 11.1 (Sept. 2020). DOI: 10.1038/s41467-020-18642-y.

[38] Dale George, Paige Ahrens, and Stephen Lambert. "Satellite glial cells represent a population of developmentally arrested Schwann cells". In: *Glia* 66.7 (Mar. 2018), pp. 1496–1506. DOI: 10.1002/glia.23320.

[39] Matthias Weider et al. "Elevated In Vivo Levels of a Single Transcription Factor Directly Convert Satellite Glia into Oligodendrocyte-like Cells". In: *PLOS Genetics* 11.2 (Feb. 2015). Ed. by Ben A. Barres. DOI: 10.1371/journal.pgen.1005008.

[40] S. Britsch. "The transcription factor Sox10 is a key regulator of peripheral glial development". In: *Genes & Development* 15.1 (Jan. 2001), pp. 66–78. DOI: 10.1101/gad.186601.

[41] Vitali Belzer, Nathanael Shraer, and Menachem Hanani. "Phenotypic changes in satellite glial cells in cultured trigeminal ganglia". In: *Neuron Glia Biology* 6.4 (Nov. 2010), pp. 237–243. DOI: 10.1017/s1740925x1100007x.

[42] Ru-Rong Ji, Christopher R. Donnelly, and Maiken Nedergaard. "Astrocytes in chronic pain and itch". In: *Nature Reviews Neuroscience* 20.11 (Sept. 2019), pp. 667–685. DOI: 10.1038/s41583-019-0218-1.

[43] Peter M. Grace et al. "Pathological pain and the neuroimmune interface". In: *Nature Reviews Immunology* 14.4 (Feb. 2014), pp. 217–231. DOI: 10.1038/nri3621.

[44] Gang Chen et al. "Microglia in Pain: Detrimental and Protective Roles in Pathogenesis and Resolution of Pain". In: *Neuron* 100.6 (Dec. 2018), pp. 1292–1311. DOI: 10.1016/j.neuron.2018.11.009.

[45] Kazuhide Inoue and Makoto Tsuda. "Microglia in neuropathic pain: cellular and molecular mechanisms and therapeutic potential". In: *Nature Reviews Neuroscience* 19.3 (Feb. 2018), pp. 138–152. DOI: 10.1038/nrn.2018.2.

[46] Yu Shin Kim et al. "Coupled Activation of Primary Sensory Neurons Contributes to Chronic Pain". In: *Neuron* 91.5 (Feb. 2016), pp. 1085–1096. DOI: 10.1016/j.neuron.2016.07.044.

[47] Tian-Ying Huang, Vitali Belzer, and Menachem Hanani. "Gap junctions in dorsal root ganglia: Possible contribution to visceral pain". In: *European Journal of Pain* 14.1 (Jan. 2010), 49.e1–49.e9. DOI: 10.1016/j.ejpain.2009.02.005.

[48] Douglas B. Weibel, Willow R. DiLuzio, and George M. Whitesides. "Microfabrication meets microbiology". In: *Nature Reviews Microbiology* 5.3 (Mar. 2007), pp. 209–218. DOI: 10.1038/nrmicro1616.

[49] Anita Niedworok. "Developing a 3-dimensional electrophysiological assay for functional studies on human iPSC-derived neurons". MA thesis. University of Hohenheim, 2015.

[50] James N. Sleigh, Greg A. Weir, and Giampietro Schiavo. "A simple, step-by-step dissection protocol for the rapid isolation of mouse dorsal root ganglia". In: *BMC Research Notes* 9.1 (Feb. 2016). DOI: 10.1186/s13104-016-1915-8.

[51] Beatriz Molina Martínez. "Development of a novel 3D microphysiological system for functional and morphological assessment of neuronal networks". PhD thesis. University of Tübingen, 2020.

[52] C. R. Legendy and M. Salcman. "Bursts and recurrences of bursts in the spike trains of spontaneously active striate cortex neurons". In: *Journal of Neurophysiology* 53.4 (Apr. 1985), pp. 926–939. DOI: 10.1152/jn.1985.53.4.926.

[53] Isabel Devesa et al. "αCGRP is essential for algesic exocytotic mobilization of TRPV1 channels in peptidergic nociceptors". In: *Proceedings of the National Academy of Sciences* (2014). ISSN: 0027-8424. DOI: 10.1073/pnas.1420252111.

[54] Linda R. Watkins and Steven F. Maier. "Beyond Neurons: Evidence That Immune and Glial Cells Contribute to Pathological Pain States". In: *Physiological Reviews* 82.4 (Jan. 2002), pp. 981–1011. DOI: 10.1152/physrev.00011.2002.

[55] L. Urban and A. Dray. "Actions of capsaicin on mouse dorsal root ganglion cells in vitro". In: *Neuroscience Letters* 157.2 (July 1993), pp. 187–190. DOI: 10.1016/0304-3940(93)90733-2.

[56] Makoto Tominaga and Tomoko Tominaga. "Structure and function of TRPV1". In: *Pflügers Archiv - European Journal of Physiology* 451.1 (June 2005), pp. 143–150. DOI: 10.1007/s00424-005-1457-8.

[57] Jeffrey T. Lock, Ian Parker, and Ian F. Smith. "A comparison of fluorescent Ca^{2+} indicators for imaging local Ca^{2+} signals in cultured cells". In: *Cell Calcium* 58.6 (Dec. 2015), pp. 638–648. DOI: 10.1016/j.ceca.2015.10.003.

[58] R. Alan North. "P2X3receptors and peripheral pain mechanisms". In: *The Journal of Physiology* 554.2 (Jan. 2004), pp. 301–308. DOI: 10.1113/jphysiol.2003.048587.

[59] Karen Kage et al. "Alteration of dorsal root ganglion P2X 3 receptor expression and function following spinal nerve ligation in the rat". In: *Experimental Brain Research* 147.4 (Dec. 2002), pp. 511–519. DOI: 10.1007/s00221-002-1263-x.

[60] William A. Catterall. “Signaling complexes of voltage-gated sodium and calcium channels”. In: *Neuroscience Letters* 486.2 (Dec. 2010), pp. 107–116. DOI: 10.1016/j.neulet.2010.08.085.

[61] Zainab A. Mohammed et al. “Veratridine produces distinct calcium response profiles in mouse Dorsal Root Ganglia neurons”. In: *Scientific Reports* 7.1 (Mar. 2017). DOI: 10.1038/srep45221.

[62] François Marceau et al. “Bradykinin receptors: Agonists, antagonists, expression, signaling, and adaptation to sustained stimulation”. In: *International Immunopharmacology* 82 (May 2020), p. 106305. DOI: 10.1016/j.intimp.2020.106305.

[63] Matthew Thakur et al. “Defining the nociceptor transcriptome”. In: *Frontiers in Molecular Neuroscience* 7 (Nov. 2014). DOI: 10.3389/fnmol.2014.00087.

[64] Abcam. *Immunocytochemistry and immunofluorescence protocol*. 2020. URL: https://www.abcam.com/protocols/immunocytochemistry-immunofluorescence-protocol.

[65] Zhihui Yang and Kevin K.W. Wang. “Glial fibrillary acidic protein: from intermediate filament assembly and gliosis to neurobiomarker”. In: *Trends in Neurosciences* 38.6 (June 2015), pp. 364–374. DOI: 10.1016/j.tins.2015.04.003.

[66] Zdenek Lukas et al. “Expression of class III beta-tubulin in normal and neoplastic human tissues”. In: *Histochemistry and Cell Biology* 109.3 (Feb. 1998), pp. 231–239. DOI: 10.1007/s004180050222.

[67] Hind Abdo et al. “Specialized cutaneous Schwann cells initiate pain sensation”. In: *Science* 365.6454 (Aug. 2019), pp. 695–699. DOI: 10.1126/science.aax6452.

[68] Zayra V. Garavito et al. “Is S-100 protein a suitable marker for adult Schwann cellls?” In: *In Vitro Cellular & Developmental Biology - Animal* 36.5 (2000), p. 281. DOI: 10.1290/1071-2690(2000)036<0281:ispasm>2.0.co;2.

[69] Sino Biological. *Fluorescence Activated Cell Sorting (FACS)*. 2020. URL: https://www.sinobiological.com/category/fcm-facs-facs.

[70] Addgene Protocols. *Isolating a Monoclonal Cell Population by Limiting Dilution*. 2020. URL: https://www.addgene.org/protocols/limiting-dilution/.

[71] Rui Liu, Gou Lin, and Hanpeng Xu. “An Efficient Method for Dorsal Root Ganglia Neurons Purification with a One-Time Anti-Mitotic Reagent Treatment”. In: *PLoS ONE* 8.4 (Apr. 2013). Ed. by Joao carlos Bettencourt de Medeiros Relvas, e60558. DOI: 10.1371/journal.pone.0060558.

[72] Roberta Bianchi, Ileana Giambanco, and Rosario Donato. "S-100 Protein, but Not Calmodulin, Binds to the Glial Fibrillary Acidic Protein and Inhibits Its Polymerization in a Ca2+-dependent Manner". In: *The Journal of Biological Chemistry* 268.17 (1993), pp. 12669–12674.

[73] Juliana Karl Frizzo et al. "S100B-Mediated Inhibition of the Phosphorylation of GFAP Is Prevented by TRTK-12". In: *Neurochemical Research* 29.4 (Apr. 2004), pp. 735–740. DOI: 10.1023/b:nere.0000018844.51009.40.

[74] K. Watabe et al. "Spontaneously immortalized adult mouse Schwann cells secrete autocrine and paracrine growth-promoting activities". In: *Journal of Neuroscience Research* 41.2 (June 1995), pp. 279–290. DOI: 10.1002/jnr.490410215.

[75] Kazunori Sango et al. "Immortalized Adult Rodent Schwann Cells as In Vitro Models to Study Diabetic Neuropathy". In: *Experimental Diabetes Research* 2011 (2011), pp. 1–9. DOI: 10.1155/2011/374943.

[76] 10X Genomics. *Chromium Single Cell Gene Expression*. 2020. URL: https://www.10xgenomics.com/products/single-cell-gene-expression/.

[77] Byungjin Hwang, Ji Hyun Lee, and Duhee Bang. "Single-cell RNA sequencing technologies and bioinformatics pipelines". In: *Experimental & Molecular Medicine* 50.8 (Aug. 2018), pp. 1–14. DOI: 10.1038/s12276-018-0071-8.

[78] Douglas M. Lopes et al. "Sex differences in peripheral not central immune responses to pain-inducing injury". In: *Scientific Reports* 7.1 (Nov. 2017). DOI: 10.1038/s41598-017-16664-z.

[79] Wuping Sun et al. "A Transcriptomic Analysis of Neuropathic Pain in Rat Dorsal Root Ganglia Following Peripheral Nerve Injury". In: *NeuroMolecular Medicine* 22.2 (Dec. 2019), pp. 250–263. DOI: 10.1007/s12017-019-08581-3.

[80] H.-S. Xiao et al. "Identification of gene expression profile of dorsal root ganglion in the rat peripheral axotomy model of neuropathic pain". In: *Proceedings of the National Academy of Sciences* 99.12 (June 2002), pp. 8360–8365. DOI: 10.1073/pnas.122231899.

[81] Weizmann Institute of Science. *GeneCards*. 2020. URL: https://www.genecards.org/.

[82] UniProt Consortium. *UniProt*. 2020. URL: https://www.uniprot.org/.

[83] Alan D. Wickenden. "Overview of Electrophysiological Techniques". In: *Current Protocols in Pharmacology* 11.1 (Dec. 2000). DOI: 10.1002/0471141755.ph1101s64.

[84] Estrela Neto et al. "Compartmentalized Microfluidic Platforms: The Unrivaled Breakthrough of In Vitro Tools for Neurobiological Research". In: *The Journal of Neuroscience* 36.46 (Nov. 2016), pp. 11573–11584. DOI: 10.1523/jneurosci.1748-16.2016.

[85] Hong Cao and Yu-Qiu Zhang. "Spinal glial activation contributes to pathological pain states". In: *Neuroscience & Biobehavioral Reviews* 32.5 (July 2008), pp. 972–983. DOI: 10.1016/j.neubiorev.2008.03.009.

[86] Luc Jasmin et al. "Can satellite glial cells be therapeutic targets for pain control?" In: *Neuron Glia Biology* 6.1 (Feb. 2010), pp. 63–71. DOI: 10.1017/s1740925x10000098.

[87] E. A. Kolos and D. E. Korzhevskii. "Glutamine Synthetase-Containing Cells of the Dorsal Root Ganglion at Different Stages of Rat Ontogeny". In: *Russian Journal of Developmental Biology* 49.3 (May 2018), pp. 179–183. DOI: 10.1134/s1062360418030049.

[88] Novusbio. *Immunocytochemistry (ICC) handbook*. 2020. URL: https://images.novusbio.com/design/BR_ICCguide.pdf.

[89] D. Bianchini et al. "GFAP expression of human Schwann cells in tissue culture". In: *Brain Research* 570.1-2 (Jan. 1992), pp. 209–217. DOI: 10.1016/0006-8993(92)90583-u.

[90] Kristjn R. Jessen, Robin Thorpe, and Rhona Mirsky. "Molecular identity, distribution and heterogeneity of glial fibrillary acidic protein: an immunoblotting and immunohistochemical study of Schwann cells, satellite cells, enteric glia and astrocytes". In: *Journal of Neurocytology* 13.2 (Apr. 1984), pp. 187–200. DOI: 10.1007/bf01148114.

[91] Filipa Alexandra Leite Costa and Fani Lourença Moreira Neto. "Satellite glial cells in sensory ganglia: its role in pain". In: *Brazilian Journal of Anesthesiology (English Edition)* 65.1 (Jan. 2015), pp. 73–81. DOI: 10.1016/j.bjane.2013.07.013.

[92] Peter T. Ohara et al. "Gliopathic Pain: When Satellite Glial Cells Go Bad". In: *The Neuroscientist* 15.5 (Oct. 2009), pp. 450–463. DOI: 10.1177/1073858409336094.

[93] Marc R. Suter et al. "Do glial cells control pain?" In: *Neuron Glia Biology* 3.3 (Aug. 2007), pp. 255–268. DOI: 10.1017/s1740925x08000100.

[94] Menachem Hanani. "Intercellular communication in sensory ganglia by purinergic receptors and gap junctions: Implications for chronic pain". In: *Brain Research* 1487 (Dec. 2012), pp. 183–191. DOI: 10.1016/j.brainres.2012.03.070.

[95] Tian-Ying Huang et al. "Dye coupling among satellite glial cells in mammalian dorsal root ganglia". In: *Brain Research* 1036.1-2 (Mar. 2005), pp. 42–49. DOI: 10.1016/j.brainres.2004.12.021.

[96] David E. Weinstein and Rina Wu. "Isolation and Purification of Primary Schwann Cells". In: *Current Protocols in Neuroscience* 8.1 (Aug. 1999). DOI: 10.1002/0471142301.ns0317s08.

[97] Henrika Honkanen et al. "Isolation, purification and expansion of myelination-competent, neonatal mouse Schwann cells". In: *European Journal of Neuroscience* 26.4 (Aug. 2007), pp. 953–964. DOI: 10.1111/j.1460-9568.2007.05726.x.

[98] CP. *Stable Isotope Labeling Using Amino Acids in Cell Culture (SILAC): Principles, Workflow, and Applications*. 2018. URL: https://www.creative-proteomics.com/blog/index.php/stable-isotope-labeling-using-amino-acids-in-cell-culture-silac-principles-workflow-and-applications/.

[99] Claire Horlock. *Enzyme-linked immunosorbent assay (ELISA)*. 2021. URL: https://www.immunology.org/public-information/bitesized-immunology/experimental-techniques/enzyme-linked-immunosorbent-assay.

[100] Quanterix. *Simoa® Technology*. 2021. URL: https://www.quanterix.com/simoa-technology/.

[101] Jeremy Schwartzentruber et al. "Molecular and functional variation in iPSC-derived sensory neurons". In: *Nature Genetics* 50.1 (Dec. 2017), pp. 54–61. DOI: 10.1038/s41588-017-0005-8.

[102] Chenling Xiong et al. "Human Induced Pluripotent Stem Cell Derived Sensory Neurons are Sensitive to the Neurotoxic Effects of Paclitaxel". In: *Clinical and Translational Science* (June 2020). DOI: 10.1101/2020.06.04.134262.

Appendix

Appendix

A.1 Descriptive statistics

(a) Descriptive statistics for capsaicin

Condition	after 3 hours		after 24 hours		after 72 hours	
	Purified	Non-purified	Purified	Non-purified	Purified	Non-purified
Number of values	1365	1466	1375	1330	825	664
Mean	3.516	7.776	8.364	30.68	2.303	35.09
Std. Deviation	18.43	26.79	27.69	46.13	15.01	47.76
Std. Error of Mean	0.4987	0.6997	0.7469	1.265	0.5225	1.853
Lower 95% CI of Mean	2.538	6.404	6.899	28.20	1.277	31.45
Upper 95% CI of Mean	4.495	9.149	9.829	33.16	3.329	38.73

(b) Unpaired t test for capsaicin

Entry	after 3 hours	after 24 hours	after 72 hours
P value	<0.0001	<0.0001	<0.0001
P value summary	****	****	****
Significantly different (P<0.05)?	Yes	Yes	Yes
One- or Two-tailed P value?	Two-tailed	Two-tailed	Two-tailed
t, df	t=4.895, df=2829	t=15.31, df=2703	t=18.61, df=1487
Mean of purified	3.516	8.364	2.303
Mean of non-purified	7.776	30.68	35.09
Difference between means ± SEM	4.260 ± 0.8703	22.31 ± 1.458	32.79 ± 1.762
95% confidence interval	2.553 to 5.966	19.46 to 25.17	29.33 to 36.24
R squared (eta squared)	0.008398	0.07978	0.1889

Table A.1: Descriptive statistics and unpaired t-test for capsaicin

(a) Descriptive statistics for αβ-ATP

Condition	Non-purified	Purified
Number of values	560	741
Mean	47.32	4.453
Std. Deviation	49.97	20.64
Std. Error of Mean	2.112	0.7583
Lower 95% CI of Mean	43.17	2.965
Upper 95% CI of Mean	51.47	5.942

(b) Unpaired t test for αβ-ATP

Entry	Value
P value	<0.0001
P value summary	****
Significantly different (P<0.05)?	Yes
One- or Two-tailed P value?	Two-tailed
t, df	t=21.09, df=1299
Mean of non-purified	47.32
Mean of purified	4.453
Difference between means ± SEM	42.87 ± 2.032
95% confidence interval	38.88 to 46.85
R squared (eta squared)	0.2551

Table A.2: Descriptive statistics and unpaired t-test for αβ-ATP

(a) Descriptive statistics for veratridine

Condition	Non-purified	Purified
Number of values	467	637
Mean	23.91	3.651
Std. Deviation	42.54	18.66
Std. Error of Mean	1.968	0.7395
Lower 95% CI of Mean	20.04	2.199
Upper 95% CI of Mean	27.77	5.104

(b) Unpaired t test for veratridine

Entry	Value
P value	<0.0001
P value summary	****
Significantly different (P<0.05)?	Yes
One- or Two-tailed P value?	Two-tailed
t, df	t=10.70, df=1102
Mean of non-purified	23.91
Mean of purified	3.651
Difference between means ± SEM	20.25 ± 1.894
95% confidence interval	16.54 to 23.97
R squared (eta squared)	0.09406

Table A.3: Descriptive statistics and unpaired t-test for veratridine

(a) Descriptive statistics for bradykinin

Condition	Non-purified	Purified
Number of values	238	795
Mean	12.18	2.767
Std. Deviation	32.78	16.41
Std. Error of Mean	2.125	0.5821
Lower 95% CI of Mean	7.999	1.625
Upper 95% CI of Mean	16.37	3.910

(b) Unpaired t test for bradykinin

Entry	Value
P value	<0.0001
P value summary	****
Significantly different (P<0.05)?	Yes
One- or Two-tailed P value?	Two-tailed
t, df	t=5.979, df=1031
Mean of non-purified	12.18
Mean of purified	2.767
Difference between means ± SEM	9.418 ± 1.575
95% confidence interval	6.327 to 12.51
R squared (eta squared)	0.03351

Table A.4: Descriptive statistics and unpaired t-test for bradykinin

(a) Descriptive statistics for mean frequency in burst

Condition	caps		αβATP		vtr		BK	
	P	NP	P	NP	P	NP	P	NP
Number of values	19	233	33	265	49	175	22	75
Mean	11.41	9.317	4.536	4.486	26.44	22.60	1.748	1.246
Std. Deviation	12.58	9.723	3.329	11.55	31.51	32.98	1.901	1.031
Std. Error of Mean	2.886	0.6369	0.5794	0.7093	4.501	2.493	0.4053	0.1191
Lower 95% CI of mean	5.346	8.062	3.356	3.090	17.39	17.68	0.9054	1.009
Upper 95% CI of mean	17.47	10.57	5.717	5.883	35.49	27.52	2.591	1.484

(b) Unpaired t test for mean frequency in burst (for each agonist, purified DRGs were tested against non-purified DRGs)

Entry	caps	αβATP	vtr	BK
P value	0.3790	0.9804	0.4676	0.1079
P value summary	ns	ns	ns	ns
Significantly different (P<0.05)?	No	No	No	No
One- or Two-tailed P value?	Two-tailed	Two-tailed	Two-tailed	Two-tailed
t, df	t=0.8813, df=250	t=0.02464, df=296	t=0.7276, df=222	t=1.623, df=95
Mean of purified	11.41	4.536	26.44	1.748
Mean of non-purified	9.317	4.486	22.60	1.246
Difference between means ± SEM	2.093 ± 2.375	0.04986 ± 2.023	3.842 ± 5.280	0.5020 ± 0.3093
95% confidence interval	-2.585 to 6.772	-3.932 to 4.031	-6.564 to 14.25	-0.1120 to 1.116
R squared (eta squared)	0.003097	2.052e-006	0.002379	0.02698

Table A.5: Descriptive statistics and unpaired t-test for mean frequency in burst

Condition	Capsaicin			Veratridine		
	P MEA	NP MEA	P imaging	P MEA	NP MEA	P imaging
Number of values	825	664	106	637	467	73
Mean	2.303	35.09	33.96	3.651	23.91	90.41
Std. Deviation	15.01	47.76	47.58	18.66	42.54	29.65
Std. Error of Mean	0.5225	1.853	4.622	0.7395	1.968	3.470
Lower 95% CI of Mean	1.277	31.45	24.80	83.49	2.199	20.04
Upper 95% CI of Mean	3.329	38.73	43.13	97.33	5.104	27.77

Table A.6: Descriptive statistics for calcium imaging experiments

(a) Unpaired t test for purified DRGs with capsaicin on MEA vs. imaging

Entry	Value
P value	<0.0001
P value summary	****
Significantly different (P<0.05)?	Yes
One- or Two-tailed P value?	Two-tailed
t, df	t=14.37, df=929
Mean of capsaicin purified MEA	2.303
Mean of capsaicin purified imaging	33.96
Difference between means ± SEM	31.66 ± 2.203
95% confidence interval	27.34 to 35.98
R squared (eta squared)	0.1819

(b) Unpaired t test for purified DRGs with imaging vs. non-purified DRGs on MEA

Entry	Value
P value	0.8213
P value summary	ns
Significantly different (P<0.05)?	No
One- or Two-tailed P value?	Two-tailed
t, df	t=0.2259, df=768
Mean of capsaicin non-purified MEA	35.09
Mean of capsaicin purified imaging	33.96
Difference between means ± SEM	1.128 ± 4.993
95% confidence interval	-8.673 to 10.93
R squared (eta squared)	6.646e-005

Table A.7: Unpaired t-test for calcium imaging experiments part I

(a) Unpaired t test for purified DRGs with veratridine on MEA vs. imaging

Entry	Value
P value	<0.0001
P value summary	****
Significantly different (P<0.05)?	Yes
One- or Two-tailed P value?	Two-tailed
t, df	t=35.01, df=708
Mean of veratridine purified MEA	90.41
Mean of veratridine purified imaging	23.91
Difference between means ± SEM	86.76 ± 2.478
95% confidence interval	81.89 to 91.63
R squared (eta squared)	0.6338

(b) Unpaired t test for veratridine on purified DRGs in imaging vs. non-purified DRGs on MEA

Entry	Value
P value	<0.0001
P value summary	****
Significantly different (P<0.05)?	Yes
One- or Two-tailed P value?	Two-tailed
t, df	t=12.87, df=538
Mean of veratridine non-purified MEA	23.91
Mean of veratridine purified imaging	90.41
Difference between means ± SEM	66.51 ± 5.166
95% confidence interval	56.36 to 76.65
R squared (eta squared)	0.2355

Table A.8: Unpaired t-tests for Calcium imaging experiments part II

Entry	150mV	250mV	350mV	450mV
P value	0.19	0.0019	0.0404	0.5234
P value summary	ns	**	*	ns
Significantly different (P<0.05)?	No	Yes	Yes	No
One- or Two-tailed P value?	Two-tailed	Two-tailed	Two-tailed	Two-tailed
t, df	t=1.383, df=13	t=3.890, df=13	t=2.277, df=13	t=0.6559, df=13
Mean of non-purified DRG	8.911	45.05	63.91	74.24
Mean of purified DRG	0.000	5.000	31.89	64.89
Difference between means ± SEM	8.911 ± 6.444	40.05 ± 10.29	32.02 ± 14.06	9.349 ± 14.25
95% confidence interval	-5.010 to 22.83	17.81 to 62.29	1.638 to 62.40	-21.45 to 40.14
R squared (eta squared)	0.1282	0.5379	0.2851	0.03203

Table A.9: Unpaired t test for MF-MEA with for different mV stimulation

(a) Descriptive statistics for experiments with different % of glial cells: total number of neurons

Condition	90%		75%		50%		mixed	
	DIV3	DIV6	DIV3	DIV6	DIV3	DIV6	DIV3	DIV6
Number of values	10	6	6	6	6	6	6	6
Mean	1289	1339	1288	1398	1459	1404	1265	1285
Std. Deviation	179.0	165.5	211.9	262.5	282.7	197.0	200.8	152.6
Std. Error of Mean	56.61	67.58	86.52	107.2	115.4	80.43	81.99	62.30
Lower 95% CI of mean	1161	1166	1066	1122	1162	1197	1055	1125
Upper 95% CI of mean	1417	1513	1510	1673	1756	1611	1476	1445

(b) Ordinary one-way ANOVA for total number of neurons in glia experiments

	SS	DF	MS	F (DFn, DFd)	P value
Treatment (between columns)	4785	3	1595	F (3, 24) = 12.13	P<0.0001
Residual (within columns)	3154	24	131.4		
Total	7939	27			

(c) Descriptive statistics for experiments with different % of glial cells: capsaicin response

Condition	90%		75%		50%		mixed	
	DIV3	DIV6	DIV3	DIV6	DIV3	DIV6	DIV3	DIV6
Number of values	610	337	395	404	407	405	399	348
Mean	9.180	25.22	24.05	34.90	28.75	28.40	45.11	39.37
Std. Deviation	28.90	43.49	42.79	47.72	45.31	45.15	49.82	48.93
Std. Error of Mean	1.170	2.369	2.153	2.374	2.246	2.243	2.494	2.623
Lower 95% CI of Mean	6.882	20.56	19.82	30.23	24.33	23.98	40.21	34.21
Upper 95% CI of Mean	11.48	29.88	28.28	39.57	33.16	32.81	50.02	44.53

Table A.10: Descriptive statistics for glia experiments

(a) Unpaired t test for 90% condition DIV3 vs. DIV6

Entry	Value
P value	<0.0001
P value summary	****
Significantly different (P<0.05)?	Yes
One- or Two-tailed P value?	Two-tailed
t, df	t=6.793, df=945
Mean of 90% DIV3	9.180
Mean of 90% DIV6	25.22
Difference between means ± SEM	16.04 ± 2.362
95% confidence interval	11.41 to 20.68
R squared (eta squared)	0.04655

(b) Unpaired t test for 75% condition DIV3 vs. DIV6

Entry	Value
P value	0.0008
P value summary	***
Significantly different (P<0.05)?	Yes
One- or Two-tailed P value?	Two-tailed
t, df	t=3.381, df=797
Mean of 75% DIV3	24.05
Mean of 75% DIV6	34.90
Difference between means ± SEM	10.85 ± 3.209
95% confidence interval	4.551 to 17.15
R squared (eta squared)	0.014114

Table A.11: Unpaired t-test for capsaicin response in glia experiments I

(a) Unpaired t test for 50% condition DIV3 vs. DIV6

Entry	Value
P value	0.9118
P value summary	ns
Significantly different (P<0.05)?	No
One- or Two-tailed P value?	Two-tailed
t, df	t=0.1108, df=810
Mean of 50% DIV3	28.75
Mean of 50% DIV6	28.40
Difference between means ± SEM	0.3519 ± 3.175
95% confidence interval	-5.880 to 6.583
R squared (eta squared)	1.517e-005

(b) Unpaired t test for mixed condition DIV3 vs. DIV6

Entry	Value
P value	0.1133
P value summary	ns
Significantly different (P<0.05)?	No
One- or Two-tailed P value?	Two-tailed
t, df	t=1.585, df=745
Mean of mixed DIV3	45.11
Mean of mixed DIV6	39.37
Difference between means ± SEM	5.745 ± 3.624
95% confidence interval	-1.369 to 12.86
R squared (eta squared)	0.003362

Table A.12: Unpaired t-test for capsaicin response in glia experiments II

Condition	90%		75%		50%		mixed	
	DIV3	DIV6	DIV3	DIV6	DIV3	DIV6	DIV3	DIV6
Number of values	10	6	6	6	6	6	6	6
Mean	1.302	2.272	2.847	4.337	3.881	5.230	5.575	7.467
Std. Deviation	0.3023	0.9011	0.4935	1.259	1.079	0.8369	0.7325	1.148
Std. Error of Mean	0.09559	0.3679	0.2015	0.5141	0.4405	0.3416	0.2990	0.4689
Lower 95% CI of mean	1.086	1.326	2.329	3.016	2.749	4.352	4.806	6.262
Upper 95% CI of mean	1.518	3.217	3.365	5.659	5.013	6.108	6.344	8.672

Table A.13: Descriptive statistics for ratio glia:neurons

(a) Unpaired t test for ratio glia:neurons 90% condition DIV3 vs. DIV6

Entry	Value
P value	<0.0067
P value summary	**
Significantly different (P<0.05)?	Yes
One- or Two-tailed P value?	Two-tailed
t, df	t=3.181, df=14
Mean of 90% DIV3	1.302
Mean of 90% DIV6	2.272
Difference between means ± SEM	0.9699 ± 0.3049
95% confidence interval	0.3158 to 1.624
R squared (eta squared)	0.4195

(b) Unpaired t test for ratio glia:neurons 75% condition DIV3 vs. DIV6

Entry	Value
P value	0.0223
P value summary	*
Significantly different (P<0.05)?	Yes
One- or Two-tailed P value?	Two-tailed
t, df	t=2.699, df=10
Mean of 75% DIV3	2.847
Mean of 75% DIV6	4.337
Difference between means ± SEM	1.490 ± 0.5521
95% confidence interval	0.26 to 2.72
R squared (eta squared)	0.4215

Table A.14: Unpaired t-test for ratio glia:neurons part I

(a) Unpaired t test for ratio glia:neurons 50% condition DIV3 vs. DIV6

Entry	Value
P value	0.0361
P value summary	*
Significantly different (P<0.05)?	Yes
One- or Two-tailed P value?	Two-tailed
t, df	t=2.419, df=10
Mean of 50% DIV3	3.881
Mean of 50% DIV6	5.230
Difference between means ± SEM	1.349 ± 0.5575
95% confidence interval	0.1066 to 2.591
R squared (eta squared)	0.3692

(b) Unpaired t test for ratio glia:neurons mixed condition DIV3 vs. DIV6

Entry	Value
P value	0.0068
P value summary	**
Significantly different (P<0.05)?	Yes
One- or Two-tailed P value?	Two-tailed
t, df	t=3.402, df=10
Mean of mixed DIV3	5.575
Mean of mixed DIV6	7.467
Difference between means ± SEM	1.892 ± 0.5561
95% confidence interval	0.6527 to 3.131
R squared (eta squared)	0.5364

Table A.15: Unpaired t-test for ratio glia:neurons part II

(a) Descriptive statistics for experiments with commercial antibodies

Entry	DRG + SC	DRG + EC	DRG + SGCs	DRG + FB	Purified DRG	Non-purified DRG
Number of values	347	366	362	397	825	664
Mean	5.764	6.831	3.867	3.275	2.303	35.09
Std. Deviation	23.34	25.26	19.31	17.82	15.01	47.76
Std. Error of Mean	1.253	1.320	1.015	0.8943	0.5225	1.853
Lower 95% CI of mean	3.299	4.234	1.872	1.516	1.277	31.45
Upper 95% CI of mean	8.228	9.427	5.863	5.033	3.329	38.73

(b) Unpaired t test for purified DRGs vs. DRG + single glial cells or non-purified DRGs

Entry	DRG + SC	DRG + EC	DRG + SGCs	DRG + FB	Non-purified DRG
P value	0.0025	0.0001	0.1314	0.3196	<0.0001
P value summary	**	***	ns	ns	****
Significantly different (P<0.05)?	Yes	Yes	No	No	Yes
One- or Two-tailed P value?	Two-tailed	Two-tailed	Two-tailed	Two-tailed	Two-tailed
t	t=3.025	t=3.842	t=1.510	t=0.9956	t=18.61
df	df=1170	df=1189	df=1185	df=1220	df=1487
Mean of Purified	2.303	2.303	2.303	2.303	2.303
Mean of co-culture	5.764	6.831	3.867	3.275	35.09
Difference between means ± SEM	3.461 ± 1.144	4.528 ± 1.178	1.564 ± 1.036	0.9715 ± 0.9758	32.79 ± 1.762
95% confidence interval	1.216 to 5.705	2.216 to 6.839	-0.4689 to 3.598	-0.9429 to 2.886	29.33 to 36.24
R squared (eta squared)	0.007759	0.01226	0.001919	0.0008118	0.1889

Table A.16: Descriptive statistics and unpaired t-test for co-cultures DRG-glia

(a) Descriptive statistics for experiments with IMS32 cells

Entry	Purified	Purified + IMS32	Non-purified
Number of values	1512	1764	1260
Mean	1.257	2.381	18.49
Std. Deviation	11.14	15.25	38.84
Std. Error of Mean	0.2866	0.3631	1.094
Lower 95% CI of Mean	0.6945	1.669	16.35
Upper 95% CI of Mean	1.819	3.093	20.64

(b) Unpaired t test for purified DRGs vs. purified DRGs + IMS32

Entry	Value
P value	0.0176
P value summary	*
Significantly different (P<0.05)?	Yes
One- or Two-tailed P value?	Two-tailed
t, df	t=2.375, df=3274
Mean of Purified	1.257
Mean of Purified + IMS32	2.381
Difference between means ± SEM	1.124 ± 0.4735
95% confidence interval	0.1960 to 2.053
R squared (eta squared)	0.001719

(c) Unpaired t test for purified DRGs + IMS32 vs. non-purified DRGs

Entry	Value
P value	<0.0001
P value summary	****
Significantly different (P<0.05)?	Yes
One- or Two-tailed P value?	Two-tailed
t, df	t=15.80, df=3022
Mean of Purified + IMS32	2.381
Mean of Non-purified	18.49
Difference between means ± SEM	16.11 ± 1.020
95% confidence interval	14.11 to 18.11
R squared (eta squared)	0.07632

Table A.17: Descriptive statistics and unpaired t-test for experiments with co-cultures DRG-IMS32

Condition	wt		non conc		w/o factors		conc		High
	P	NP	ctrl	cond	ctrl	cond	ctrl	cond	density
Number of values	409	664	422	445	581	780	787	825	1373
Mean	5.134	35.09	3.555	4.270	4.475	3.718	19.82	27.27	2.185
Std. Deviation	22.10	47.76	18.54	20.24	20.69	18.93	39.89	44.56	14.62
Std. Error of Mean	1.093	1.853	0.9024	0.9595	0.8585	0.6779	1.422	1.551	0.3947
Lower 95% CI of Mean	2.987	31.45	1.781	2.384	2.789	2.387	17.03	24.23	1.411
Upper 95% CI of Mean	7.282	38.73	5.328	6.155	6.161	5.049	22.61	30.32	2.959

Table A.18: Descriptive statistics for experiments with conditioned medium

(a) Purified DRGs vs. purified DRGs treated with conditioned concentrated medium

Entry	Value
P value	<0.0001
P value summary	****
Significantly different (P<0.05)?	Yes
One- or Two-tailed P value?	Two-tailed
t, df	t=9.484, df=1232
Mean of Purified	5.134
Mean of conditioned concentrated medium	27.27
Difference between means ± SEM	22.14 ± 2.334
95% confidence interval	17.56 to 26.72
R squared (eta squared)	0.06804

(b) Purified DRGs vs. purified DRGs treated with control concentrated medium

Entry	Value
P value	<0.0001
P value summary	****
Significantly different (P<0.05)?	Yes
One- or Two-tailed P value?	Two-tailed
t, df	t=6.914, df=1194
Mean of Purified	5.134
Mean of Control concentrated medium	19.82
Difference between means ± SEM	14.69 ± 2.124
95% confidence interval	10.52 to 18.86
R squared (eta squared)	0.03850

(c) Purified DRGs vs. purified DRGs treated with conditioned medium derived from high-density glial cells

Entry	Value
P value	0.0017
P value summary	**
Significantly different (P<0.05)?	Yes
One- or Two-tailed P value?	Two-tailed
t, df	t=3.147, df=1780
Mean of Purified	5.134
Mean of Control concentrated medium	2.185
Difference between means ± SEM	2.949 ± 0.9372
95% confidence interval	1.111 to 4.788
R squared (eta squared)	0.005534

Table A.19: Unpaired t-tests for experiments with conditioned medium

(a) Descriptive statistics for experiments with Millicell® inserts

Entry	Filters control	Filters with cells	Purified	Non-purified
Number of values	692	1399	825	664
Mean	3.613	19.09	2.303	35.09
Std. Deviation	18.67	39.31	15.01	47.76
Std. Error of Mean	0.7099	1.051	0.5225	1.853
Lower 95% CI of Mean	17.02	1.277	31.45	2.219
Upper 95% CI of Mean	21.15	3.329	38.73	5.007

(b) Unpaired t test for purified DRGs vs. purified DRGs co-cultured with filters w/o cells (control)

Entry	Value
P value	0.1302
P value summary	ns
Significantly different (P<0.05)?	Ns
One- or Two-tailed P value?	Two-tailed
t, df	t=1.514, df=1515
Mean of Purified	2.303
Mean of Filters control	3.613
Difference between means ± SEM	1.310 ± 0.8650
95% confidence interval	-0.3870 to 3.006
R squared (eta squared)	0.001511

(c) Unpaired t test for purified DRGs vs. purified DRGs co-cultured with filters with cells

Entry	Value
P value	<0.0001
P value summary	****
Significantly different (P<0.05)?	Yes
One- or Two-tailed P value?	Two-tailed
t, df	t=11.77, df=2222
Mean of Purified	2.303
Mean of Filters with cells	19.09
Difference between means ± SEM	16.78 ± 1.426
95% confidence interval	13.98 to 19.58
R squared (eta squared)	0.05865

Table A.20: Descriptive statistics and unpaired t-test for experiments with Millicell ® inserts

A.2 Media and buffers

Chemical	Quantity	Final concentration
Boric acid	1.55 g	50 mM
Sodium tetracarborate	2.375 g	12.5 mM
Milli Q water	500 ml	
pH		8.4

Table A.21: Borate buffer

Chemical	Quantity	Final concentration
PEI	0.03 g	0.075%
Borate buffer	40 ml	
Filter	0.4µM	

Table A.22: PEI solution

Chemical	Quantity	Final concentration
Laminin	10 µl	20 mg/ml
DPBS with calcium and magnesium	490 µl	

Table A.23: Laminin solution

Chemical	Quantity	Final concentration
Glucose	9 mg	3.6 mg/ml
Collagenase type IV	7.5 mg	3 mg/ml
Neutral Protease	15 mg	6 mg/ml
DMEM + GlutaMAX	2.5 ml	

Table A.24: Enzymatic solution "CD"

Chemical	Quantity	Final concentration
Glucose	9 mg	1.8 mg/ml
Neutral Protease	15 mg	3 mg/ml
DMEM + GlutaMAX	5 ml	

Table A.25: Enzymatic solution "D"

Chemical	Quantity	Final concentration
DNAse	60 µl	1 unit/ml
Gradient medium	6 ml	

Table A.26: DNAse solution

Chemical	Quantity	Final concentration
Neurobasal-A	19.4 ml	
GlutaMAX	200 µl	1X
SM1	200 µl	0.5X
Penicillin-Streptomycin	100 µl	0.5X
N2 Supplement-A	100 µl	0.5X
NGF	8 µl	100 ng/µl

Table A.27: Modified Neurobasal-A medium for primary DRG cultures

Chemical	Quantity	Final concentration
Neurobasal-A	19.9 ml	
Penicillin-Streptomycin	100 µl	0.5X

Table A.28: Modified Neurobasal-A medium for primary DRG cultures without factors

Chemical	Quantity	Final concentration
Prigrow III	44.5 ml	
FBS	5 ml	10%
Penicillin-Streptomycin	500 µl	1%

Table A.29: Modified Prigrow III medium for immortalized mouse Schwann cells (IMS32)

Chemical	Quantity	Final concentration
DMEM + GlutaMAX	17.9 ml	
FBS	2 ml	10%
Penicillin-Streptomycin	100 µl	0.5%

Table A.30: Modified DMEM medium for non-neuronal cells (limiting dilution)

Chemical	Quantity	Final concentration
DMEM + GlutaMAX	22.5 ml	
HS	2.5 ml	5%
Penicillin-Streptomycin	125 µl	0.5%

Table A.31: Gradient medium

Chemical	Volume
Optiprep^{TM}	4 ml
Gradient medium	2 ml

Table A.32: Working solution

Solution	Volume of Working solution	Volume of Gradient medium
8%	0.8 ml	3.2 ml
15%	1.5 ml	2.5 ml
28%	2.8 ml	1.2 ml

Table A.33: Gradient solutions

Chemical	Quantity	Final concentration
DPBS with calcium and magnesium	14 ml	
BSA	200 µl	0.5%

Table A.34: BSA buffer

Chemical	Quantity	Final concentration
NaCl	8.1816 mg	140 mM
KCl	0.298 mg	4 mM
$CaCl_2$	0.294 mg	2 mM
$MgCl_2$	0.203 mg	1 mM
HEPES	2.383 mg	10 mM
Milli-Q water	1 l	
pH	7.4	

Table A.35: EC

Chemical	Quantity	Final concentration
NaCl	4.325 mg	74 mM
KCl	5.219 mg	70 mM
$CaCl_2$	0.294 mg	2 mM
$MgCl_2$	0.203 mg	1 mM
HEPES	2.383 mg	10 mM
Milli-Q water	1 l	
pH	7.4	

Table A.36: EC high K

Chemical	Quantity	Final concentration
EC	50 ml	
Glucose	40 mg	4 mM

Table A.37: EC for recording

Chemical	Quantity	Final concentration
Neurobasal-A	400 µl	
NeuroFluor^{TM} NeuO	1 µl	250 nM

Table A.38: NeuroFluor^{TM} NeuO staining solution

Chemical	Quantity	Final concentration (v/v)%
Milli-Q water	250 ml	50
DPBS without calcium and magnesium	250 ml	50
Paraformaldehyde	20 g	20
Sucrose	20 g	20

Table A.39: PFA 4%

Chemical	Quantity	Final concentration
DPBS without calcium and magnesium	250 ml	
Gelatin from cold-water fish	0.5 g	0.2%

Table A.40: Washing buffer

Chemical	Quantity	Final concentration
Washing buffer	5 ml	
Triton^{TM} X-100	25 µl	0.1%

Table A.41: Permeabilization buffer

Chemical	Quantity	Final concentration
Washing buffer	18 ml	
Permeabilization buffer	1 ml	0.005% Triton^{TM} X-100
Donkey serum	1 ml	5%

Table A.42: Blocking buffer/Ab carrier solution

A.3 Chemicals and consumables

Name	Manufacturer	Catalog number
Adenosine 5'-triphosphate (ATP) disodium salt	Tocris/Biotechne	3245
Boric acid	Sigma-Aldrich	B-9645
Bradykinin	Tocris/Biotechne	3004
BSA	Sigma-Aldrich	A7979
Cal-520®, AM	AAT Bioquest	21130
Calcium chloride ($CaCl_2$)	Carl Roth	5239.2
Capsaicin	Tocris/Biotechne	0462
Collagenase Type IV	Worthington	LS004186
Deoxyribonuclease I	Worthington	LS002139
Donkey serum	Dianova	017-000-121
DMEM + GlutaMAX	Thermo Fisher	31966-021
DPBS with calcium and magnesium	Thermo Fisher	14040-091
DPBS without calcium and magnesium	Thermo Fisher	14190-094
Gelatin from cold-water fish skin, 45% in H2O	Sigma-Aldrich	G7765
Glucose	Carl Roth	HN06.3
GlutaMAX	Thermo Fisher	35050-038
HBSS without calcium and magnesium	Thermo Fisher	14175-129
HEPES	Carl Roth	9105.3
Horse Serum (HS)	Thermo Fisher	26050-070
Laminin[1]	Sigma-Aldrich	L2020-1MG
Magnesium dichloride ($MgCl_2$)	Carl Roth	2189.1
N2 Supplement-A	Stemcell	7152
Neurobasal-A	Thermo Fisher	10888-022
NeuroFluor™ NeuO	Stemcell	01801
Neuron Isolation Kit	Miltenyi Biotec	130-115-390
Neutral Protease (Dispase)	Worthington	LS02109
NGF 2.5S	Promega	G5141
NucBlue® Live ReadyProbes®	Thermo Fisher	R37605
OptiPrep™	Sigma-Aldrich	D1556-250ML
Paraformaldehyde	Carl Roth	0335.3
Penicillin-Streptomycin	Sigma-Aldrich	P4333-20ML
PEI	Sigma-Aldrich	408727-250ML

Continued on next page

[1] From Engelbreth-Holm-Swarm murine sarcoma

Table A.43 – Continued from previous page

Name	Manufacturer	Catalog number
Potassium chloride (KCl)	Carl Roth	6781.1
Prigrow III	ABM	TM003
Propan-2-ol	Carl Roth	9781.1
Sylgard ™ Silicone elastomer kit	Dowsil, USA	1673921
SM1	Stemcell	5711
Sodium chloride (NaCl)	Carl Roth	9265.1
Sucrose	Carl Roth	9097.2
Tergazyme	Sigma-Aldrich	Z273287
Triton™ X-100	Sigma-Aldrich	X100-100ML
Trypsin-EDTA 0.25%	Sigma-Aldrich	T4049
Veratridine	Tocris/Biotechne	2918

Table A.43: List of chemicals

Name	Manufacturer	Cat. nr.	Labelling	Reactivity	Host	Concentration
TUBB3 (purified anti-Tubulin βIII)	Biolegend	801201	Dendrites, axons	H, M, R	M	1:500
S100b	Abcam	ab52642	Schwann cells	H, M, R	Rb	1:100
GFAP	Biolegend	PKC-591P	Astrocytes	H, M, R	Ch	1:500
ProLong™ Glass Antifade Mountant with DAPI	Thermo Fisher	P36980	Nuclei	-	-	20 µl

Table A.44: Primary antibodies

Name	Manufacturer	Cat. nr.	Host	Abs-Em (λ)	Concentration
Alexa Fluor 488- conjugated Anti-Rabbit	Dianova	711-545-152	Donkey	488 nm	1:500
Alexa Fluor 568- conjugated Anti-Mouse	Thermo	1917938	Donkey	568 nm	1:500
Alexa Fluor 647- conjugated Anti-Chicken	Dianova	703-605-155	Donkey	647 nm	1:500

Table A.45: Secondary antibodies

Name	Manufacturer	Catalog number
6-well plate	Corning, Germany	3736
24-well plate	Corning, Germany	3524
Amicon® Ultra 15 mL Centrifugal Filters	Merck, Germany	UFC900308
Bio Puncher 3mm Biopunch®	Ted Pella, Inc, USA	15111-30
Bottle Top Vacuum Filter	Corning, Germany	431118
Dissection forceps	Fine Science Tools, Germany	11295-20
Forceps 2	Fine Science Tools, Germany	06 100 003
Glass coverslips round 12mm	Carl Roth, Germany	P231.1
Glass coverslips 24 x 32 mm	Carl Roth, Germany	H877.2
Millicell® Cell Culture Inserts	Merck, Germany	PICM01250
Parafilm®	Bemis, USA	PM999
Petri dishes 35mm	Corning, Germany	3294
Petri dishes 60mm	Corning, Germany	430166
Petri dishes 100mm	Corning, Germany	430167
Petri dishes 150mm	Corning, Germany	430599
Scalpels	Swann-Morton, England	0205
Scissors	Fine Science Tools, Germany	14070-12
Serological pipettes 5ml	Gilson, Germany	F110126
Serological pipettes 10ml	Gilson, Germany	F110128
Serological pipettes 25ml	Gilson, Germany	F110130
Serological pipettes 50ml	Gilson, Germany	F110131
Tips for p10 pipettes*	Greiner Bio-One, Germany	765290
Tips for p2, p10, and p20 pipettes*	Integra, Germany	4402
Tips for p100*	Greiner Bio-One, Germany	685290
Tips for p100*	Integra, Germany	4422
Tips for p1000*	Greiner Bio-One, Germany	686290
Tips for p1000*	Integra, Germany	4442

Note: * denotes in-house sterilization

Table A.46: List of chemicals

Name	Manufacturer	Catalog number	Notes
Cell culture incubator	Binder	990049	37°C, 5% CO2
Centrifuge	Eppendorf, Germany	5804	
Dissection microscope	Motic, Germany	SMZ-171-TLED	
Fineplacer® lambda	Finetech GmbH, Germany	-	
Gas controller	Okolab S.R.L., Italy	CO2-UNIT-BL	
Humidity controller	Okolab S.R.L., Italy	HM-ACTIVE	
Incubation chamber	Okolab S.R.L., Italy	H301-T-UNIT-BL-PLUS	
MEA2100 recording system	MultiChannel Systems GmbH, Germany		
Minishaker	IKA, Germany	MS1	
pH-Meter	Knick, Germany	766 Calimatic	
Plasma cleaner	Harrick, USA	PDC32G	
RETbasic magnetic stirrer	IKA, Germany	G023	
Scale	Sartorius, Germany	CP153	
Scale	Sartorius, Germany	CP225D	
SpeedMixer	FlackTec Inc., USA	DAC 150.1 FVZ-K	
Ultrasonic cleaner	VWR, Germany	USC100T	
UV chamber	Bio-Rad, USA	GS Gene Linker ™	
Horizontal laminar flow hood	Kendro GmbH, Germany	Hera Safe KS12	
Water bath	Julabo GmbH, Germany	5B	

Table A.47: List of electrical devices